



**British  
Geological Survey**

NATURAL ENVIRONMENT RESEARCH COUNCIL

# The IEA Weyburn CO<sub>2</sub> Monitoring and Storage Project

## Final report of the European research team

Research Report RR/05/03



**British  
Geological Survey**  
NATURAL ENVIRONMENT RESEARCH COUNCIL



**Quintessa**





BRITISH GEOLOGICAL SURVEY

RESEARCH REPORT RR/05/03

# The IEA Weyburn CO<sub>2</sub> Monitoring and Storage Project

## Final report of the European research team

James B Riding<sup>2</sup> and Christopher A Rochelle<sup>2</sup>

### *Keywords*

Carbon dioxide, economics, enhanced oil recovery, geochemistry, geological storage, geoscientific monitoring, safety assessment studies, Weyburn

### *Front cover*

Well head infrastructure at the Weyburn oilfield, Saskatchewan, Canada. M H Strutt, BGS © NERC

### *Bibliographical reference*

RIDING, J B and ROCHELLE, C A  
2005. The IEA Weyburn CO<sub>2</sub>  
Monitoring and Storage Project.  
Final Report of the European  
Research Team. *British Geological  
Survey Research Report*  
RR/05/03 54pp.

ISBN 085272 507 8

Copyright in materials derived from the British Geological Survey's work is owned by the Natural Environment Research Council (NERC) and/or the authority that commissioned the work. You may not copy or adapt this publication without first obtaining permission. Contact the BGS Intellectual Property Rights Section, British Geological Survey, Keyworth, e-mail [ipr@bgs.ac.uk](mailto:ipr@bgs.ac.uk). You may quote extracts of a reasonable length without prior permission, provided a full acknowledgement is given of the source of the extract.

**THE IEA WEYBURN CO<sub>2</sub> MONITORING AND STORAGE PROJECT  
FINAL REPORT OF THE EUROPEAN RESEARCH TEAM**

**Contributors:**

<sup>1</sup>Pascal Audigane  
<sup>1</sup>Mohamed Azaroual  
<sup>2</sup>Keith Bateman  
<sup>3</sup>Jean-Claude Baubron  
<sup>4</sup>Steven Benbow  
<sup>5</sup>Roberto Bencini  
<sup>6</sup>Stan E Beaubien  
<sup>2</sup>David J Birchall  
<sup>5</sup>Barbara Cantucci  
<sup>5</sup>Carlo Cardellini  
<sup>2</sup>Ben D Charlton  
<sup>5</sup>Daniele Cinti  
<sup>1</sup>Isabelle Czernichowski-Lauriol  
<sup>1</sup>Pierre Durst  
<sup>1</sup>Hubert Fabriol  
<sup>5</sup>Gianfranco Galli  
<sup>1</sup>Irina Gaus  
<sup>5</sup>Domenico Granieri  
<sup>7</sup>Panchali Guha  
<sup>2</sup>David G Jones  
<sup>2</sup>Simon J Kemp  
<sup>1</sup>Yves-Michel Le Nindre  
<sup>6</sup>Salvatore Lombardi  
<sup>4</sup>Philip Maul  
<sup>2</sup>John A McKervey  
<sup>8</sup>Dan Olsen  
<sup>2</sup>Jonathan M Pearce  
<sup>9</sup>Lynden Penner  
<sup>5</sup>Luca Pizzino  
<sup>5</sup>Fedora Quattrocchi  
<sup>2</sup>Shaun Reeder  
<sup>2</sup>James B Riding  
<sup>2</sup>Nicholas J Riley  
<sup>2</sup>Christopher A Rochelle  
<sup>10</sup>David Savage  
<sup>2</sup>Richard A Shaw  
<sup>8</sup>Niels Springer  
<sup>8</sup>Niels Stenft  
<sup>2</sup>Michael H Strutt  
<sup>2</sup>Helen Taylor  
<sup>2</sup>Gren Turner  
<sup>5</sup>Nunzia Voltattorni  
<sup>2</sup>Doris Wagner  
<sup>2</sup>Joanna Wragg

- <sup>1</sup> Bureau de Recherches Géologiques et Minières, 3 Avenue Claude Guillemin, BP 6009, 45060 Orléans Cedex 2, France
- <sup>2</sup> British Geological Survey, Keyworth, Nottingham NG12 5GG, UK
- <sup>3</sup> Bureau de Recherches Géologiques et Minières, Service Géologique Régional Lorraine, 1 Avenue du Parc de Brabois, 54500 Vandoeuvre-lès-Nancy, France
- <sup>4</sup> Quintessa Limited, Dalton House, Newtown Road, Henley-on-Thames, Oxfordshire RG9 1HG, UK
- <sup>5</sup> Istituto Nazionale di Geofisica e Vulcanologia, Via di Vigna Murata 605, 00143, Rome, Italy
- <sup>6</sup> University of Rome 'La Sapienza', Department of Earth Sciences, P.le Aldo Moro 5, 00185 Rome, Italy
- <sup>7</sup> British Geological Survey, Maclean Building, Crowmarsh Gifford, Wallingford, Oxfordshire OX10 8BB, UK
- <sup>8</sup> Geological Survey of Denmark and Greenland, Øster Voldgade 10, DK-1350 Copenhagen, Denmark
- <sup>9</sup> J D Mollard and Associates Limited, 2002 Victoria Avenue, 810 Avord Tower, Regina, Saskatchewan, Canada S4P 0R7
- <sup>10</sup> Quintessa Limited, 24 Trevor Road, West Bridgford, Nottingham NG2 6FS, UK

# Contents

## Executive summary v

## 1 Introduction 1

- 1.1 Overview 1
- 1.2 Geology 1
  - 1.2.1 The geology and petroleum geology of the Williston Basin 1
  - 1.2.2 The geology of the Weyburn oilfield 1
- 1.3 The CO<sub>2</sub>-EOR operation at Weyburn 3

## 2 Reservoir monitoring and characterisation 4

- 2.1 Introduction 4
- 2.2 Core analysis 4
- 2.3 Hydrochemical baseline characterisation 5
- 2.4 Analysis of reservoir fluids and dissolved gases 7
  - 2.4.1 Introduction 7
  - 2.4.2 Approach and methodology 7
  - 2.4.3 Dissolved gases and trace metals 8
  - 2.4.4 Strontium isotope ratios (<sup>87</sup>Sr/<sup>86</sup>Sr) 10
- 2.5 Hydrogeological, hydrochemical modelling and geochemical reactions 11
  - 2.5.1 Introduction 11
  - 2.5.2 Experiments 12
  - 2.5.3 Modelling 18
- 2.6 Microseismic monitoring 22
  - 2.6.1 Introduction 22
  - 2.6.2 Data acquisition and processing 22
  - 2.6.3 Interpretation 23
  - 2.6.4 Summary and conclusions 23

## 3 Caprock, overlying formations and engineered seals 25

- 3.1 Introduction 25
- 3.2 Core analysis of the Midale Evaporite Unit caprock 25
- 3.3 Characterisation and hydrochemical modelling of the overburden 26
  - 3.3.1 The Watrous Formation 26
  - 3.3.2 Other formations 27
- 3.4 Geochemical reactions of caprocks; the Midale Evaporite Unit and the Watrous Formation 28
  - 3.4.1 Experiments 28
  - 3.4.2 Modelling 29
- 3.5 Geochemical reactions of borehole cement 30

## 4 Monitoring and characterisation of near-surface processes 32

- 4.1 Soil gas monitoring 32
  - 4.1.1 Introduction 32
  - 4.1.2 Methodology 32
  - 4.1.3 Results 33
  - 4.1.4 Conclusions 35
- 4.2 Till characterisation in the Weyburn Oilfield 36
  - 4.2.1 Introduction 36
  - 4.2.2 Background 36
  - 4.2.3 Geochemistry, sedimentology and mineralogy of the tills, and their relationship to soil gas 36
  - 4.2.4 Palynology 37
  - 4.2.5 Conclusions and recommendations 37

## 5 Safety assessment studies 39

- 5.1 Introduction 39
- 5.2 The FEP database 39
  - 5.2.1 Accessing the FEP database 39
  - 5.2.2 Database structure and content 39
  - 5.2.3 The assessment basis 40
  - 5.2.4 External factors 40
  - 5.2.5 Carbon dioxide storage 41
  - 5.2.6 Carbon dioxide properties, interactions and transport 41
  - 5.2.7 The geosphere 41
  - 5.2.8 Boreholes 42
  - 5.2.9 The near-surface environment 42
  - 5.2.10 Human behaviour 42
  - 5.2.11 Impacts 42
- 5.3 System-level modelling 43
  - 5.3.1 Model development 43
  - 5.3.2 The treatment of uncertainty 43
  - 5.3.3 The use of the FEP database 43
- 5.4 Other uses of the database 43
- 5.5 Discussion 43

## 6 Economics 45

- 6.1 The economics of the CO<sub>2</sub> source: The Great Plains Synfuel Plant, North Dakota, USA 45
  - 6.1.1 Introduction 45
  - 6.1.2 Background 45
  - 6.1.3 Outline of the Great Plains Synfuels Plant, the syngas process and by-products 45
  - 6.1.4 The CO<sub>2</sub> stream 46
  - 6.1.5 The price of CO<sub>2</sub> 46
  - 6.1.6 The syngas market 46
- 6.2 The Economics of enhanced oil recovery using CO<sub>2</sub>: the Weyburn case 46
  - 6.2.1 Introduction 46
  - 6.2.2 Incremental production 47
  - 6.2.3 Revenue from CO<sub>2</sub>-EOR 47
  - 6.2.4 Costs 47
  - 6.2.5 The interface between CO<sub>2</sub> sequestration and enhanced oil recovery 47

## 7 Conclusions 48

## 8 Acknowledgements 51

## 9 References 52

### TABLES

- 1 Comparisons between Weyburn core data on gas permeability and porosity determined in this study, and field average data taken from Malik and Islam (2000) 5
- 2 Details of borehole fluid monitoring surveys conducted at the Weyburn oilfield 7
- 3 Statistical summary of the 2001–2003 strontium isotope ratios 12
- 4 Mass balance calculation for samples GEUS 1, GEUS 2, and GEUS 3 18
- 5 Conventional core analysis data measured for the Midale Marly M1 Unit/Midale Evaporite Unit transition zone 27

- 6 Changes in weight of cement monolith samples after two weeks reaction with 'free CO<sub>2</sub>' and dissolved CO<sub>2</sub> 30

## FIGURES

- 1 The location of the Weyburn oilfield and the route of the CO<sub>2</sub> pipeline 2
- 2 Stratigraphical correlation of the Mississippian in Saskatchewan, North Dakota, Montana and Manitoba. Modified from Kent (1984) and Wegelin (1984) 2
- 3 Schematic diagram illustrating how a miscible CO<sub>2</sub>-enhanced oil recovery flood produces incremental oil 3
- 4 An example of core material used in the flow and batch reaction experiments 4
- 5 A back-scattered electronmicrograph of a sample of the Midale Marly M2 Unit 5
- 6 Modelling of the natural migration pathways within the Mississippian aquifer; observed salinity distribution and simulated streamlines 6
- 7 Gas-brine equilibrium system and CO<sub>2</sub> solubility versus total dissolved solids in Weyburn oilfield brines 7
- 8 Contour maps illustrating dissolved CO<sub>2</sub> contents, sampled at the surface (i.e. CO<sub>2</sub>(DGCS)), between the M5 and M8 surveys 9
- 9 Ternary plots of dissolved CO<sub>2</sub>-nitrogen-hydrogen and methane-nitrogen-hydrogen contents for the 2001 to 2004 surveys 9
- 10 Normal probability plots of dissolved CO<sub>2</sub> (top), dissolved methane (lower left) and dissolved hydrogen (lower right) 10
- 11 Contour maps showing dissolved methane, sampled at the surface between the M5 and M8 surveys 11
- 12 Normal probability plot of dissolved hydrogen sulphide in the different surveys expressed as percentage of dissolved gas 11
- 13 Hydrostratigraphical delineation and nomenclature for the Williston Basin (modified from Bachu and Hichon, 1996) 12
- 14 <sup>87</sup>Sr/<sup>86</sup>Sr contour maps of produced aqueous fluids within the Phase 1A CO<sub>2</sub> injection area at Weyburn for monitoring campaigns M1 (2001), M5 (2002) and M8 (2003) 13
- 15 Evolution of calcium concentrations within the static batch experiments on Midale Beds material 14
- 16 Evolution of magnesium concentrations within experiments using samples of Midale Beds material 15
- 17 The inlet end of sample GEUS 1 (Midale Marly Unit, M1 zone), before the CO<sub>2</sub> flooding experiment (top left), and after the experiment (top right and bottom right) 15
- 18 Sample GEUS 1 (Midale Marly Unit, M1 zone) after CO<sub>2</sub> flooding. Thin-section micrograph with plane polarized light from the central part of the sample 16
- 19 Backscatter electron microscope images of sample GEUS 2 (Midale Marly Unit, M2 zone) 16
- 20 Output fluid concentrations of Ca<sup>2+</sup> and Mg<sup>2+</sup> during the CO<sub>2</sub> flooding experiments 17
- 21 Scanning electron photomicrograph of a monolith of the Midale Vuggy Unit, showing a well-developed 'tide mark' with increased dissolution within the water-rich phase (i.e. the lower half of the image) 18
- 22 Scanning electron photomicrographs of Midale Vuggy Unit monoliths showing well-developed secondary growth of gypsum crystals within the aqueous phase 19
- 23 The saturation index (SI) potentially reacting, i.e. dissolving and/or precipitating, minerals in the BGS experimental system 19
- 24 The saturation index (SI) of potentially reacting, i.e. dissolving and/or precipitating, minerals in the CO<sub>2</sub> flooding experiment system of GEUS 20
- 25 The saturation index (SI) of potentially reacting, i.e. dissolving and/or precipitating, minerals in the BGS flow experiments 21
- 26 The saturation index (SI) of potentially reacting, i.e. dissolving and/or precipitating, minerals in the BGS experimental system 21
- 27 Sulphate mineral (anhydrite and gypsum) behaviour in the Weyburn reservoir brines under CO<sub>2</sub> injection pressure, temperature and pCO<sub>2</sub> conditions 22
- 28 Hypocentral location of 'high' frequency events in horizontal view and vertical/sectional view, recorded on September 9th and October 20th 2003 and on March 18th and 19th 2004 by ESG 23
- 29 Comparison of gas production in well 191/11-08 and the cumulative seismic moment of the microseismic events recorded during January and February 2004 24
- 30 Comparison of the oil production rate in well 191/09-08 and the cumulative seismic moment of events located south of the observation well 24
- 31 Regional NNW-SSE cross-section of the Mississippian succession through the Weyburn oilfield illustrating the truncation by the Lower Watrous Formation 25
- 32 Conceptual sketch of CO<sub>2</sub> diffusion in the Lower Watrous Formation 26
- 33 A back-scattered electron micrograph of a sample of the Midale Evaporite Unit 26
- 34 Calculated porosity changes in the base of the Lower Watrous Formation for composition 1 (left) and composition 2 (middle) after 350 years and for composition 1 after 20 000 years (right) 28
- 35 Scanning electron photomicrographs of two samples of a monolith sample of the Midale Evaporite Unit 29
- 36 The saturation index (SI) of potentially dissolving and/or precipitating minerals in the experiments 30
- 37 Soil gas measurement in the Phase 1 CO<sub>2</sub> injection area of the Weyburn oilfield 32
- 38 Maps illustrating the locations of the various studied sites, and detail of the grid area showing sampling points, surface water, wells and air photo lineaments 33
- 39 Contoured distribution of CO<sub>2</sub> flux and soil gas CO<sub>2</sub> for the three sampling campaigns 34
- 40 Plot illustrating the relationship between CO<sub>2</sub>, O<sub>2</sub> and N<sub>2</sub> for the grid dataset from Weyburn in July, 2001 as compared to data collected from Cava dei Selci in Italy, a dormant volcanic site which has known gas vents due to deep thermometamorphic reactions 35
- 41 Ternary diagram of grain size variations (after Shepard, 1954) for the <2 mm fraction 36
- 42 (a) A typical view of till matrix with detrital angular to rounded, silt to sand sized grains in a clay matrix. (b) A relict, oxidised ferromagnesian grain now replaced by iron and manganese oxides 37
- 43 Clast density. The number of clasts larger than 50 mm within 5 m of a grid point for the main soil gas grid 38
- 44 The periglacial effects FEP 40
- 45 Crystal Geyser, Utah 41
- 46 Stratigraphical section at the Weyburn oilfield (from Whittaker and Rostron, 2001) 42
- 47 Aerial photograph of the Great Plains Synfuels Plant, Beulah, North Dakota, USA 45

## Executive summary

The IEA Weyburn Carbon Dioxide (CO<sub>2</sub>) Monitoring and Storage Project has analysed the effects of a miscible CO<sub>2</sub> flood into a carbonate reservoir rock at an onshore Canadian oilfield. Anthropogenic CO<sub>2</sub> is being injected as part of an enhanced oil recovery operation. The European research was aimed at analysing long-term migration pathways of CO<sub>2</sub> and the effects of CO<sub>2</sub> on the hydrochemical and mineralogical properties of the reservoir rock. The long-term safety and performance of CO<sub>2</sub> storage was assessed by the construction of a features, events and processes (FEP) database which provides a comprehensive knowledge base for the geological storage of CO<sub>2</sub>. The pre-CO<sub>2</sub> injection hydrogeological, hydrochemical and petrographical conditions in the reservoir were investigated in order to recognise changes caused by the CO<sub>2</sub> flood and assess the long-term fate of the CO<sub>2</sub>. The Mississippian aquifer has a salinity gradient in the Weyburn area, where flows are oriented SW–NE. The baseline gas fluxes and CO<sub>2</sub> concentrations in groundwater and soil were also researched. The dissolved gas in the reservoir waters has allowed potential transport pathways to be identified. Experimental studies of CO<sub>2</sub>-porewater-rock interactions in the Midale Marly Unit have indicated slight dissolution of carbonate and silicate minerals, followed by

relatively rapid saturation with respect to carbonate minerals. Equivalent studies on the overlying and underlying units show similar reaction processes, but secondary gypsum precipitation was also observed. Carbon dioxide flooding experiments on samples of the Midale Marly Unit demonstrated that porosity and gas permeability increased significantly through corrosion of calcite and dolomite. Hydrogeological modelling indicates that if any dissolved CO<sub>2</sub> entered the main aquifers, it would migrate from Weyburn in an E–NE direction at a rate of about 0.2 m/year due to regional groundwater flow. Analysis of reservoir fluids proved that dissolved CO<sub>2</sub> and CH<sub>4</sub> increased significantly in the injection area between 2002 and 2003 and that solubility trapping accounts for the majority of the injected CO<sub>2</sub>, with little apparent mineral trapping. Twelve microseismic events were recorded and these are provisionally interpreted as being possibly related to small fractures formed by injection-driven fluid migration within the reservoir. Pre- and post-injection soil gas data are consistent with a shallow biological origin for the measured CO<sub>2</sub> in soil gases. Isotopic ( $\delta^{13}\text{C}$ ) data values are higher than in the injected CO<sub>2</sub>, and confirm this interpretation. No evidence for leakage of the injected CO<sub>2</sub> to ground level has so far been detected.

## BRITISH GEOLOGICAL SURVEY

The full range of Survey publications is available from the BGS Sales Desks at Nottingham, Edinburgh and London; see contact details below or shop online at [www.geologyshop.com](http://www.geologyshop.com)

The London Information Office also maintains a reference collection of BGS publications including maps for consultation.

The Survey publishes an annual catalogue of its maps and other publications; this catalogue is available from any of the BGS Sales Desks.

*The British Geological Survey carries out the geological survey of Great Britain and Northern Ireland (the latter is an agency service for the government of Northern Ireland), and of the surrounding continental shelf, as well as its basic research projects. It also undertakes programmes of British technical aid in geology in developing countries as arranged by the Department for International Development and other agencies.*

*The British Geological Survey is a component body of the Natural Environment Research Council.*

## *British Geological Survey offices*

### **Keyworth, Nottingham NG12 5GG**

☎ 0115-936 3100 Fax 0115-936 3200  
e-mail: [sales@bgs.ac.uk](mailto:sales@bgs.ac.uk)  
[www.bgs.ac.uk](http://www.bgs.ac.uk)  
Online shop: [www.geologyshop.com](http://www.geologyshop.com)

### **Murchison House, West Mains Road, Edinburgh EH9 3LA**

☎ 0131-667 1000 Fax 0131-668 2683  
e-mail: [scotsales@bgs.ac.uk](mailto:scotsales@bgs.ac.uk)

### **London Information Office at the Natural History Museum (Earth Galleries), Exhibition Road, South Kensington, London SW7 2DE**

☎ 020-7589 4090 Fax 020-7584 8270  
☎ 020-7942 5344/45 e-mail: [bgs london@bgs.ac.uk](mailto:bgs london@bgs.ac.uk)

### **Forde House, Park Five Business Centre, Harrier Way, Sowton, Exeter, Devon EX2 7HU**

☎ 01392-445271 Fax 01392-445371

### **Geological Survey of Northern Ireland, Colby House, Stranmillis Court, Belfast BT9 5BF**

☎ 028-9038 8462 Fax 028-9038 8461

### **Maclean Building, Crowmarsh Gifford, Wallingford, Oxfordshire OX10 8BB**

☎ 01491-838800 Fax 01491-692345

### **Sophia House, 28 Cathedral Road, Cardiff, CF11 9LJ**

☎ 029-2066 0147 Fax 029-2066 0159

## *Parent Body*

### **Natural Environment Research Council, Polaris House, North Star Avenue, Swindon, Wiltshire SN2 1EU**

☎ 01793-411500 Fax 01793-411501

# 1 Introduction

(James B Riding)

## 1.1 OVERVIEW

The IEA Weyburn CO<sub>2</sub> Monitoring and Storage Project studied the geological storage of carbon dioxide (CO<sub>2</sub>) during a commercial enhanced oil recovery (EOR) operation at the Weyburn oilfield, Saskatchewan, Western Canada. The project ran from January 2001 to June 2004 and was a collaborative initiative involving a large team of research workers from Europe and North America (White et al., 2004). It was performed under the auspices of the International Energy Agency Greenhouse Gas Research and Development Programme (IEA GHG). In North America the project was co-ordinated by the Petroleum Technology Research Centre (PTRC) in Regina, Canada, under the control of a management committee and major stakeholders such as EnCana Resources (formerly PanCanadian Resources), the Dakota Gasification Company and the project sponsors. The European and North American researchers worked in close collaboration, but were funded differently, i.e. partly by the European Commission (EC) and from national funds, and through PTRC respectively. The EC project was co-funded by the EC Framework 5 Energy, Environment and Sustainable Development Programme, partner institutions and other sponsors.

The European research was undertaken by a collaboration of five partners; the British Geological Survey (BGS), the Bureau de Recherches Géologiques et Minières (BRGM), the Geological Survey of Denmark and Greenland (GEUS), the Istituto Nazionale di Geofisica e Vulcanologia (INGV) and Quintessa Limited. The University of Rome 'La Sapienza' and the Institut Français du Pétrole were research subcontractors to INGV and BRGM respectively. The British Geological Survey co-ordinated the European work and the International Energy Agency Greenhouse Gas R&D Programme and the Petroleum Technology Research Centre Inc. (PTRC) facilitated linkages and integration. The European research effort was described briefly in Riding et al. (2003).

The work programme of the European team comprised four objectives:

- To address the issues of the long-term safety and performance of CO<sub>2</sub> storage by the use of scenario development and system analysis, together with economic issues.
- To consider the baseline conditions of the Weyburn oilfield prior to CO<sub>2</sub> injection, in particular those impacting upon hydrochemical, hydrogeological and geochemical properties of the reservoir, and their likely impact upon future reservoir performance.
- To consider the effects of injecting significant quantities of CO<sub>2</sub> on the above.
- To encourage collaboration among European and international CO<sub>2</sub> sequestration programmes in considering the key issues.

The overall objective of the project was to enhance scientific knowledge pertaining to the underground storage of CO<sub>2</sub> associated with EOR using several different techniques in

geoscientific monitoring. Another major strand to this work was the promotion of international collaboration on carbon management research between scientists in Canada, the USA and Europe. It is anticipated that the results will help to guide policy makers on carbon management issues. This report is a synthesis of the principal findings of the European research effort and an assessment of how successfully the project objectives have been met.

## 1.2 GEOLOGY

### 1.2.1 The geology and petroleum geology of the Williston Basin

The Weyburn oilfield lies within the Williston Basin. This major structure is a large, approximately circular depression, covering approximately 800 000 square kilometres, and straddling the Canadian-US border. The basin started to subside during the Ordovician, and underwent sporadic subsidence throughout the remainder of the Phanerozoic. The basin contains a relatively complete sedimentary rock record from the Ordovician to the Tertiary (Heck et al., 2000). It is a structurally simple feature, the fill being thickest in its centre, and thinning towards the margins. The deepest point is believed to be near Williston, North Dakota where the Precambrian surface is approximately 5 km below the surface. Most of the hydrocarbons from the basin are produced from Palaeozoic rocks, although some Mesozoic strata are also productive. Since the initial discovery of hydrocarbons in the basin, the Madison Group of Mississippian age has produced the most oil, but significant volumes have also been found in the Red River (Ordovician) and Duperow (Devonian) formations. Some natural gas has also been produced from the basin.

### 1.2.2 The geology of the Weyburn oilfield

The Weyburn oilfield is in south-east Saskatchewan, Canada (Figure 1) and lies in the north-east of the Williston Basin. It was discovered in 1954 and covers some 180 square kilometres of prairie. The oilfield is now operated by EnCana Resources. Medium gravity sour crude oil (25 to 34 degree API) is produced from the uppermost Midale Beds of the Charles Formation. The Charles Formation is part of the Madison Group, a 400–700 m thick carbonate and evaporite succession of upwards-shoaling shallow marine deposits (Mundy and Roulston, 1998) (Figure 2). The Madison Group spans the majority of the Mississippian (early Carboniferous) part of the Williston Basin fill and includes many transgressive-regressive cycles, the top of each typically is marked by a thin, fine-grained bed.

The Midale Beds represent one of these transgressive-regressive cycles and this unit comprises a succession of upwards shoaling, shallow marine carbonate-evaporite sediments of Mississippian (Osagean) age (Figure 2). This unit comprises the Frobisher Evaporite and the overlying Midale Carbonates. Three subdivisions of the Midale Carbonates are present, which range from deep water limestones, through an upward-shallowing succession of

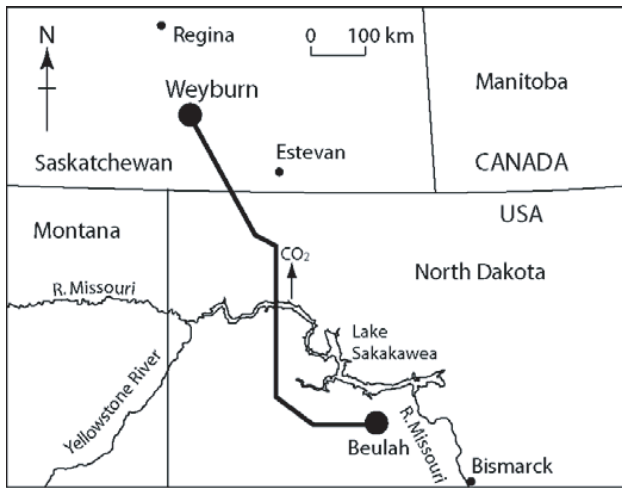


**Figure 1** The location of the Weyburn oilfield and the route of the CO<sub>2</sub> pipeline.

dolomitic mudstones, to supratidal evaporites. These units are the Midale Vuggy, Midale Marly and Midale Evaporite respectively. A thin, iron-stained, fine-grained marker bed with mud intraclasts and algal fragments lies between the Frobisher Evaporite and the Midale Carbonates. This is a lag deposit associated with the change from the restricted lagoonal conditions of the Frobisher Evaporite to the

deeper water, more open marine palaeoenvironment of the lower Midale Carbonates (Wegelin, 1984).

The lowermost subdivision of the Midale Carbonates is the Midale Vuggy Unit, which is a succession of highly fractured and permeable vuggy, heterolithic, stylonitic limestones (packstones and wackestones) that were deposited in relatively deep water (Wegelin, 1987). Wegelin (1984) subdivided the unit into six lithotypes, which were amalgamated into three zones, the Lower, Main and Upper units (Matiisen and Shehata, 1987). The Lower Midale Vuggy Unit is characterised by abundant secondary anhydrite that is of metasomatic origin, and emplaced during the Late Cretaceous according to Kendall and Walters (1978). Porosity and permeability are both highly variable, these parameters average 7% and 1 mD respectively (Wegelin, 1984). The Midale Vuggy Unit is overlain by the cryptocrystalline dolomites (packstones and mudstones) of the Midale Marly Unit, which represent the onset of restricted, shallow water conditions (Wegelin, 1987). The Midale Marly Unit contains the majority of the remaining oil reserves and is the target for the miscible CO<sub>2</sub> flood (Figure 3). It has been subdivided into a lower porous and permeable zone (M3), an upper less porous zone (M1), separated by a less porous packstone (M2) by Matiisen and Shehata (1987). Porosity in this unit is on average about 17%, the pores are approximately 5 µm across and the average permeability is 17 mD (Wegelin, 1984). The Midale Evaporite Unit represents an emergent, supratidal environment and comprises interbedded anhydrites and dolomites. It formed in a highly restricted hypersaline sabkha setting.

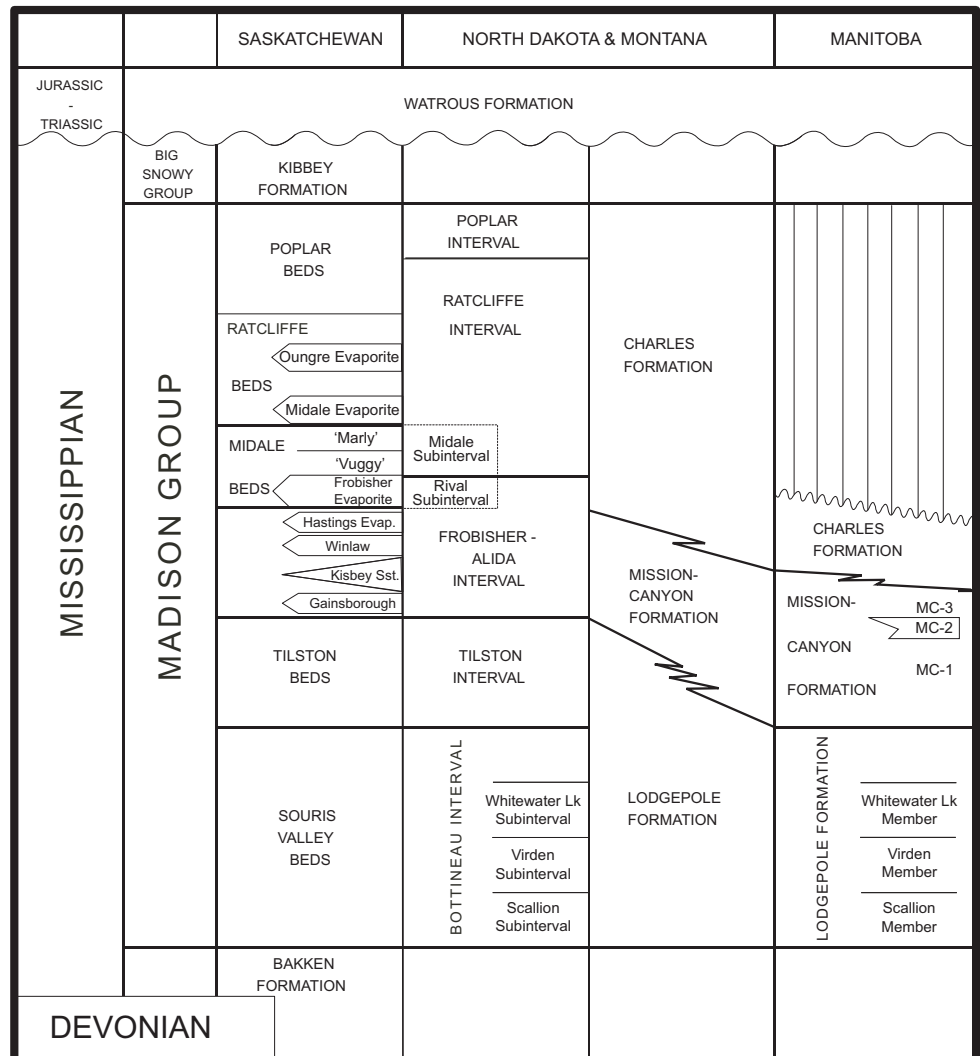


**Figure 2** Stratigraphical correlation of the Mississippian in Saskatchewan, North Dakota, Montana and Manitoba. Modified from Kent (1984) and Wegelin (1984).

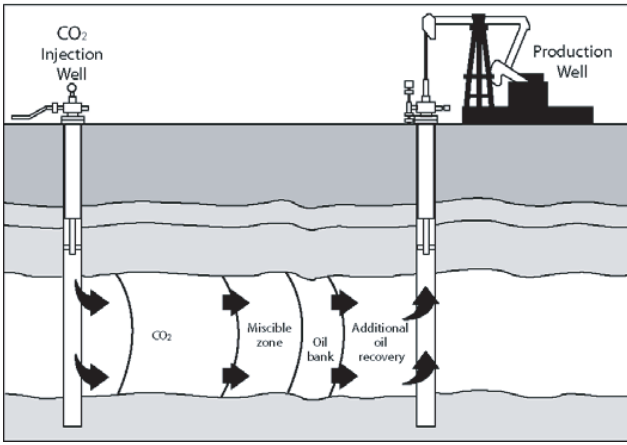


**Figure 3** Schematic diagram illustrating how a miscible CO<sub>2</sub>-enhanced oil recovery flood produces incremental oil. At Weyburn, the depth to the reservoir unit is about 1400 m.

### 1.3 THE CO<sub>2</sub>-EOR OPERATION AT WEYBURN

EnCana Resources (formerly PanCanadian Resources) began injecting a 95% pure CO<sub>2</sub> stream into the oil reservoir, the Midale Beds, at Weyburn during September 2000. At the conclusion of this EOR operation, in 2025–2030, it is anticipated that between 15 and 20 million tonnes of

anthropogenic CO<sub>2</sub> will have been permanently and safely stored in these Mississippian strata, which are about 1.4 km underground. Hence, greenhouse gas emissions will have been significantly reduced as part of a cost-effective industrial operation. Since 1964, water injection has been used as a secondary oil recovery strategy and has efficiently swept incremental oil from the Midale Vuggy Beds due to the high permeability of this unit. The water flood helped the field to achieve its peak production in 1965. The field was revitalized in 1991 by the drilling of horizontal wells. The Midale Marly Beds are less permeable and CO<sub>2</sub> injection is an effective method of extracting oil from this unit. This is because CO<sub>2</sub> is an excellent solvent and dissolves into the oil, simultaneously reducing its viscosity and increasing its volume. The reduced viscosity makes the oil flow more easily and the swelling of the CO<sub>2</sub>-rich oil enhances reservoir pressure. It is anticipated that this CO<sub>2</sub>-EOR operation (Figure 3) will extend the life of the Weyburn oilfield by approximately 25 years with the production of an extra 130 million barrels of oil. The injection of CO<sub>2</sub> was started in September 2000 as Phase 1A and the initial injection rate was 5000 tonnes per day. Injection was originally in 18 patterns of nine wells, each at the west end of the oilfield. The CO<sub>2</sub> flood has been extended in a south-easterly direction and the ultimate aim is to flood 75 patterns in phases over the next 15 years. The CO<sub>2</sub> used is a purchased by-product of coal gasification and supplied to Weyburn through a 320 km long pipeline from the Great Plains Synfuels Plant in Beulah, North Dakota, USA that is operated by the Dakota Gasification Company (Figure 1) (Stelter, 2001).

## 2 Reservoir monitoring and characterisation

### 2.1 INTRODUCTION

This section describes the research on the monitoring and characterisation of the Weyburn oilfield reservoir rocks. It is subdivided into six sections on core analysis, the analysis of reservoir fluids and dissolved gases, hydrogeological and hydrochemical modelling, geochemical reactions and microseismic monitoring. These studies allowed accurate modelling of key reservoir changes caused by the injection of CO<sub>2</sub>.

### 2.2 CORE ANALYSIS

(Jonathan M Pearce and Niels Springer)

Core material from the reservoir zone at Weyburn was selected for CO<sub>2</sub> flow and batch reaction experiments (Figure 4; Pearce and Springer, 2001). The core characterisation is summarised below. A more comprehensive account was given by Springer et al. (2002).

The core material was selected from wells within the phase 1A CO<sub>2</sub> flooding area and plugs and full core samples were prepared for flow and batch reaction experiments (Figure 4). Core analysis data clearly demonstrated that the samples are representative, i.e. they are consistent with the average porosity and permeability data measured for the Weyburn oilfield (Table 1). Macroscopic descriptions of the core samples were undertaken in order to determine the principal petrographical characters, such as mineralogy and sedimentary structures. This also served to check if the samples were representative for the core box interval and to determine if certain structures, such as solution seams and fractures, may influence reservoir



**Figure 4** An example of core material used in the flow and batch reaction experiments. A typical sample of the M1 Midale Marly Unit. This is an oil-stained dolostone with irregular, darker oil-stained shaly laminae. From Pearce and Springer (2001).

quality (porosity and permeability). It was possible to subdivide the cores from the reservoir zone into two groups, according to their sedimentary facies:

- Massive to fine-porous, bioturbated limestones, partly dolomitic, partly calcitic, belonging to the Midale Marly M1 to M3 units. The Marly M2 Unit and parts of M3 are dolomitic.
- Massive fine-porous and/or vuggy calcitic limestones belonging to the Midale Vuggy V2 Unit.

The thin sections of the Midale Marly M1 Unit consist of a finely crystalline dolomite with subordinate calcite. The crystals are 15–30 µm in diameter. An intercrystalline porosity is present in the dolomite and small vugs are common. Samples of the Midale Marly M1 Unit, and the transition between units M1 and M2, show a scale-dependent variation in the dolomite/anhydrite ratios from plug to full core sample. Anhydrite is present as small, scattered grains throughout the rock. The Midale Marly M2 Unit resembles the M1 Unit. However some of the small vugs are fusiform, being formed after dissolution of gypsum crystals (Figure 5). One of the Midale Marly M3 Unit thin sections is rich in skeletal grains that are surrounded by a fine, compact calcite matrix. The scattered pores and vugs are isolated from each other by this matrix. The other Midale Marly M3 Unit samples are dolomitic mudstones with a ‘chalky’ appearance, with abundant small pores between the dolomite crystals that are 15–25 µm in diameter. The thin sections of the calcitic Midale Vuggy V2 Unit comprise numerous poorly-preserved coated grains. These rocks are oncoidal or ooidal grainstones or packstones. They are rich in intergranular and intragranular pores and solution vugs. These appear to have fair reservoir quality, despite some of the cavities not being interconnected in areas with massive biomicrite or non-porous sparry calcite cement.

Alkali feldspar, calcite, celestine, fluorite and gypsum were identified in minor or trace amounts in the reservoir rocks by scanning electron microscope energy dispersive spectrometry (SEM-EDS) analysis. Clay mineralogical analysis by X-ray diffraction show that the Midale rocks contain illite, illite-smectite, quartz and smectite in the <2 µm fraction. There is approximately 2% clay in Midale Marly units M2 and M3.

Grain or crystal sizes were evaluated from thin sections or back-scattered electronmicrograph (BSE) imaging of four samples representing the different lithologies. The dolomite crystals that appear as subhedral to euhedral crystals in three of the samples show a general increase in grain size passing from the Midale Evaporite to the Midale Marly M3 Unit. This is seaward in sedimentary facies, from supratidal to burrowed intertidal/subtidal. The calcite crystals in the Midale Vuggy V2 Unit sample, which may represent a back-shoal facies are significantly larger. This is also reflected in specific surface area measurements. The Midale Marly units have surface areas of approximately 1 m<sup>2</sup>/g, whereas those of the Midale Vuggy units are around 0.3 m<sup>2</sup>/g.

**Table 1** Comparisons between Weyburn core data on gas permeability and porosity determined in this study, and field average data taken from Malik and Islam (2000) (asterisked). The comparisons demonstrate that the samples taken here are representative of the Weyburn reservoir.

Lithological unit	BGS plugs		Field average*	BGS plugs		Field average*	BGS plugs
	Gas permeability (mD)		Gas permeability (mD)	Porosity (%)		Porosity (%)	Grain density range (g/cm <sup>3</sup> )
	Range	Mean		Range	Mean		
Midale Marly	0.15–33	11	10	10–35	24	26	2.69–2.85
Midale Vuggy	2.7–57	22	15	12–15	14	11	2.71–2.73

### 2.3 HYDROGEOLOGICAL AND HYDRO-CHEMICAL BASELINE CHARACTERISATION

(Mohamed Azaroual, Isabelle Czernichowski-Lauriol, Yves-Michel Le Nindre and Pascal Audigane)

The potential long-term migration pathways and reactivity of CO<sub>2</sub> within the reservoir unit are largely controlled by the regional hydrodynamics and geochemistry of the aquifer system. In order to model the migration pathways and CO<sub>2</sub> reactivity, what is needed is a detailed compilation of published data on the structure, hydrology and water chemistry of the Mississippian aquifer. This was undertaken, and focused on a block of 240 x 230 km<sup>2</sup> centered on Weyburn. This dataset was then completed by unpublished well control data using the following data sources:

- Isopach, structure, salinities and pressure data from the Western Canada Sedimentary Basin provided by the Alberta Geological Survey. These have been combined and krigged according to the present grid.
- Recent well data prepared specifically for this project by Saskatchewan Energy and Mines (Saskatchewan Industry and Resources).
- Structural data processed by the Dakota Geological Survey; these were used for the reconstruction of tectonic features in the south of the area such as the Nesson anticline.
- Fluid chemical data from the baseline sampling survey of the Weyburn oilfield, carried out in August 2000 by the University of Calgary to analyse reservoir fluid chemistry prior to CO<sub>2</sub> injection.

Also needed were the structural surfaces, total dissolved solid concentrations and potentiometric surfaces for the Mississippian aquifer. These were modelled using geostatistic tools such as the GDM® BRGM software and georeferenced grids. These results are given in Czernichowski-Lauriol et al. (2001) and Le Nindre et al. (2002).

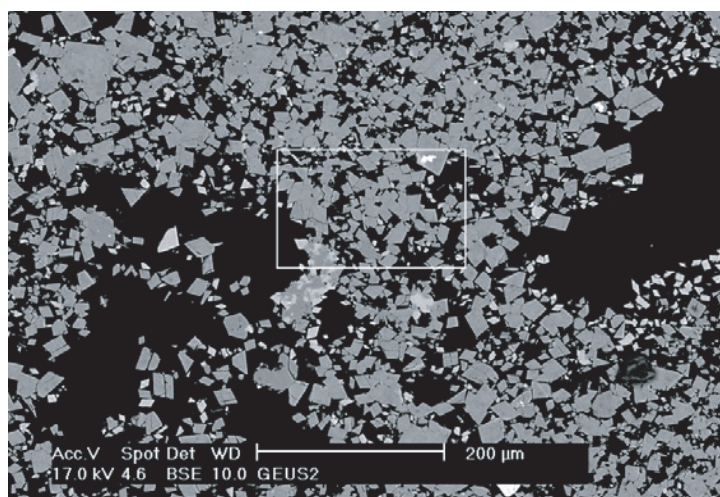
The formation water in the Mississippian aquifer exhibits a very contrasted salinity field (Figure 6). The deeper part of the basin reaches 310 g/l, whereas in southwestern Saskatchewan it is influenced by a fresh/brackish water influx (20 g/l). The Weyburn oilfield is located on a steep salinity gradient, as confirmed by recent field sampling. This may have important consequences on the long-term fate of CO<sub>2</sub> at Weyburn because:

- The water density varies from 1010 to 1210 g/l, which can significantly affect regional hydrodynamics and the migration of CO<sub>2</sub>.
- The solubility of CO<sub>2</sub> in aquifer waters is strongly influenced by salinity, from 1 mole/kg H<sub>2</sub>O of dissolved CO<sub>2</sub> at low salinities, to 0.7 mole/kg H<sub>2</sub>O at high salinities. This can affect CO<sub>2</sub> solubility trapping and chemical reactions with the reservoir rocks and brines.

Detailed investigations on both of these above points were carried out.

Assessments of the salinity gradient and the associated density contrast of the formation water implies the revision of the regional fluid flow which had been previously

**Figure 5** A back-scattered electronmicrograph of a sample of the Midale Marly M2 Unit. This is a dolomite with an idiotopic fabric and numerous small inter-crystalline pores and two small vugs. The vugs are the dark areas at the left and right margins. From Springer et al. (2002).



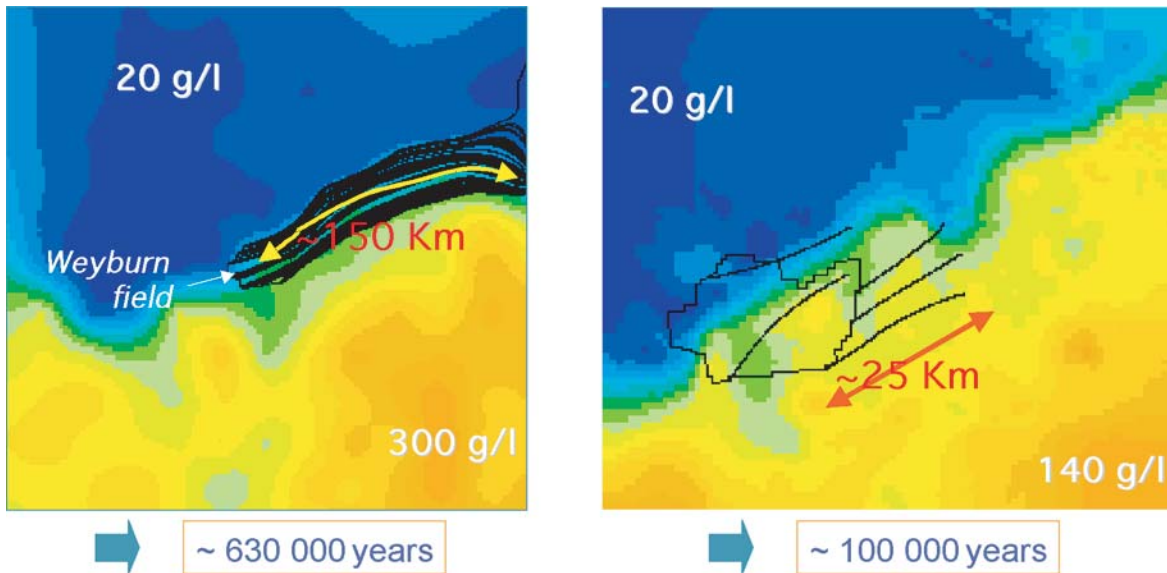


**Figure 6** Modelling of the natural migration pathways within the Mississippian aquifer; observed salinity distribution and simulated streamlines. The left hand panel illustrates the regional scale (i.e. the 240 x 230 km<sup>2</sup> block). The right hand panel illustrates the local scale.

assessed from the potentiometric surfaces. Considering fresh water or environmental hydraulic head gradients, lead to a different overall fluid flow orientation. These are NE–SW for fresh water and NW–SE for environmental hydraulic heads. To cope with these interpretations of the potentiometric surface gradient, two approaches were considered (Audigane and Le Nindre, 2004):

- Initially, an analytical approach quantifying and minimising the error in assessing the regional fluid flow of a variable-density formation in deep sloping aquifers from hydraulic head measurements was used (Bachu, 1995). This method uses an environmental hydraulic head field, calculated with a constant average formation water density of approximately 1088 g/l at Weyburn. From this hydraulic head field, a new W to E fluid flow direction trend was estimated.
- Secondly, the inversion tool of the fluid flow simulator MARTHE (Thiéry, 1990) was used for retrieving streamline patterns for the regional fluid flow. Taking into account the density variability of the fluid, MARTHE can resolve a 2D fluid flow model able to reproduce, with calculated quality criteria, the measured environmental hydraulic head field by calibrating a permeability field.

A comparison between these analytical and numerical methods gave the same result, i.e. a W–E trend of the regional fluid flow within the Mississippian aquifer. The numerical model was then used for determining the streamline set leaving the Weyburn oilfield area (Figure 6). The model effectively illustrates how the salinity gradient acts as barrier for fluid flow and how streamlines are re-oriented in order to avoid the high salinity gradient present in the aquifer. Assuming pure advective transport of dissolved CO<sub>2</sub>, this modelling shows that natural aquifer flow is capable of transporting dissolved CO<sub>2</sub> approximately 25 km away from the Weyburn oilfield towards the E–NE in 100 000 years; this equates to approximately 0.2 m/year (Audigane and Le Nindre, 2004).

Geochemical modelling with SCALE2000 (Azaroual et al., 2004) and PHREEQC (Parkhurst and Appelo, 1999) has indicated the main in situ baseline chemical characteristics of the fluids in the Mississippian reservoir at the Weyburn oilfield. It has also enabled a reliable assessment of CO<sub>2</sub> solubility in Weyburn brines. In the reservoir, dissolved organic acid anions do not have a significant effect on the alkalinity, or the pH-buffering capacity. By contrast, sulphide (HS<sup>-</sup>) concentrations may represent more than 60% of the total alkalinity. Redox disequilibrium is present in the Mississippian aquifer waters at the Weyburn oilfield. Anthropogenic contributions due to oil production and enhanced recovery has amplified this tendency. Furthermore, the Mississippian waters are largely in thermodynamic equilibrium with respect to anhydrite, barite, calcite, dolomite and a silica phase with a thermodynamic stability between that of chalcedony and quartz. Dissolved aluminium concentrations could be due to one of several mineral phases encountered in oil-bearing sedimentary basins, i.e., illite, K-feldspar, kaolinite or montmorillonite. It has proved difficult to demonstrate possible control of sulphide concentrations by a precise mineral reaction. Thermodynamic calculations including fugacity and activity corrections for non-ideality show that no more than 1 mole of CO<sub>2</sub> can dissolve in 1 kg of water for typical Weyburn reservoir brines with a salinity range from 35 to 110 g/l at 50°C and 14 MPa (Figure 7). The steep salinity gradient in the Weyburn oilfield area will greatly affect CO<sub>2</sub> solubility, migration and reactivity.

For an initial regional approach at the scale of a 240 x 230 km<sup>2</sup> block, and based on the data available at the start of the Weyburn project, this baseline hydrogeological and hydrochemical characterisation was performed at the entire Mississippian aquifer level. More refined studies at the scale of the 10 km buffer zone around the injection patterns would need to consider a multilayer aquifer system. The Midale Beds reservoir unit and the underlying and overlying strata should be studied in terms of characteristics such as permeability, pressure, salinity and thickness.

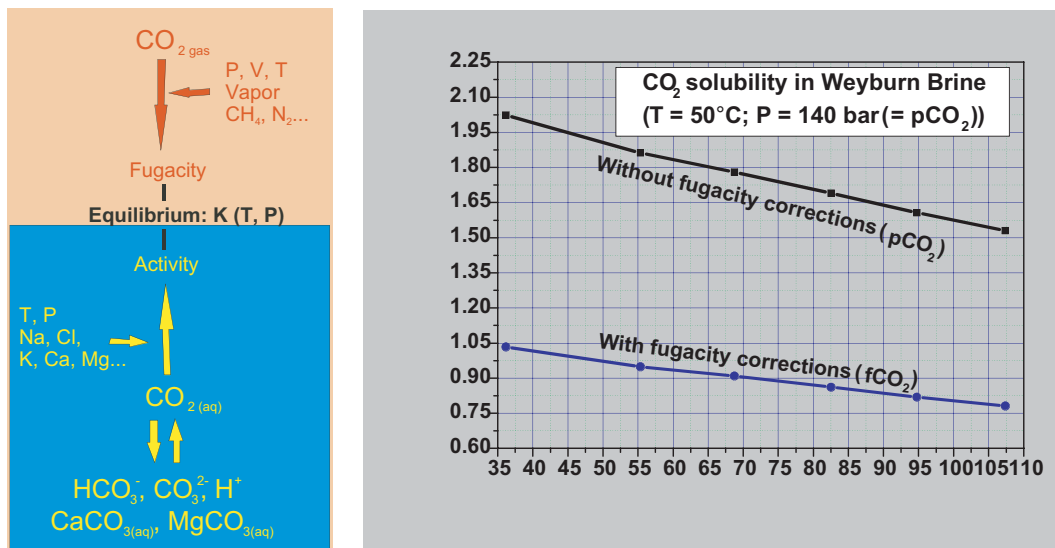


**Figure 7** Gas-brine equilibrium system and CO<sub>2</sub> solubility versus total dissolved solids in Weyburn oilfield brines.

## 2.4 ANALYSIS OF RESERVOIR FLUIDS AND DISSOLVED GASES

(Fedora Quattrocchi, Roberto Bencini, Barbara Cantucci, Daniele Cinti, Domenico Granieri, Luca Pizzino and Nunzia Voltattorni)

### 2.4.1 Introduction

During and after CO<sub>2</sub> injection operations, the presence of supercritical CO<sub>2</sub> will result in chemical disequilibria and the initiation of various reactions. It is important to understand the direction, rate and magnitude of such reactions, both in terms of their impact upon the ability of the Midale Beds and the overlying lithological units to safely contain the injected CO<sub>2</sub>, and in terms of the longevity of CO<sub>2</sub> containment.

A three-pronged approach has been used to study the impact of CO<sub>2</sub> upon reservoir geochemistry:

- Monitoring changes in actual reservoir fluids from deep boreholes at Weyburn.

- Laboratory experiments to simulate in situ conditions within the reservoir.
- Predictive modelling of evolving conditions within the reservoir.

The above approaches are complementary, and by combining and assimilating all their results, it is possible to obtain a coherent assessment of the geochemical evolution at the Weyburn oilfield.

The following subsections provide a summary of results from the monitoring of the reservoir fluids. These are important because they give direct evidence for geochemical changes at a reservoir scale. Information about the experiments and predictive modelling is described in section 2.5.

### 2.4.2 Approach and methodology

A joint study by INGV and the University of Calgary, Canada sampled waters from the Weyburn oilfield, in order to analyse for dissolved gases, minor elements, strontium isotope ratios and trace metals (Table 2).

**Table 2** Details of borehole fluid monitoring surveys conducted at the Weyburn oilfield. All the surveys involved the University of Calgary and the Alberta Research Council. Fluids from some of these surveys were provided to INGV for subsequent laboratory analysis. Other fluids were collected by INGV in collaboration with the University of Calgary.

Survey	Dissolved gases	Chemical analyses (major, minor and trace elements)	<sup>87</sup> Sr/ <sup>86</sup> Sr ratio
Baseline (B0), August 2000	NO	NO	Partially
Monitor 1 (M1), March 2001	YES	YES	YES
Monitor 2 (M2), July 2001	NO	NO	NO
Monitor 3 (M3), September 2001	NO	NO	NO
Monitor 4 (M4), March 2002	NO	NO	NO
Monitor 5 (M5), June 2002	YES	YES	YES
Monitor 6 (M6), September 2002	NO	NO	NO
Monitor 7 (M7), April 2003	NO	NO	YES
Monitor 8 (M8), June 2003	YES	NO	NO
Monitor 9 (M9), September 2003	YES	YES	YES
Monitor 10 (M10), March 2004	YES	YES	YES

The sampled fluids were analysed for the following:

- Major elements/ions using standard procedures of *Dionex*<sup>TM</sup> liquid chromatography. Calcium, chlorine, magnesium, potassium, sodium and SO<sub>4</sub> were analysed.
- Minor and trace elements using *ELAN*<sup>TM</sup> 6000 ICP-Plasma. Aluminium, arsenic, barium, beryllium, boron, bromine, cadmium, caesium, chromium, copper, iron, lead, manganese, nickel, rubidium, silicon, silver, strontium and zinc were analysed.
- Alkalinity data, measured in the field by titration, were provided by the University of Calgary to complete the anionic-cationic balances.

Dissolved gases (i.e. carbon monoxide, CO<sub>2</sub>, helium, hydrogen, hydrogen sulphide, methane, neon, nitrogen and oxygen) were analysed by gas chromatography. They were extracted by creating a temporary vacuum in the head-space above a fluid sample, and allowing the gases to accumulate (Capasso and Inguaggiato, 1998; Quattrocchi, 1999; Quattrocchi et al., 1999, 2000; Salvi et al., 2000). This methodology for analysing dissolved gases was based on equilibrium partitioning of gases between the liquid and gas phases. It was possible to derive the initial concentrations of the dissolved gases in the liquid phase from concentrations in the gas phase, by using partitioning coefficients for the different species. For the same well fluids, an isotope of radon, <sup>222</sup>Rn, was analysed by gamma spectrometry (Quattrocchi et al., 1999) within four days of sampling. However, this was only measured in the M1 survey because it was found to occur in extremely low concentrations, well below the detection limit of 0.5 Bq/L. Conversely, the <sup>222</sup>Rn content in shallow groundwater, up to 100 m depth, was found to range up to 5 Bq/L in the Hal Bakusko shallow well.

The strontium isotope (<sup>87</sup>Sr/<sup>86</sup>Sr) ratios were measured by adding 100 ml of sample to 50 mg of sodium carbonate (Na<sub>2</sub>CO<sub>3</sub>) to transform barium and strontium sulphates (BaSO<sub>4</sub> and SrSO<sub>4</sub> respectively) to carbonates. The final product of this reaction was filtered and washed to eliminate sulphate ions. The carbonates were then dissolved with 2.5 N hydrochloric acid (HCl) and the resulting solution completely evaporated. The resulting solid was again dissolved with 2.5 N hydrochloric acid, and the strontium separated from the other elements by cationic exchange using DOWEX resin. The strontium was then placed onto a tantalum filament as strontium nitrate (Sr(NO<sub>3</sub>)<sub>2</sub>) and the <sup>87</sup>Sr/<sup>86</sup>Sr ratio measured by a VG 54E mass spectrometer. The <sup>87</sup>Sr/<sup>86</sup>Sr values were normalised to the standard ratio of 0.1194. The uncertainty in the analytical measurements was expressed as twice the standard deviation, i.e. ± 0.00002.

## 2.4.3 Dissolved gases and trace metals

### 2.4.3.1 DISSOLVED GASES

The free gas phase was sampled at the wellhead and immediately analysed by the University of Calgary using gas chromatography. This free gas composition at the surface (FGPS), is the residual composition of the dissolved gas composition at the surface (DGCS). The DGCS is derived from the real dissolved gas composition at depth (DGCD), before the degassing in the wells. Hence the unknown DGCD will have a closer similarity to the DGCS than the FGPS, at least in terms of relative gas abundances.

The CO<sub>2</sub> partial pressure at depth (i.e. CO<sub>2(DGCD)</sub>) is a key parameter affecting the in situ pH. In oilfield brines,

this is normally different from the pH measured at surface. This is the most important parameter for modelling the geochemistry of the Weyburn system, over both the short and long timescales. To date, the actual CO<sub>2</sub> partial pressure in the Weyburn reservoir (CO<sub>2(DGCD)</sub>) has not been available to researchers. However, it is likely that the dissolved gas method employed in this study provides some of the closest measurements to the actual in situ values. This, coupled with the pH values measured by the University of Calgary, provides directly measured data that can be useful for modelling geochemistry at Weyburn as they allow hypotheses to be built about ongoing water-rock interactions.

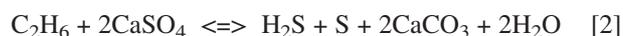
The key results indicated by the dissolved gas data are:

- Dissolved CO<sub>2</sub> generally increased from the M5 to M10 surveys (June 2002 to March 2004). This varied from 0–30 cc/L (at STP) in 2002, to 1–270 cc/L in 2003, to 20–470 cc/L in 2004. The maximum values were 0.028, 0.40 and 0.80 moles/L respectively, assuming a 16.5 MPa reservoir pressure (Figures 8, 9 and 10).
- The CO<sub>2</sub> anomaly became wider in 2003; at this time it was no longer centered on a single well, but evenly spread throughout the entire Phase 1A CO<sub>2</sub> injection area that was investigated.
- Dissolved methane increased from the M1 to M10 surveys (March 2001 to March 2004), varying from 0–0.35 cc/L (Figures 9, 10 and 11).

Dissolved helium and hydrogen decreased in the 2003 and 2004 surveys, after an initial increase in the injection area in 2002. This is probably due to the release of trapped helium and hydrogen from rocks during the initial reaction with the injected CO<sub>2</sub> (Figures 9 and 10).

The range of dissolved hydrogen sulphide compositions shows a similar pattern of increase between the M1 and M10 surveys (March 2001 to March 2004). It varies from 0–3.5% to 0–5% (Figure 12). The hydrogen sulphide anomaly shifted southwards between the 2002 and 2003 surveys, and was slightly enlarged in 2003 throughout the entire Phase 1A injection area.

Methane and other light hydrocarbons could react during thermochemical sulphate reduction reactions such as:



However, these are thought to be negligible due to the relatively low reservoir temperature.

The sampling and analytical methods used in this phase of the project were used to give a preliminary indication of broad changes in dissolved gases. One remaining uncertainty is the precise behaviour of the fluids immediately before and during sampling. As the fluids rise up the borehole and are sampled, they will degas as they drop from the reservoir pressure of 16.5 MPa pressure to atmospheric pressure, 0.1 MPa. This can occur in different ways; for example, degassing could occur progressively during ascent. Here, the degassing/stripping factor could be calculated for each dissolved gas species on the basis of the Henry's law, i.e. knowing the pumping rate and the stripping effects. However, information from the operator suggests that the pressure drop may occur at the surface only, and not inside the pipeline, i.e. at the fluid sampling valve at the wellhead. In this case, the stripping effects during sampling at atmospheric pressure would be constant for each of the surveys because it took a similar time to fill the large volume plastic sample bottles. After the initial sampling, the dissolved gas

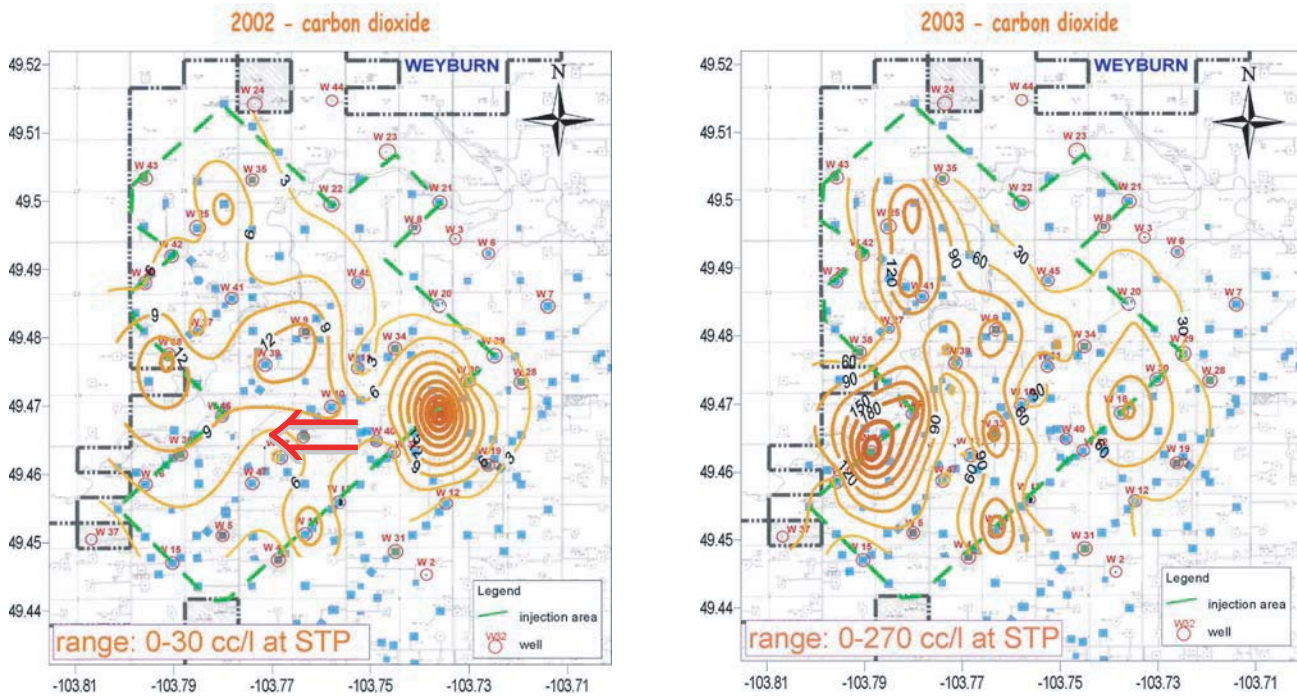


**Figure 8** Contour maps illustrating dissolved CO<sub>2</sub> contents, sampled at the surface (i.e. CO<sub>2(DGCS)</sub>), between the M5 and M8 surveys. There are large differences between the 2002 and 2003 data, strongly suggesting similar large differences in the dissolved CO<sub>2</sub> contents at depth (i.e. CO<sub>2(DGCD)</sub>) and in situ pH.

could not escape from solution because they were rapidly transferred to glass 250–500 cm<sup>3</sup> vials. The degassing/stripping of the gas phase from the water phase is not an instantaneous process. As an approximation, it was estimated that 20–30% of the total dissolved gases were exsolved during depressurisation to atmospheric conditions, although an exact value for this has not been determined. Future sampling procedures could be improved by the use of high-pressure steel isokinetic sample vessels, coupled to a miniseparator. The high-pressure steel isokinetic sample vessels would reduce uncertainties and are currently under development.

#### 2.4.3.2 TRACE METALS

Over the M1 to M5 monitoring period (March 2001 to June 2002), there was a general increase in concentrations of aluminium, barium, beryllium, chromium and iron. However, there was a general decrease in arsenic, copper, nickel and zinc. The processes controlling these changes have not been determined. However, factors that are likely to be involved include; metal complexation, the presence and evolution of hydrogen sulphide, precipitation of sulphides, and the role of geochemical barriers.

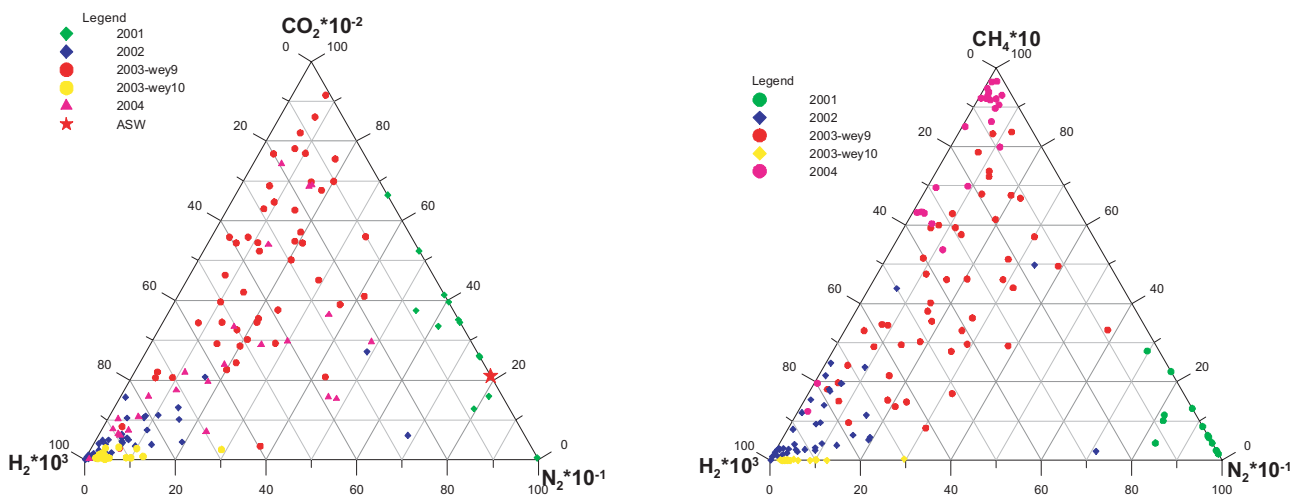


**Figure 9** Ternary plots of dissolved CO<sub>2</sub>-nitrogen-hydrogen and methane-nitrogen-hydrogen contents for the 2001 to 2004 surveys.

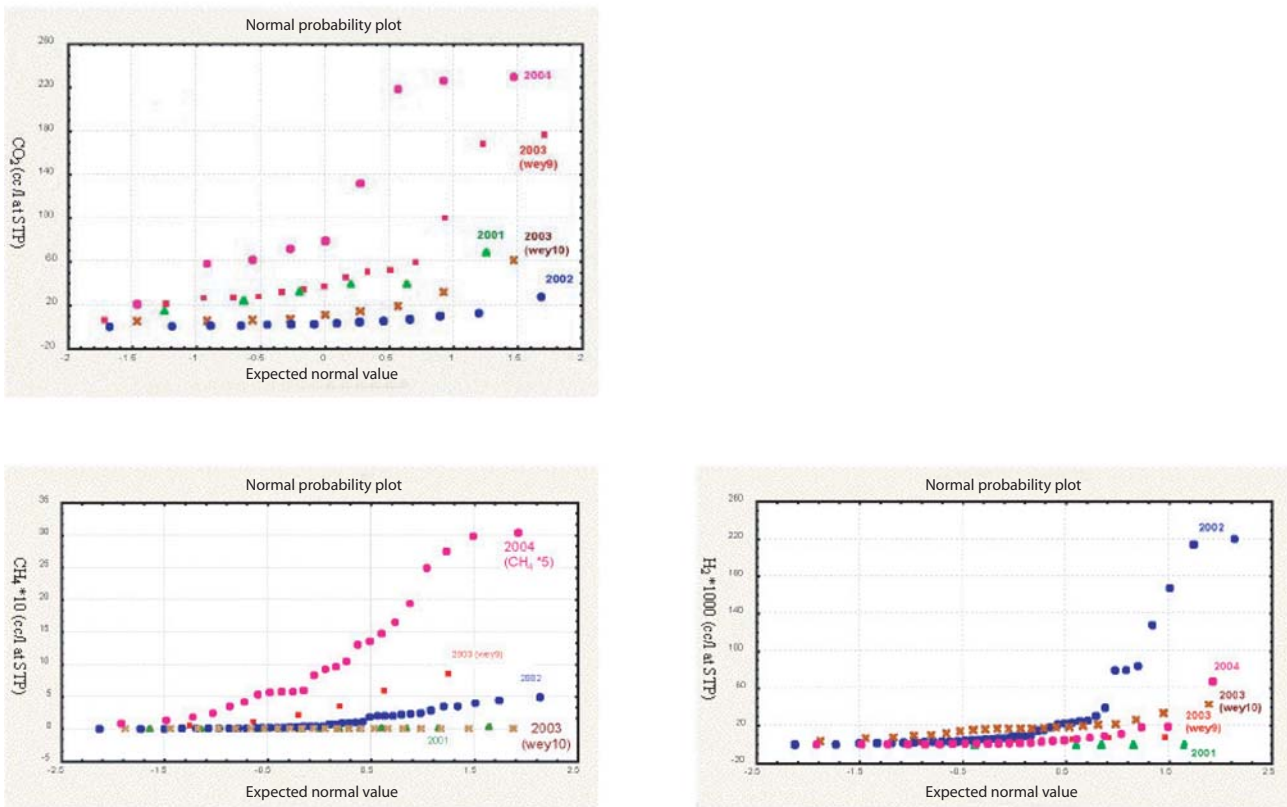


**Figure 10** Normal probability plots of dissolved CO<sub>2</sub> (top), dissolved methane (lower left) and dissolved hydrogen (lower right).

According to the basinal brine theory of Kharaka et al. (1987), high dissolved metal concentrations in the presence of aqueous sulphide species require acid solutions with pH values lower than those generally obtained in basinal brines (Anderson, 1983). Injection of large quantities of CO<sub>2</sub> can generate such acid solutions, and so this might facilitate high dissolved metal concentrations. Conversely however, the presence of hydrogen sulphide can also lead to the precipitation of metal sulphides such as sphalerite (ZnS) from solution. This may explain the decrease in zinc concentration from 2002 to 2003. Sulphide formation would consume some dissolved hydrogen sulphide, and lead to its transfer from the gaseous phase to the water phase (Kharaka et al., 1987). This process could continue until virtually all the available metals are precipitated as sulphides. The dissolved hydrogen sulphide (H<sub>2</sub>S<sub>(DGCS)</sub>) and the free gas phase hydrogen sulphide (H<sub>2</sub>S<sub>(FGCS)</sub>), should be measured in order to understand their relationship to trace metal concentrations and to possibly calculate the H<sub>2</sub>S<sub>(DGCD)</sub>, and combine this with data on the trace metals content.

#### 2.4.4 Strontium isotope ratios (<sup>87</sup>Sr/<sup>86</sup>Sr)

Strontium isotope ratios for produced fluids from the Midale Beds vary between 0.7077 and 0.7082 (Table 3). These are consistent with published values for Mississippian fluids and carbonate minerals, which are approximately 0.7076 to 0.7082 (Figure 13; Bruckschen et al., 1995).

The Mannville aquifer has been used as a source of water for the water-flooding of the Weyburn oilfield since 1959. It is a Cretaceous sandstone, with <sup>87</sup>Sr/<sup>86</sup>Sr values ranging between 0.7072 and 0.7073 (Jones et al., 1994). A small component of the water recycled during oil production is

derived from the Mannville aquifer, and this is re-injected back into the Midale Beds via a water-alternating-gas (WAG) enhanced oil recovery technique. Strontium isotopes were first analysed for this study in 2001, approximately 40 years after the start of water flooding operations. Despite this relatively long period of time, the strontium isotope ratios of the produced waters were closer to those of the Mississippian Midale Beds reservoir, although some of the strontium isotope ratios could be related to the injected Mannville aquifer component. The lowest strontium isotope ratios recorded may therefore represent higher levels of mixing of the Midale Beds fluids by re-injected Mannville aquifer make-up water, i.e. the highest injection volumes. The average strontium ratios and mass balance calculations suggest that as much as 25% of the produced fluids in 2001 were derived from the Mannville aquifer, although this appears to have decreased to 15% in 2003. It is significant that there is no known natural mixing between the Mississippian and Mannville aquifers, because they are separated by a large aquitard (Figure 13).

The positive trend in the strontium isotope ratios from 2001 to 2003 may be due to either:

- Dissolution of the Midale Beds reservoir rocks, because leaching of strontium from these Mississippian carbonates would drive the strontium composition of the produced waters to heavier values, thereby masking the Mannville aquifer contribution.
- A smaller Mannville aquifer component in the water flood over the last three years. However, this study found no evidence that the operators of the oilfield significantly reduced the injection of Mannville aquifer fluids into the Midale Beds oil reservoir.

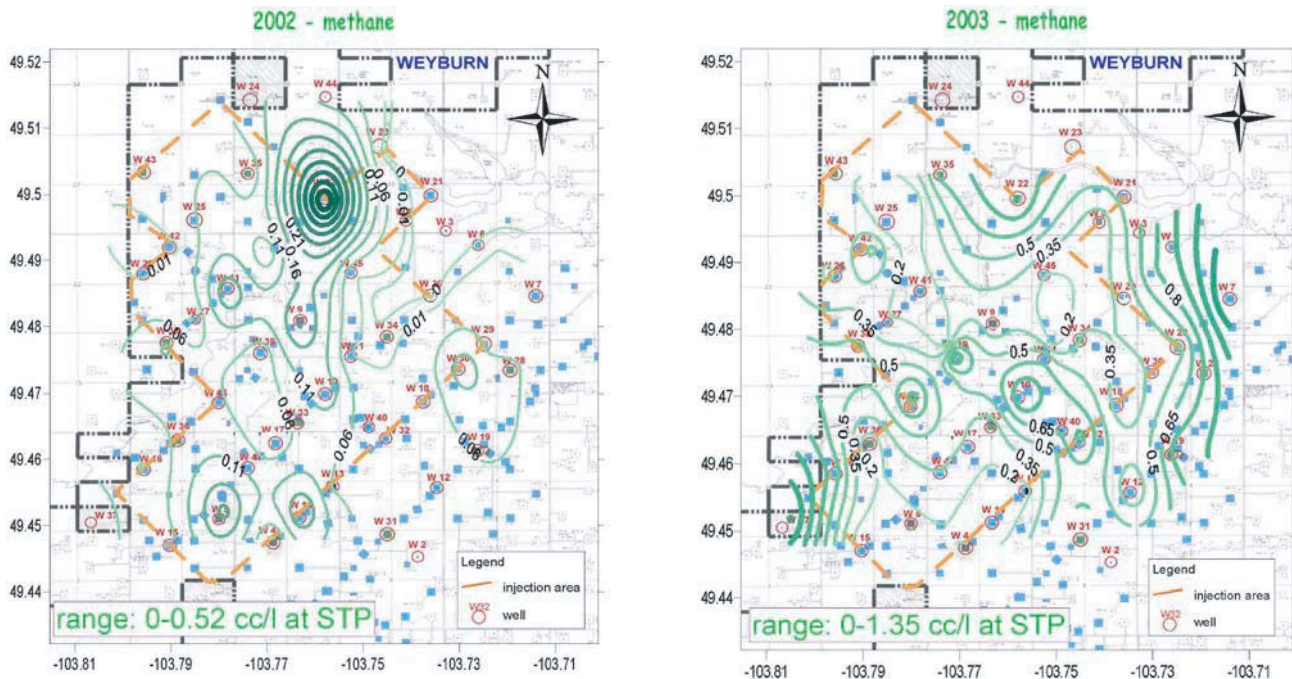


**Figure 11** Contour maps showing dissolved methane, sampled at the surface between the M5 and M8 surveys.

If the leaching of the Midale Beds oil reservoir increased, for example triggered by CO<sub>2</sub> injection, a progressive approach toward the pre-water-flooding strontium isotope baseline values may be expected. This would act to reverse the isotopic impact of 40 years of water-flooding, which has resulted in the oilfield fluids being contaminated by up to 25% Mannville aquifer fluids. This appears to be happening in the oilfield, as an apparent progressive decrease in Mannville aquifer contamination was observed from 2001 to 2003. Therefore, the progressive approach of the <sup>87</sup>Sr/<sup>86</sup>Sr values to the Midale Beds reservoir values points to zones of carbonate dissolution as a direct result of CO<sub>2</sub> injection.

The changes in the strontium isotope ratios can be used to monitor the injection of Mannville aquifer make-up water. They may also monitor the injection of CO<sub>2</sub>, causing carbonate dissolution via more recent increases in the strontium isotope ratio. The strontium isotope ratios between 2001 and 2003 measured on monitoring campaigns M1, M5 and M8 are illustrated in Figure 14.

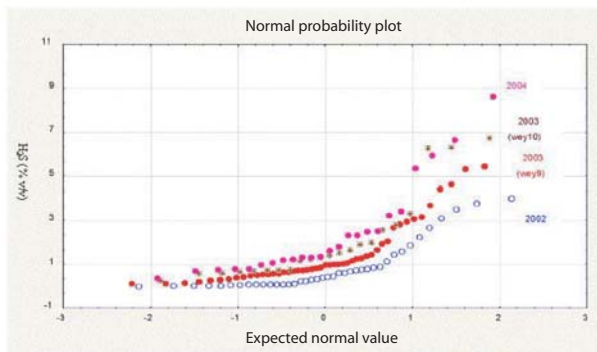


**Figure 12** Normal probability plot of dissolved hydrogen sulphide in the different surveys expressed as percentage of dissolved gas.

The hypothesis of carbonate dissolution caused by CO<sub>2</sub> injection is supported by other chemical data, as well as δ<sup>13</sup>C data, for produced bicarbonate and CO<sub>2</sub> analysed by the University of Calgary. For example, the injected CO<sub>2</sub> initially had a distinctive δ<sup>13</sup>C signature of -35‰. However, since 2002, CO<sub>2</sub> recycling and re-injection had changed this signature to between -20 to -25‰. It is hoped that future chemical and isotopic monitoring will be able to further monitor the evolution of this complex multi-phase and multi-component system.

## 2.5 HYDROCHEMICAL MODELLING AND GEO-CHEMICAL REACTIONS

*(Christopher A Rochelle, Mohamed Azaroual, Keith Bateman, David J Birchall, Isabelle Czernichowski-Lauriol, Dan Olsen, Niels Stenoft, Niels Springer and Pierre Durst)*

### 2.5.1 Introduction

During and after CO<sub>2</sub> injection operations, the presence of supercritical CO<sub>2</sub> will result in chemical disequilibria and the initiation of various reactions. Some of these will be important in helping CO<sub>2</sub> to dissolve into the formation water (i.e. 'solubility trapping'). Other reactions will facilitate its precipitation as carbonate phases, i.e. 'mineral trapping', Bachu et al. (1994). Both these trapping mechanisms will reduce the potential of buoyancy-driven fluid flow and aid the long-term containment of CO<sub>2</sub>.

A three-pronged approach has been used to study the impact of CO<sub>2</sub> upon reservoir geochemistry:

- Monitoring changes in actual reservoir fluids from deep boreholes at Weyburn (see section 2.4)
- Laboratory experiments to simulate in situ conditions within the reservoir. These are important in that they

**Table 3** Statistical summary of the 2001–2003 strontium isotope ratios. The data were normalised to the Mississippian value of 0.7082 and expressed as  $\delta\%$ . Note the shift toward the Mississippian aquifer/host rock component from 2001 (M1) to 2003 (M8). For reference, the  $^{87}\text{Sr}/^{86}\text{Sr}$  isotopic ratio of the Mannville aquifer is 0.7073, and that of the Mississippian aquifer is 0.7082 (see Figure 13)

Sampling trip	$^{87}\text{Sr}/^{86}\text{Sr}$			Equivalent Manville component	Sampling trip	$\delta\text{ }^{87}\text{Sr}$		
	Min.	Max.	Mean			Min.	Max.	Mean
M1	0.70775	0.70825	0.70798	25%	M1	-0.63	0.08	-0.31
M5	0.70800	0.70818	0.70804	—	M5	-0.28	-0.03	-0.23
M8	0.70797	0.70818	0.70807	15%	M8	-0.32	-0.03	-0.19

can provide the detailed, well-constrained quantitative information identified in the point above. They have a limitation in that they cannot replicate the temporal or spatial scales of an actual injection operation.

- Predictive modelling of evolving conditions within the reservoir. This uses data from the previous two approaches to improve, constrain, and build confidence in the geochemical models of the shorter-term evolution of the Weyburn reservoir system. These can then be extended to predict the impacts of  $\text{CO}_2$  in the longer-term, after injection operations have ceased.

The above approaches are complementary, and by combining and assimilating all their results, it is possible to obtain a coherent assessment of the geochemical evolution at the Weyburn oilfield.

The following sections provide a summary of results from the experiments and modelling. The monitoring of reservoir fluids was described in section 2.4.

### 2.5.2 Experiments

A series of laboratory experiments has been undertaken where samples of well-characterised borehole material from the Midale Beds were reacted with both  $\text{CO}_2$  and synthetic reservoir formation waters under simulated in situ conditions. The aims of this work were as follows:

- to identify and characterise fluid-mineral reactions caused by the presence of  $\text{CO}_2$
- to determine how these reactions might impact the petrophysical properties of the reservoir rocks, especially porosity/permeability
- to provide well-defined ‘benchmarks’ which could be used as test cases for comparison with predictions from geochemical computer models

Addressing the above aims was achieved via two experimental approaches:

$^{87}\text{Sr}/^{86}\text{Sr}$	System	Hydrostratigraphy	
	Quaternary	Upper Aquifer System	
	Tertiary	(1.4 <TDS < 46 g/l)	
	Cretaceous	Cretaceous Aquitard System	
		Viking Aquifer (< 36 g/l)	
		Joli Fou Aquitard	
0.7073	140 Ma	Mannville Aquifer System (< 80 g/l)	
0.7072	Jurassic 200 Ma	Jurassic Aquifer (4–250 g/l)	
	Triassic	Mississippian Jurassic Aquitard System	
	Permian		
	Pennsylvanian		
0.7082	330 Ma	Mississippiian Aquifer System (<310 g/l; Weyburn: 40–120 g/l)	
0.7076	350 Ma	Bakken Aquitard	
	Devonian	Devonian Aquifer System (< 300 g/l)	
		Prairie Aquiclude	
		Winnipegosis Aquifer (40–330 g/l)	
	Silurian	Silurian Devonian Aquitard	
	Ordovician	Basal Aquifer System (TDS ~ 335 g/l)	
	Cambrian		
	Precambrian		Basement

**Figure 13** Hydrostratigraphical delineation and nomenclature for the Williston Basin (modified from Bachu and Hichon, 1996). The arrow (I) indicates that water from the Mannville Aquifer System is used for water flooding. The symbols (?) are added to indicate the possibility of using shallower aquifers for water flooding. The arrow (II) inside the Mississippiian Aquifer System is to indicate that water used for flooding is continuously being re-injected.

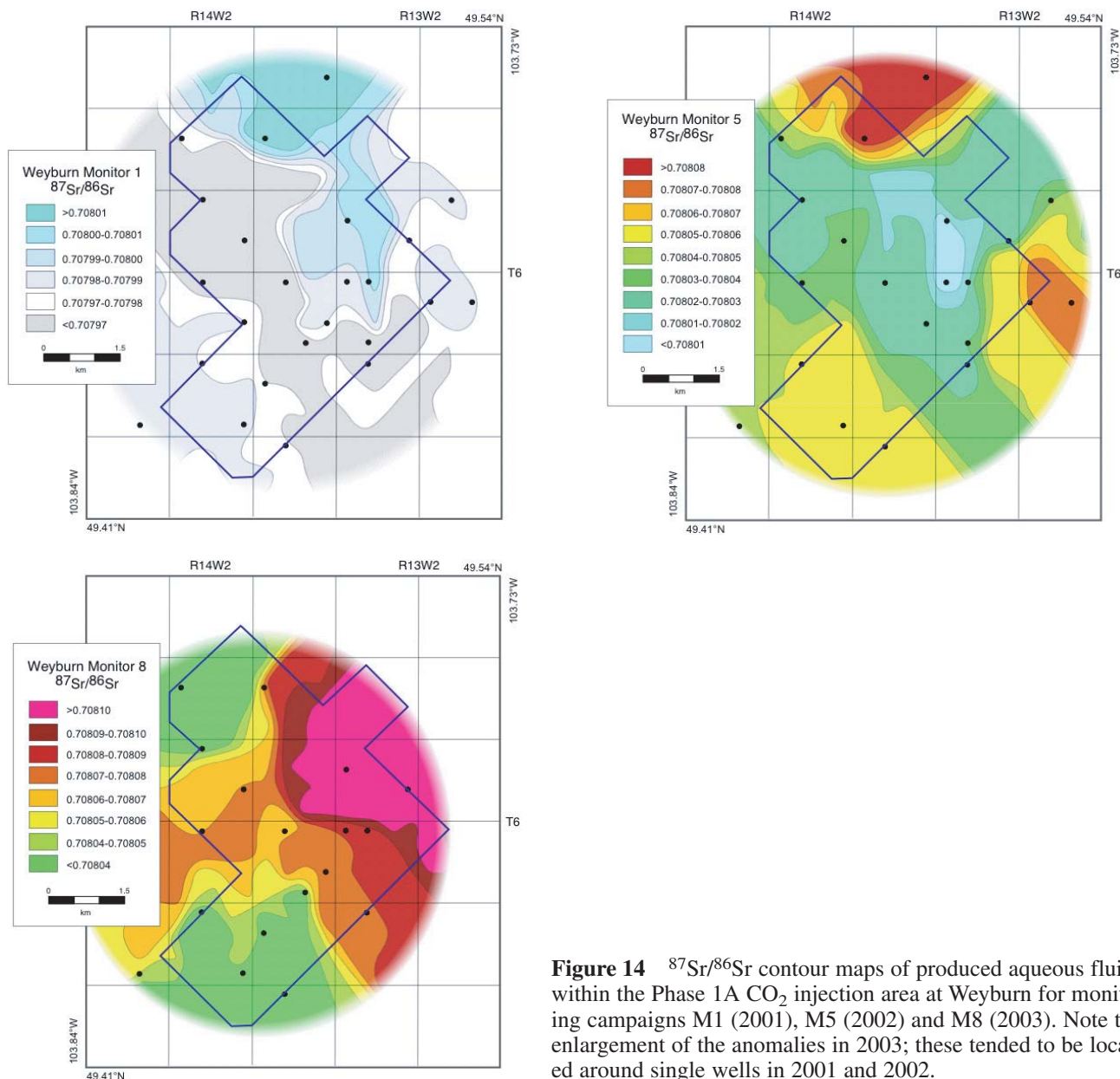


**Figure 14**  $^{87}\text{Sr}/^{86}\text{Sr}$  contour maps of produced aqueous fluids within the Phase 1A  $\text{CO}_2$  injection area at Weyburn for monitoring campaigns M1 (2001), M5 (2002) and M8 (2003). Note the enlargement of the anomalies in 2003; these tended to be located around single wells in 2001 and 2002.

- **Static batch experiments.** These used fixed quantities of rock, brine and  $\text{CO}_2$  that were allowed to react for a prolonged period of time. This approach facilitates the development of steady-state conditions towards a point where the fluid composition becomes unchanging, and where the rates of dissolution/precipitation reactions fall towards zero. Further details were given by Rochelle, Bateman and Birchall (2002).
- **Flow experiments.** These continually pass fresh  $\text{CO}_2$ -rich formation water through the rock samples. This approach tends to maintain 'far from equilibrium' conditions, and so tends to maximise the degree of rock dissolution.

These different approaches allow simulation of different parts of the storage system at Weyburn. For example, conditions of relatively high fluid flow will exist close to the wells. Conversely, further from them, groundwater flow will be controlled by regional-scale flow regimes, which are likely to be slow or near static.

It was decided to maximise the amounts of  $\text{CO}_2$  available for reaction, by making the synthetic formation waters  $\text{CO}_2$ -saturated. This was done in part to facilitate the observation

of geochemical changes, and in part because it was easier to maintain experimentally. However, it also ensured that the study considered a maximum reaction limiting case. It is recognised though, that variable degrees of  $\text{CO}_2$  saturation will exist in the Weyburn reservoir itself.

#### 2.5.2.1 REACTIONS OF THE MIDALE MARLY UNIT RESERVOIR ROCK

The Midale Marly Unit is the target horizon for  $\text{CO}_2$  injection because it still retains most of its original oil. As a consequence,  $\text{CO}_2$  concentrations, and rates of fluid movement, will be greatest within this unit. The experimental programme attempted to reflect this, by conducting flow experiments in addition to static experiments.

##### *Static batch experiments*

Approximately 30 batch experiments were completed using samples of the Midale Marly Unit material from the Weyburn oilfield (Rochelle, Birchall and Bateman, 2002; Rochelle et al., 2003a; Rochelle et al., 2004). The experiments were conducted at conditions representative of the

reservoir (60°C, 150–160 bar), or close to injection wells (60°C, 250 bar), and ran for time periods of over five months. A range of grain sizes of Midale Marly Unit samples were used (<250 µm, 250–500 µm, and small monoliths) and fluid:rock ratios were typically 10:1 or less. The Midale Marly Unit samples were reacted with synthetic formation water of realistic composition, and the experiments pressurised with either CO<sub>2</sub> ('reactive' experiments) or nitrogen (non-reacting 'baseline' experiments).

The evolution over time of a range of solutes was followed. Relative to the nitrogen 'baseline' experiments, it was found that the impact of CO<sub>2</sub> was to:

- increase the concentrations of calcium, HCO<sub>3</sub><sup>-</sup> and silicon (e.g. Figure 15)
- decrease the pH and concentration of strontium
- have little impact on the concentrations of aluminium, magnesium, manganese, and total sulphur (e.g. Figure 16).

Many of the solutes, most notably calcium, reached steady-state conditions within about one month, indicating relatively rapid control by calcite dissolution. Although aluminosilicate minerals make up a small proportion of the rock, dissolution/precipitation reactions appeared to be occurring significantly more slowly. Silicon concentrations did not reach steady-state conditions, even after five months reaction.

The above observations of fluid chemistry were mirrored by close observations of the solid reaction products, which showed no significant differences in the degree of dissolution. This applied to comparisons between the nitrogen and CO<sub>2</sub> experiments, and between the monoliths and the 250–500 µm crushed samples. No secondary precipitates were observed.

#### Core flooding experiments

Three CO<sub>2</sub> flooding experiments were completed on dolomitic carbonate samples from the Midale Marly Unit (Olsen and Stenoft, 2004). The experiments were conducted at conditions representative of the reservoir. These were: 59°C; 160 bar fluid pressure; and 100 bar net hydrostatic pressure. This is equivalent to burial at approximately

1400 m. All samples were approximately 2.5 cm diameter plugs with a length of around 7 cm. Two of the experiments were normal flooding experiments lasting 21 and 37 days, with fluid velocities of respectively 29 cm/day and 16 cm/day. The third experiment was a 'fracture' flow experiment lasting 35 days. The fluids used were synthetic formation brines prepared from fluid analyses of actual well fluids, with the addition of sufficient CO<sub>2</sub> to fully saturate the fluids (0.9 mol l<sup>-1</sup>; Chang et al., 1998).

The CO<sub>2</sub> flooding experiments caused the porosity in the samples to increase by 0.5–1.9 porosity units, and grain density to increase by 0.002–0.027 g/cm<sup>3</sup>. Matrix gas permeability increased by 8–19%. During one of the experiments (GEUS 1) the liquid permeability increased initially, remained stable for a long period, and finally reduced significantly. This response is interpreted as resulting from initial permeability enhancement by dissolution, followed by progressive plugging by migrating fines. When the sample was removed from the core holder after the experiment, abundant fine material was found to be present at the fluid inlet end of the core.

All three samples underwent significant corrosion during the experiments, and this was concentrated within 3 mm of where the CO<sub>2</sub>-saturated brine entered the samples (Figure 17). More scattered evidence of corrosion was found further inside the samples. Two of the samples had significant calcite contents, and widespread evidence of calcite corrosion was found. In sample GEUS 1, the calcite was present mainly in small irregular peloids, while much of the calcite of sample GEUS 14 was present in fossil fragments. Calcite in both the peloids (Figure 18) and the fossil fragments was strongly corroded. Dolomite, being the principal mineral in all three samples, showed more restricted evidence of corrosion. However, characteristic hollowed-out grains were widespread, particularly in sample GEUS 2 that did not contain calcite (Figure 19). Where present, anhydrite and gypsum (Figure 18) usually showed evidence of corrosion, while alkali feldspar, celestine, fluorite, pyrite and quartz did not. Evidence for the precipitation of minerals, especially gypsum, was sought, but not found. That corrosion was concentrated towards the inlet ends of all three samples indicated that reaction rates for the main chemical reactions were fast relative to fluid velocities (16 to 29 cm/day), sample length (6.9 to 7.3 cm), and experiment duration (21 to 37 days).

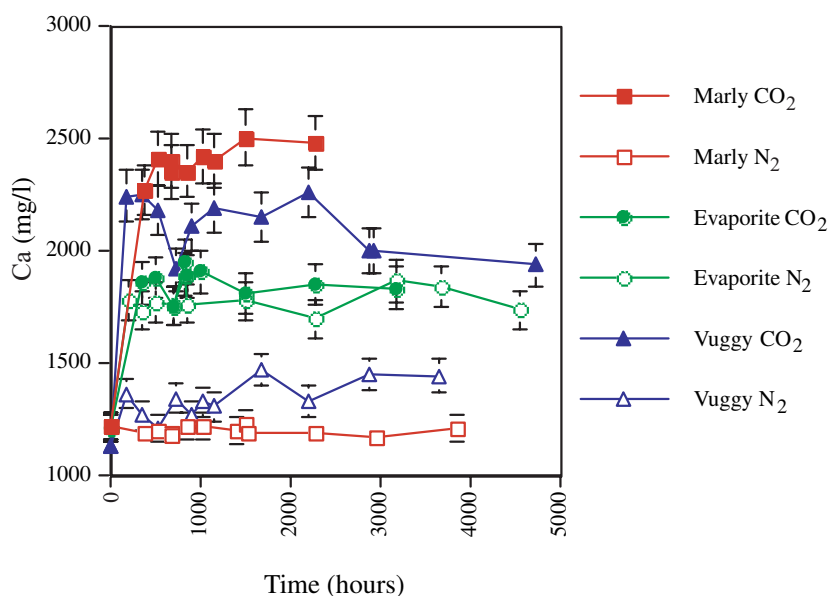


**Figure 15** Evolution of calcium concentrations within the static batch experiments on Midale Beds material. Note the enhanced calcium concentrations in the presence of CO<sub>2</sub>-rich fluids in the Marly and Vuggy Unit experiments.

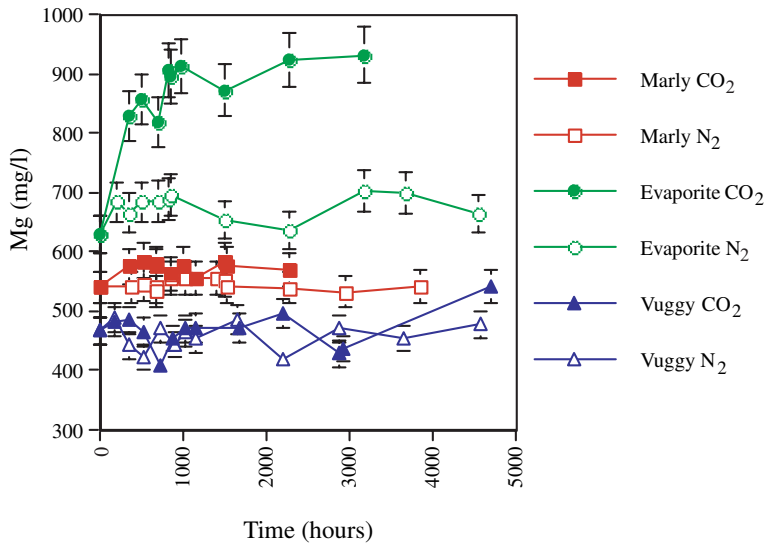


**Figure 16** Evolution of magnesium concentrations within experiments using samples of Midale Beds material. Note the enhanced magnesium concentrations in the presence of CO<sub>2</sub>-rich fluids in the Midale Evaporite experiments only.

A total of 49 fluid samples were extracted for analysis during the core flooding experiments. In terms of reacted fluid chemistry, elemental compositions changed by variable degrees, from none to significant change. For example, Figure 20 shows the results for dissolved calcium and magnesium, which are two of the elements showing significant increases as the fluid passed through the rock samples. The fluid chemical analyses gave the following results:

- Calcium, HCO<sub>3</sub><sup>-</sup>, magnesium, manganese, pH, strontium and total iron show clear evidence of chemical reactions.
- Chloride, potassium, sodium, SO<sub>4</sub><sup>2-</sup> and total sulphur do not show evidence of chemical reactions.
- HCO<sub>3</sub><sup>-</sup>, magnesium, manganese and strontium show time-dependent trends that indicate varying reaction rates.



**Figure 17** The inlet end of sample GEUS 1 (Midale Marly Unit, M1 zone), before the CO<sub>2</sub> flooding experiment (top left), and after the experiment (top right and bottom right). Numerous small pits are present in the sample surface after the experiment. They represent dissolved calcite grains (peloids). The sample diameter is 2.48 cm.

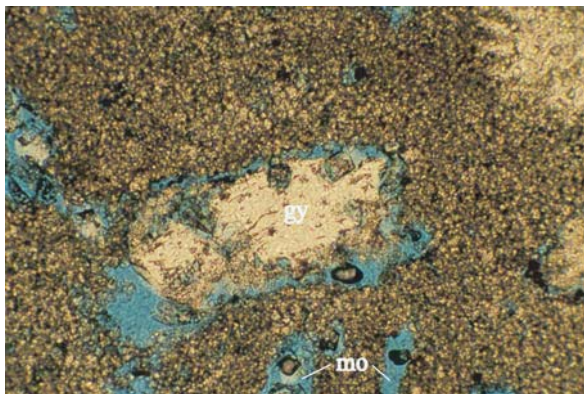


**Figure 18** Sample GEUS 1 (Midale Marly Unit, M1 zone) after CO<sub>2</sub> flooding. Thin-section micrograph with plane polarized light from the central part of the sample. A large gypsum crystal ('gy') has been partly dissolved. Calcitic peloids are locally dissolved, leaving irregular moulds ('mo'). The dolomitic matrix appears unaffected by the CO<sub>2</sub> flooding. All pores are filled with blue resin. The width of view is 0.9 mm.

- Potassium and silicon show significant variations that are not readily interpreted.
- Nickel, total iron and zinc show variations that are interpreted to result from contamination, the CO<sub>2</sub>-rich brine being aggressive towards some of the metallic components of the experimental equipment.

Geochemical mass balance calculations using the amounts of dissolved calcium and magnesium in the reacted brine show good agreement with both the total weight loss from the samples during the experiments and the petrographical

evidence of minerals actually being dissolved. The mass balance calculations indicate that the dissolution of sample GEUS 1 involved slightly more dolomite than calcite, the dissolution of sample GEUS 2 involved only dolomite, and the dissolution of GEUS 14 involved slightly more calcite than dolomite (Table 4). These results are consistent with the petrographical evidence of the samples. The total weight losses of the samples, as determined by weighing before and after the experiments, agree reasonably well with the mass balance calculations, when it is considered that some fine-grained material was lost when dismantling the samples from the experimental equipment.

#### Column experiments

An experimental study reacted a 1 m long column of crushed Midale Marly material with CO<sub>2</sub> and synthetic formation water (Bateman et al., 2004). This was reacted at 60°C, and at 150 bar under flowing conditions. A similar, non-reacting experiment pressurised with nitrogen was also undertaken. The experiment durations were 6 months. The aim of this study was to understand how the front of dissolved CO<sub>2</sub>, and the associated chemical reactions, will propagate in an open system, and to investigate the impact of mineral reaction kinetics on flowing systems.

The evolution of the reacted fluid was monitored. Relative to the nitrogen 'baseline' non-reacting experiment, it was found that the impact of CO<sub>2</sub> was to:

- increase the concentrations of calcium, HCO<sub>3</sub><sup>-</sup>, magnesium and silicon. This is different to the Midale Marly Unit batch experiments
- decrease pH values and the concentration of strontium.
- have little impact on the concentrations of chloride, iron, manganese, potassium, sodium and total sulphur
- dissolve the rock close to the inlet.

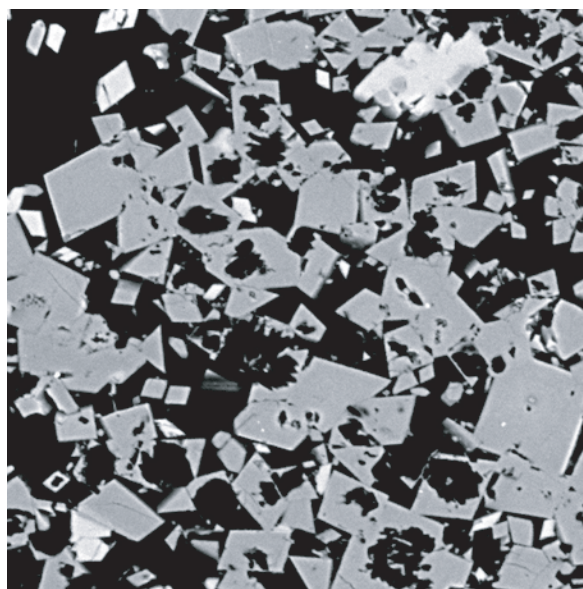
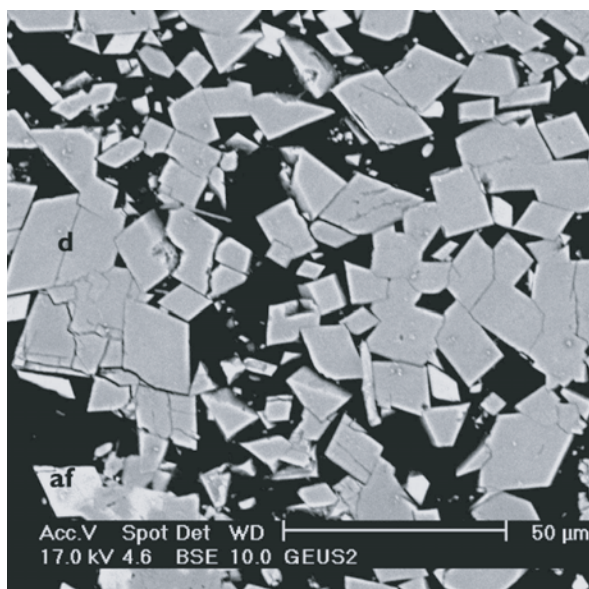


**Figure 19** Backscatter electron microscope images of sample GEUS 2 (Midale Marly Unit, M2 zone). The image on the left shows euhehdral dolomite crystals before the CO<sub>2</sub> flooding experiment. The image on the right illustrates the state after the CO<sub>2</sub> flooding experiment, with dolomite crystals that are severely corroded. Note that many grains are hollowed-out, even though their euhehdral crystal faces are almost intact. For phase identification on the left image, 'af' is alkali feldspar and 'd' is dolomite. The right image was located 0.5 mm from the inlet end of the test plug. Both images are at the same scale.

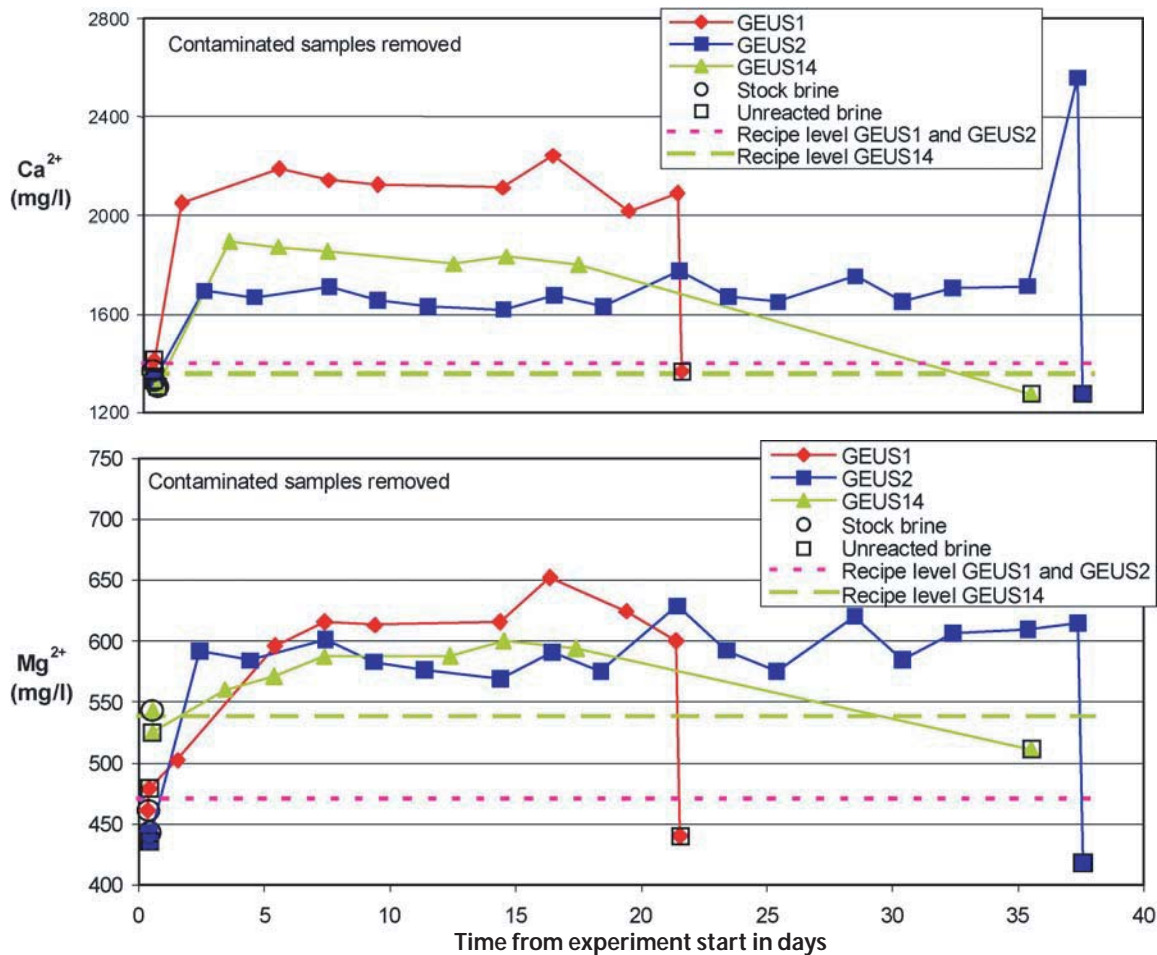


**Figure 20** Output fluid concentrations of  $\text{Ca}^{2+}$  and  $\text{Mg}^{2+}$  during the  $\text{CO}_2$  flooding experiments. Coloured markers represent geochemical analyses of pore fluids. Dashed lines represent the fluid composition at the time of preparation. Markers labelled 'Stock brine' represent brine from the stock bottle. Markers labelled 'Unreacted brine' represent brine that flowed through the reservoir condition rig exactly as the reacted brine, except that they did not flow through the rock sample. Samples of reacted brine show considerable increase in both  $\text{Ca}^{2+}$  and  $\text{Mg}^{2+}$  contents, relative to recipe level, stock brine and unreacted brine.

There also appear to be some experimental artefacts, for example the increases in iron and manganese concentrations are thought to be due to corrosion of some parts of the equipment used in the experiments.

Reaction in the  $\text{CO}_2$  column shows significant dissolution over the 20–30 cm closest to the inlet, compared to the nitrogen 'baseline' experiment. This led to an almost four-fold increase in the surface area of the Midale Marly unit material. An apparent increase in clay content over this interval was probably a result of the clay being released following dolomite dissolution. The lack of significant differences in clay mineralogy between the initial material, the nitrogen column and the  $\text{CO}_2$  column indicate that this clay was not produced during the experiment, but was incorporated within the original dolomite. Reaction between  $\text{CO}_2$  and the Midale Marly Unit therefore appears to have the potential to release previously entrapped clay, that may lead to blocking of pore throats. However, no evidence of such blocking was observed in these experiments, though evidence for migration of fines was observed.

#### 2.5.2.2 REACTIONS OF THE MIDALE VUGGY UNIT RESERVOIR ROCK

The Midale Vuggy Unit immediately underlies the Midale Marly Unit, and has had most of its original oil removed

during primary production and water-flooding operations. Although the injected  $\text{CO}_2$  will be more buoyant than the formation water, it is likely that dissolved  $\text{CO}_2$  will react with the Midale Vuggy unit. Moreover, the brines become denser when  $\text{CO}_2$  dissolves into them, and it is possible that plumes of  $\text{CO}_2$ -rich brine may eventually slowly descend into the Midale Vuggy Unit. This experimental programme attempted to reflect this, by concentrating on static experiments with  $\text{CO}_2$ -saturated formation waters.

#### Static batch experiments

Approximately 18 batch experiments were completed using samples of Midale Vuggy Unit material from the Weyburn oilfield (Rochelle et al., 2003b; Rochelle et al., 2004). The experiments were conducted at conditions representative of the reservoir, i.e.  $60^\circ\text{C}$  and 150 bar, or of injection wells, i.e.  $60^\circ\text{C}$  and 250 bar, and covered time periods of over six months. A range of grain sizes of Midale Vuggy Unit samples were used ( $<250\ \mu\text{m}$ ,  $250\text{--}500\ \mu\text{m}$ , and small monoliths) and fluid:rock ratios were typically 10:1 or less. The Midale Vuggy Unit samples were reacted with synthetic formation water of realistic composition, and the experiments pressurised with

**Table 4** Mass balance calculation for samples GEUS 1, GEUS 2, and GEUS 3. The calculation of dissolved minerals assumes a calcium/magnesium molecular ratio of  $1.46 \pm 0.04$  for dolomite, as determined by six dolomite analyses from samples GEUS 2 and GEUS 14.

	GEUS 1	GEUS 2	GEUS 14
Measured weight loss (g)	2.45	1.47	1.79
<i>Mass balance calculations based on geochemistry:</i>			
Total dissolved carbonates (g)	1.75	1.48	1.01
Dissolved dolomite (g)	1.02	1.42	0.38
Dissolved calcite (g)	0.73	0.06	0.62
<i>Petrographical evidence:</i>			
	Significant corrosion of calcite Minor corrosion of dolomite	Calcite not present in sample. Significant corrosion of dolomite, hollowed-out grains widespread.	Significant corrosion of calcite, especially shell fragments. Minor corrosion of dolomite.

either CO<sub>2</sub> ('reactive' experiments) or nitrogen (non-reacting 'baseline' experiments).

The evolution of a selection of solutes was followed. Relative to the nitrogen 'baseline' experiments, it was found that the impact of CO<sub>2</sub> was to:

- increase the concentrations of calcium, HCO<sub>3</sub><sup>-</sup> and silicon in the fluid (e.g. Figure 15)
- decrease the concentrations of total sulphur and possibly strontium and pH values
- have little impact on the concentrations of aluminium, magnesium and manganese (e.g. Figure 16).

Many of the solutes, including calcium, reached steady-state conditions within about a month, indicating relatively rapid control by anhydrite and/or calcite dissolution. Although aluminosilicate minerals make up a small proportion of the rock, dissolution/precipitation reactions occurred much more slowly. Silicon concentrations did not reach steady-state conditions, even after six months. It is noted that these changes are similar to those found in the Midale Marly Unit experiments, and it suggests that similar controls of fluid chemistry are operating in both studies.

Unlike the reacted solids from the Midale Marly Unit experiments however, samples of Midale Vuggy Unit material showed clear signs of reaction. For the monoliths these included 'tidemarks' developed on the surfaces straddling the CO<sub>2</sub>-water interface (Figure 21). Below the water line, anhydrite and calcite were corroded. The calcite dissolution was greater than in the Midale Marly unit experiments, and dissolution of the aluminosilicate minerals and anhydrite was relatively minor. After four weeks of reaction with CO<sub>2</sub>, euhedral prismatic gypsum crystals up to 500 µm long formed below the water line, and by eight weeks these were 2.5 mm long (Figure 22). After 17 weeks reaction, gypsum crystals up to 500 µm long had also developed in the baseline nitrogen experiment. In addition, most anhydrite and calcite surfaces were corroded to a depth of 10–30 µm in both the CO<sub>2</sub> and the baseline nitrogen experiments. This porosity was easily distinguishable from the vuggy porosity developed during diagenesis. Similar features were seen in the experiments using samples with finer grain sizes.

### 2.5.3 Modelling

A variety of modelling approaches were used to predict the reactions of CO<sub>2</sub> with formation water and the Midale Beds under simulated in situ conditions. Azaroual et al. (2004) gave a detailed account of this work. The aims of this research were as follows:

- to simulate and help interpret laboratory experimental studies of the reactions between the Midale Beds rock samples, porewaters and CO<sub>2</sub>
- to extend predictions of laboratory-scale systems to those on a reservoir scale.

The above aims were achieved through the use of two predictive geochemical modelling codes:

- 1) PHREEQC (V2.8). This has many capabilities for simulating fluid-rock interactions, including kinetics and transport calculations.



**Figure 21** Scanning electron photomicrograph of a monolith of the Midale Vuggy Unit, showing a well-developed 'tide mark' with increased dissolution within the water-rich phase (i.e. the lower half of the image). The sample had reacted for eight weeks with CO<sub>2</sub>.

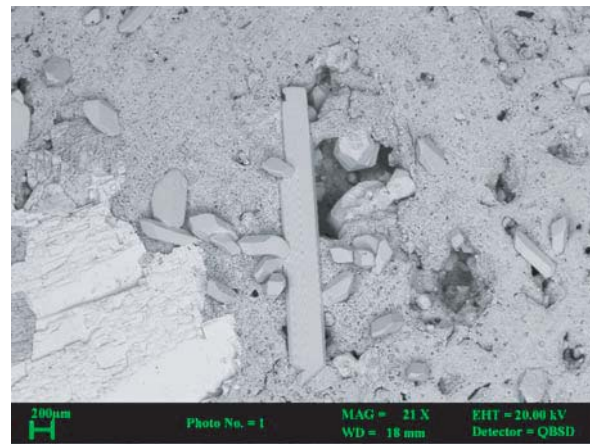
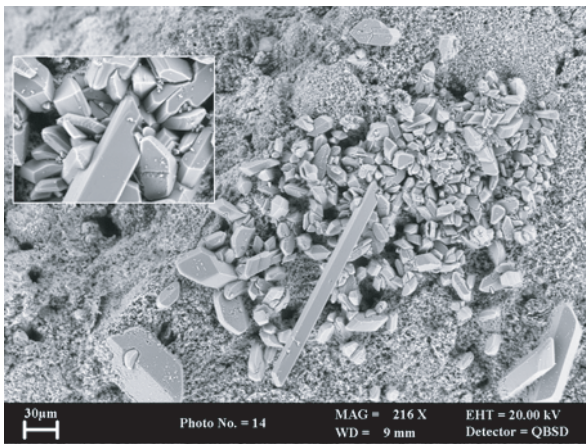


**Figure 22** Scanning electron photomicrographs of Midale Vuggy Unit monoliths showing well-developed secondary growth of gypsum crystals within the aqueous phase. After four weeks with  $\text{CO}_2$ , the crystals were up to  $500\ \mu\text{m}$  long (left hand image), and after eight weeks they were at least  $2.5\ \text{mm}$  long (right hand image).

2) SCALE 2000. This is a thermo-kinetic model, designed to evaluate the physico-chemical properties of hydrothermal, industrial and petroleum brines and the kinetics of mineral-dissolution and precipitation reactions. It can provide thermodynamic diagnoses of the precipitation of carbonate, silicate, sulphate and sulphide deposits that are common for these brines.

### 2.5.3.1 MODELLING REACTIONS OF THE MIDALE MARLY UNIT RESERVOIR ROCK

#### Static batch experiments

A simplified mineralogy of the Midale Marly Unit material was used: dolomite (60%), calcite (15%), anhydrite (10%), quartz (5%), K-feldspar (3.8%), albite (1.9%), siderite (0.6%) and kaolinite (0.5%). The experimental measurements were used as input data for saturation index (SI) calculations in order to evaluate the evolution of the thermodynamic equilibrium state of the experimental systems. The SI of dolomite (Figure 23) was initially low, at  $-4.75$ , i.e. well below saturation. This increased rapidly, i.e. in less than 200 hours, to achieve a positive value of  $+0.5$ , i.e. just above saturation.

Calcite approached thermodynamic equilibrium rapidly and remained constant for the fine fraction experiments ( $<250\ \mu\text{m}$ ). The monolith experiments had an average SI for calcite of approximately  $-0.5$ . Thermodynamic equilibrium was achieved faster ( $<200$  hours) for the fine ( $<250\ \mu\text{m}$ ) grains. It seems that the  $p\text{CO}_2$  has a significant effect on this behaviour. Carbon dioxide solubility is  $0.96$  molal at  $250$  bar, whereas its value is  $0.86$  molal at a  $p\text{CO}_2$  of  $150$  bar. The analysis of detailed aqueous carbon speciation in both conditions shows that the activity of carbonate ( $a_{\text{CO}_3^{2-}}$ ) is  $5.8 \times 10^{-8}$  for a  $p\text{CO}_2$  of  $150$  bar, and  $1.62 \times 10^{-7}$  for a  $p\text{CO}_2$  of  $250$  bar, corresponding to calcite SI values of  $-0.46$  and  $-0.09$  respectively. The activity of free calcium ( $a_{\text{Ca}^{2+}} = 1.37 \times 10^{-2}$ ) was the same in both cases.

It appears that the non-attainment of equilibrium is not linked to the kinetics of the reactions, but rather to the solubility of the  $\text{CO}_2$ . This suggestion is confirmed by the behaviour shown in Figure 23. Here the exchange surface between the Midale Marly Unit minerals and brine is reduced in the monolith samples since the calcium concentration is controlled by gypsum saturation.

Anhydrite and gypsum remain at thermodynamic equilibrium in these experiments (Figure 23). This behaviour was

also observed in the monolith experiments where the reactive surface area is reduced. Anhydrite and gypsum are linked by the activity of water, and its value is exactly the same (i.e.  $a_{\text{H}_2\text{O}}$  is about  $0.936$ ). For water activity values higher than  $0.8$ , gypsum will precipitate. If the value is lower than  $0.8$ , then anhydrite precipitates (see later). Therefore, for the  $a_{\text{H}_2\text{O}}$  in the experiments, gypsum precipitation would be expected, as is seen. Pyrrhotite, siderite and strontianite remain undersaturated.

#### Modelling the flow experiments

Three  $\text{CO}_2$  flooding experiments were carried out using Midale Marly Unit material (see earlier and Olsen and Stenoft, 2004). Figure 24 illustrates that anhydrite, dolomite and gypsum achieved thermodynamic equilibrium after 25 hours. For sample GEUS 1, dolomite became oversaturated for the remainder of the experiments, probably because of the faster kinetics of calcite dissolution increasing calcium ion concentrations. Calcite achieved thermodynamic equilibrium after 100 hours of flooding. Pyrrhotite, siderite and strontianite remained undersaturated for the entire duration of the experiments.

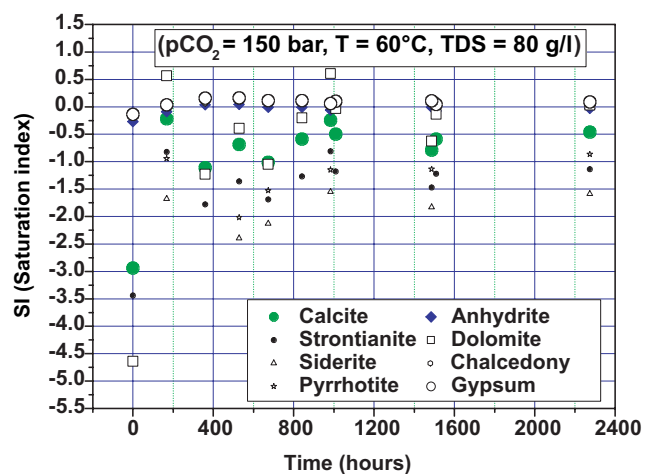


**Figure 23** The saturation index of (SI) potentially reacting, i.e. dissolving and/or precipitating, minerals in the BGS experimental system.

For sample GEUS 2, anhydrite, dolomite and gypsum moved close to saturation after 50 hours. The SI of calcite has a constant value of approximately -0.5 from 100 hours to the end of the experiment, i.e. after 900 hours. This behaviour indicates that calcite is not reacting quickly enough to release sufficient quantities of calcium in order to achieve saturation. This explanation is indirectly supported by the results from the GEUS 1 experiment. Here, calcite achieved equilibrium even though the flow rate was 1.5 times higher than that in the GEUS 2 experiment. Therefore the residence time was higher in GEUS 2, compared to GEUS 1.

Experiment GEUS 14 was designed by Olsen and Stenfort (2004) to correspond to CO<sub>2</sub>-rich fluid flowing through a fracture. As reactive surface is the crucial parameter which controls mass exchange between the Midale Beds and flowing fluids, the minerals exhibit similar behaviour to that in the GEUS 2 experiment. Anhydrite, dolomite and gypsum approached thermodynamic equilibrium after 50 hours. Calcite has the same SI value, -0.5, as in the GEUS 2 experiment. Pyrrhotite, siderite and strontianite continued to be far from equilibrium.

#### Modelling the column experiments

Two flow experiments using crushed Midale Marly Unit material were carried out (see earlier, and Bateman et al., 2004). These were the longest flow experiments that were undertaken, having durations in excess of six months. Figure 25 illustrates the thermodynamic state of the minerals that were treated in previous batch tests. The global behaviour observed in the batch experiments was reproduced. The sulphates anhydrite and gypsum remained at thermodynamic equilibrium throughout the duration of the experiment.

Calcite and dolomite approached equilibrium after 2250 hours. After this time, dolomite attained equilibrium whereas calcite did not. Both have SI values of approximately -0.5 as in the previous examples. In an open system, the stationary state cannot be interpreted unequivocally as in batch systems. This is due to the flowing conditions that may control residence times. Reaction rates at the outlet of the system are far from equilibrium. Furthermore, the increasing SI of all minerals is likely to be due to increasing reactive surface areas with time as observed by Bateman et al. (2004). At the system inlet, the surface area increased by a factor of 2–3.5 over a column length of 20–30 cm.

Chalcedony, pyrrhotite, siderite and strontianite exhibited similar behaviour to that observed in the batch experiments.

#### Modelling processes at the field scale

Geochemical modelling has been used to interpret the potential of long-term storage of CO<sub>2</sub> in the Midale Beds reservoir at Weyburn, and to interpret if geochemically reactive zones exist above and below the reservoir. The effect of CO<sub>2</sub> injection into the Midale Marly Unit was modelled for a simulated 10 000 years under in situ conditions. The pressure (*p*CO<sub>2</sub>) and temperature values used in these numerical simulations were 54°C and 150 bar, respectively. This modelling took into account mineral dissolution/precipitation reaction kinetics and coupled them with 1D advective/diffusive/dispersive transport processes. Many long-term geochemical modelling scenarios were carried out using flow rates from 0.25 to 50 m/year.

These predictions showed that anorthite would be completely exhausted from the simulated systems over scales from 400 to 4000 m, depending on the flow rates, after 10 000 years of reaction. Dawsonite (NaAl[CO<sub>3</sub>][OH]<sub>2</sub>) was predicted to precipitate over all the spatial scales considered. However, calcite was predicted to dissolve at the entrance of the system, whereas anhydrite was predicted to precipitate. Albite, illite and K-feldspar were predicted to dissolve throughout the simulations, not achieving thermodynamic equilibrium, even after a simulated 10 000 years. As a consequence of these dissolution/precipitation reactions, it was predicted that the overall porosity would increase over 10 000 years.

#### 2.5.3.2 MODELLING REACTIONS OF THE MIDALE VUGGY UNIT RESERVOIR ROCK

##### Static batch experiments

The Midale Vuggy Unit is largely calcitic in its average mineralogy. It comprises 80% calcite, 12% dolomite, 4% anhydrite and 4% silica and aluminosilicate minerals. The salinity of the synthetic aqueous solution used for these experiments is the lowest one at 64 g/l. Calcite achieved thermodynamic equilibrium rapidly, but became undersaturated with a SI of approximately -0.5 for the fine (<250 μm) fraction at 150 bars *p*CO<sub>2</sub> (Figure 26).

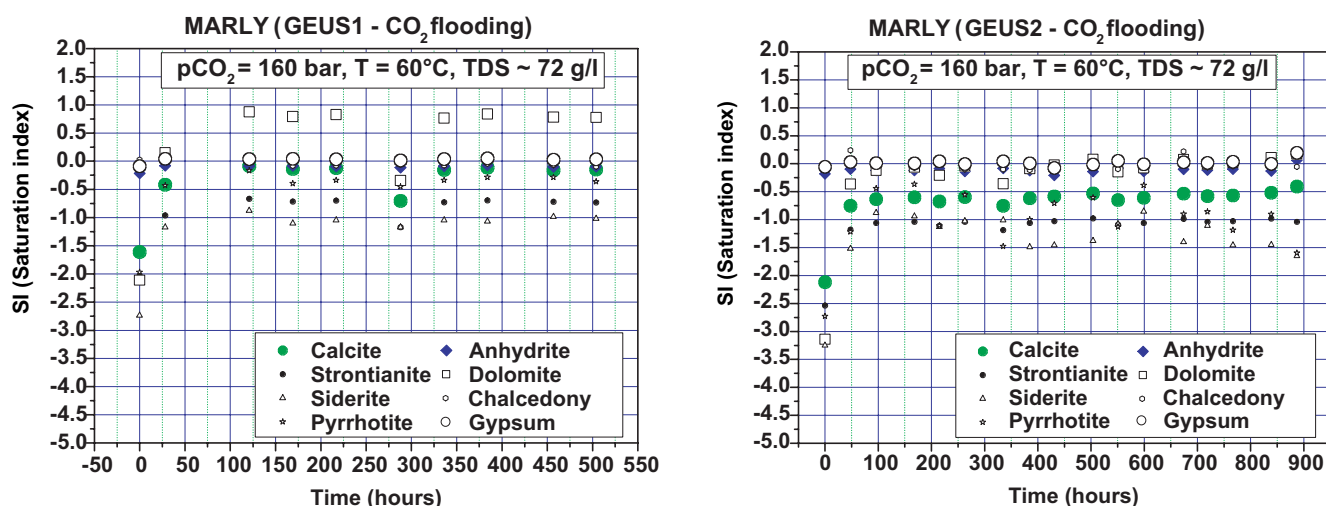


**Figure 24** The saturation index (SI) of potentially reacting, i.e. dissolving and/or precipitating, minerals in the CO<sub>2</sub> flooding experiment system of GEUS.

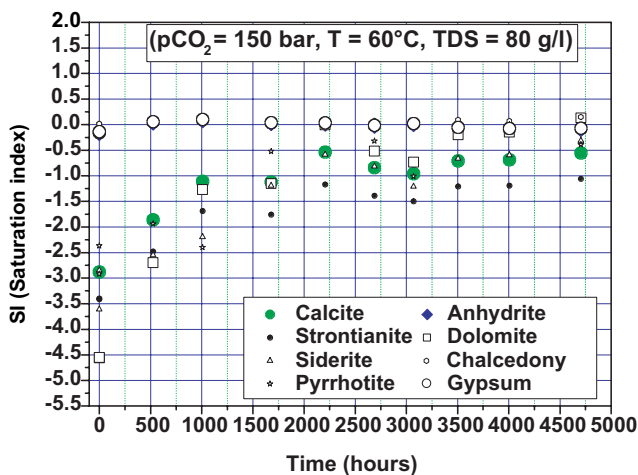


**Figure 25** The saturation index (SI) of potentially reacting, i.e. dissolving and/or precipitating, minerals in the BGS flow experiments.

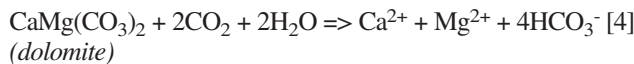
The explanation for reactions in the Midale Marly Unit experiments appears to be confirmed. Hence, even if the amount of calcite is high, e.g. 80%, the system maintains disequilibrium because of gypsum precipitation and the slow dissolution rate of anhydrite.

### 2.5.3.3 PRINCIPAL GEOCHEMICAL REACTIONS INVOLVED IN THE EXPERIMENTS

The experiments which explored the reactivity of CO<sub>2</sub>-enriched brines with Midale Beds material under EOR injection CO<sub>2</sub> conditions have highlighted many important physical/chemical mechanisms. The dissolution of CO<sub>2</sub> to form carbonic acid in the brine caused the dissolution of calcite and dolomite. It also perhaps caused aluminosilicate minerals such as albite, anorthite and kaolinite to dissolve in systems with variable salinity (i.e. 64 to 115 g/l) and pressures of between 150 and 250 bar. This behaviour was shown experimentally by using similar pressure and temperature conditions using nitrogen, rather than CO<sub>2</sub>, or a by-pass for precipitation. Silica and sulphate minerals were not affected by the acidification of the system and theoretically, they should not dissolve under CO<sub>2</sub> injection conditions.

The dissolution of carbonate minerals is kinetically-controlled and the time taken to achieve thermodynamic equilibrium varied from test to test. Calcite is the most reactive mineral, rapidly approaching equilibrium. However, it often maintains a steady state, close to equilibrium, with a SI of approximately -0.5, hence continuing to dissolve with a reduced reaction rate. However, dolomite rapidly achieved equilibrium or an oversaturated state, completely inhibiting its contribution to the evolution of the system. Gypsum was predicted to precipitate in all experiments and was observed in some. Sulphate minerals are relatively unreactive and are not directly affected by the CO<sub>2</sub> injection. At the experimental timescales, however, carbonate and sulphates are the main reacting minerals.

The two principal irreversible mineral dissolution reactions, induced by CO<sub>2</sub> injection, are as follows:



Some calcium ions from reactions [3] and [4] will combine with SO<sub>4</sub><sup>2-</sup> ions which are present in the Weyburn brines (there are 3 to 4 g/l of SO<sub>4</sub><sup>2-</sup> ions in the geochemical baseline fluids). The resultant minerals therefore affect the global equilibrium of sulphate minerals (Figure 27):



Reaction [5] will precipitate stable calcium sulphate, either anhydrite or gypsum, depending on the P-T-a<sub>H2O</sub> stability domain of the system (Figure 27). If the water activity of sulphate minerals is higher than approximately 0.8, gypsum will precipitate.

The sampled fluids after CO<sub>2</sub> injection in the Weyburn field contain high concentrations, i.e. 3 to 10 g/l, of sulphates (unpublished data from the University of Calgary). Therefore, this mechanism will be important in the Weyburn reservoir. Water activity depends on dissolved species concentrations. Consequently, for high salinity compartments in the Weyburn field, anhydrite is likely to precipitate.

Due to the high reactivity of calcite, the possible effects of surfaces were not found to be significant in the experiments. This is surprising, especially so because reactive surfaces appear to be significant in the aluminosilicate mineral kinetic studies. This is an interesting result for the short term (EOR), and long term predictive reactive transport modelling where the local equilibrium approach (LEA) can be adopted for both carbonate and sulphate minerals. However, for aluminosilicate minerals, it will be necessary to integrate dissolution-precipitation reaction kinetics because their reactivity is slower and it is important for long term modelling. Unfortunately, the experiments carried out in this study were not long enough to generate the long term (decadal) data needed to constraint long term modelling work. Also, the kinetic constants tentatively evaluated, based on aluminium or silicon concentration evolution, by Rochelle et al. (2003c) do not refer to a specific mineral, and so are difficult to apply in the modelling.

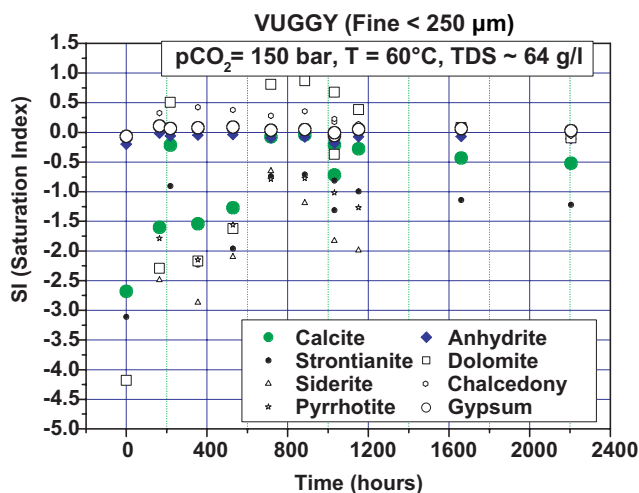


**Figure 26** The saturation index (SI) of potentially reacting, i.e. dissolving and/or precipitating, minerals in the BGS experimental system.

## 2.6 MICROSEISMIC MONITORING

(Hubert Fabriol)

### 2.6.1 Introduction

Passive microseismic monitoring has been used extensively to map rock fracturing induced by fluid injection in enhanced oil recovery (EOR), by hydraulic stimulation, or by reservoir compaction phenomena linked to hydrocarbon production. Microseismic monitoring has been undertaken as part of this project to assess any seismic hazards caused by CO<sub>2</sub> injection and to monitor the spread of injected CO<sub>2</sub> via fracturing and fracture reactivation induced by local overpressure within the reservoir.

### 2.6.2 Data acquisition and processing

Certain data gathered during active downhole seismic investigations were analysed prior to the installation of the dedicated downhole microseismic tool. The Weyburn oilfield was found to be microseismically inactive ('quiet') during a surface seismic survey carried out by the Colorado School of Mines over two to three weeks during September 2000 and during a crosswell seismic survey by the Lawrence Berkeley National Laboratory in 2002. In August 2003, a Canadian passive seismics service provider (ESG), was commissioned to install a microseismic monitoring tool in an abandoned well, number 101/06–08, which is located in the Phase 1B injection area. The microseismic data recorded from September 2003 through March 2004 are described below.

The seismic cable comprises 8 tri-axial geophones with a resonance frequency of 20 Hz, which were cemented at 25 m intervals between 1356 m to 1181 m in the observation well. Three surface calibration shots were used to orientate the horizontal sensors and to check the system. The magnitude of microseismic events recorded ranged from -3.5 to -1, which does not exceed magnitudes associated with water flood or gas injection in similar oilfields. The average velocity model used for hypocentre determination was calculated by ESG using a dipole sonic log in well 141/01–07. Errors

in location range from 30 m to 400 m, depending mainly on the quality of P and S onsets. Analysis of the main characteristics of the waveforms indicated that three types of events were recorded. The first are events related to drilling, completion work or perforation shots in nearby wells and are characterised by poor quality data and large amplitude events caused by the perforation shots. Secondly, events with a dominant frequency of approximately 20 Hz were observed. The final category are higher frequency events, with impulsive first arrivals and clear P and S phases.

#### 2.6.2.1 MICROSEISMICITY ASSOCIATED WITH DRILLING AND COMPLETION OF WELL 121/06–08

The new water alternating gas (WAG) injection well 121/06–08 is located 51 m west of the monitoring well (Figure 28). Here, water and CO<sub>2</sub> are injected in turn into the Midale Vuggy Unit, which has low porosity (8–20%), high permeability (10 to >300 Md) and a relatively high fracture density. Drilling began in October 2003 and resulted in dramatic increases in background seismic noise levels. The passive system recording logic was kept constant and a maximum number of triggered events were set in order to avoid continuous triggering. Approximately 20 events were recorded and located by ESG close to the bottom part of well 121/06–08, corresponding mainly to completion activities and perforation shots carried out in late November 2003.

#### 'Low' frequency events

Water injection in well 121/06–08 started on December 15th 2003, causing an increase in background noise levels and the virtually continuous triggering of the microseismic system until January 12th, 2004. Thirteen events were recorded by the end of this phase of water injection, between January 21st and 22nd 2004, and before the start of CO<sub>2</sub> injection. The waveform spectra are of relatively low frequency with a peak between 20 and 30 Hz, near the resonance frequency of the (undamped) geophones. Low frequencies and short separation between P and S-waves make hypocentral location difficult. A further four events with similar waveforms were recorded later.

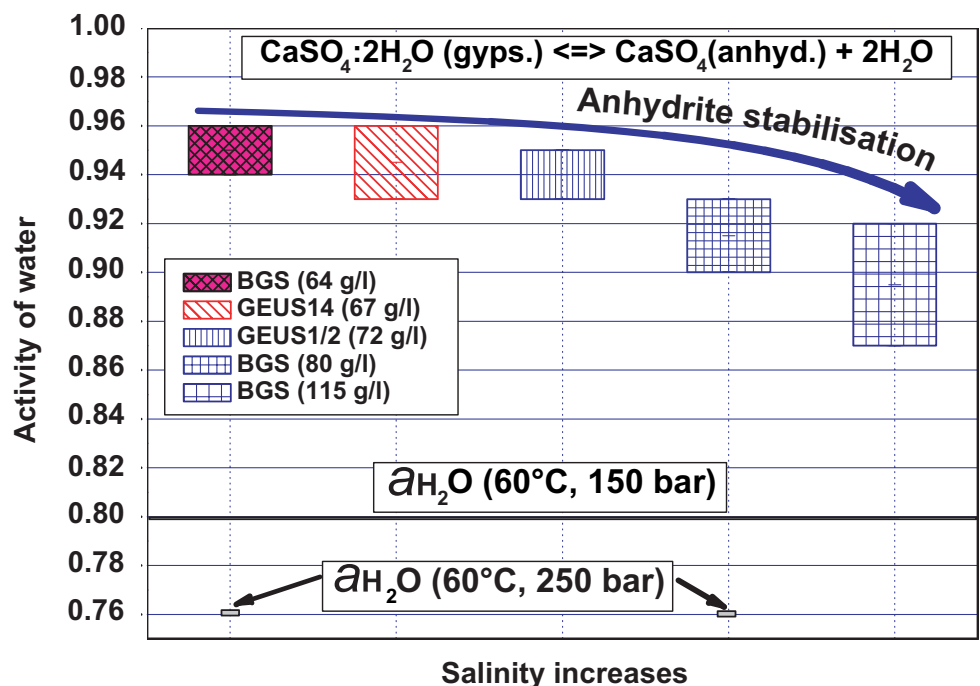


**Figure 27** Sulphate mineral (anhydrite and gypsum) behaviour in the Weyburn reservoir brines under CO<sub>2</sub> injection pressure, temperature and pCO<sub>2</sub> conditions.

### 'High' frequency microseismicity

High frequency events occurred during September 2003, October 2003 and March 2004, corresponding to periods when no drilling, completion activities or water injection were being done. These P and S phases are clear and the waveform spectra contain frequencies up to 150 Hz.

### 2.6.3 Interpretation

The 'low' frequency events are correlated with a peak of gas production in horizontal well 191/11-08 (Figure 29), which is located about 150 m west from the injection well (Figure 28). This, and the low frequency content of spectra, suggests that the inducing mechanism is gas or fluid flow within or close to the base of well 191/11-08. Except for 4 events, this microseismicity occurred prior to CO<sub>2</sub> injection and it is likely that CO<sub>2</sub> did not cause these events.

The 'high' frequency events were located 200 m to 500 m apart, south of the observation well and around the base of the vertical sections of wells 191/09-08 and 192/09-06 (Figure 28). A comparison of cumulative seismic moment and the oil and gas production rate of well 191/09-08 seems to indicate a relationship with a decrease or the entire cessation of oil production (Figure 30). Re-opening of fractures due to pressure build-up in the producing unit could induce shear failures and consequently microseismicity.

### 2.6.4 Summary and Conclusions

During August 2003, continuous passive monitoring was started within the recently initiated Phase 1B injection area using an eight-level array of three-component geophones cemented in immediately above the reservoir unit in an observation well, number 101/06-08 which had been abandoned. Carbon dioxide injection started in January 2004 in vertical

well 121/06-08 located 51 m west of the observation well. By April 2004, 62 microseismic events have been recorded with magnitude estimates ranging from -3.5 to -1; distances from the monitoring well vary from 50 m to 2500 m. This microseismicity has been classified into three groups of events:

- 1) Eighteen of the events were located close to the base of a nearby horizontal production well, and occurred during two periods when production from this well was shut down. This microseismicity is believed to relate to pressure build-up within the formation.
- 2) Twenty-one microseismic events were recorded close to the bottom part of injection well 121/06-08, corresponding mainly to completion activities and perforation shots carried out during late November 2003.
- 3) The remaining events were recorded prior to the start of CO<sub>2</sub> injection. Waveform spectra are characterised by relatively low frequencies with a peak near 20 Hz. Emergent P- and S-phases make it difficult to obtain accurate locations for these. It is suggested that these events were caused by fluid flow within or close to well 191/11-08, approximately 150 m west of the observation well.

The results to date demonstrate unequivocally that recording microseismicity in an oilfield CO<sub>2</sub>-injection operation is technically feasible. Because the injection of CO<sub>2</sub> has only recently been started, no microseismicity linked directly to the spread of CO<sub>2</sub> within the reservoir has been unambiguously identified. Nevertheless, different types of events have been recorded and appear to be related to production or completion activities. Careful analysis of waveforms, event locations and production data will be necessary to identify events induced by CO<sub>2</sub> injection. With respect to seismic hazards due to injection, the microseismicity observed to date does not exceed magnitudes associated with water floods or gas injection in other monitored oilfields.

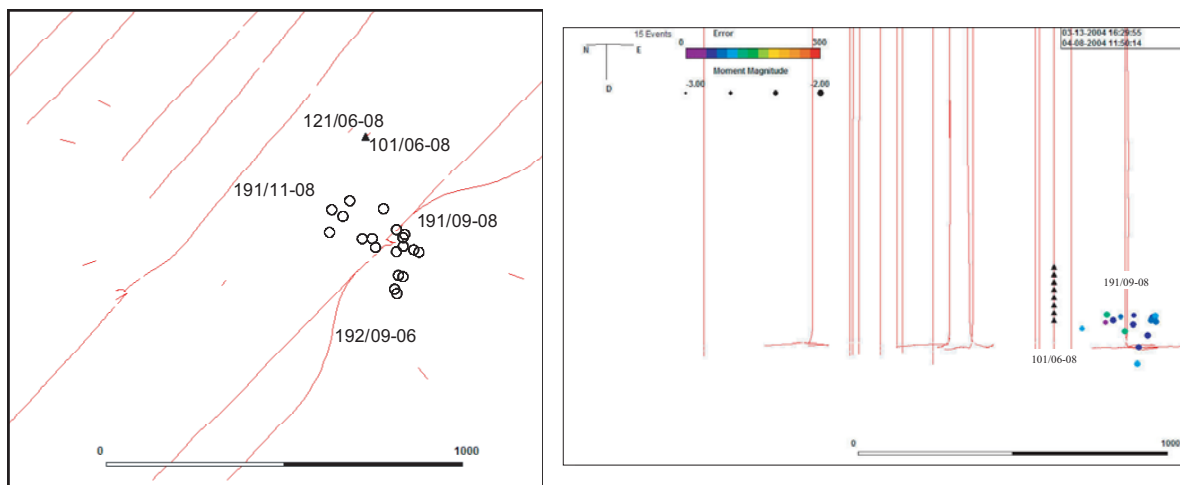


**Figure 28** Hypocentral location of 'high' frequency events in horizontal view and vertical/sectional view, recorded on September 9th and October 20th 2003 and on March 18th and 19th 2004 by ESG. The black triangles are geophones. Vertical and horizontal scales are equal. The black lines are horizontal and vertical projection of wells.

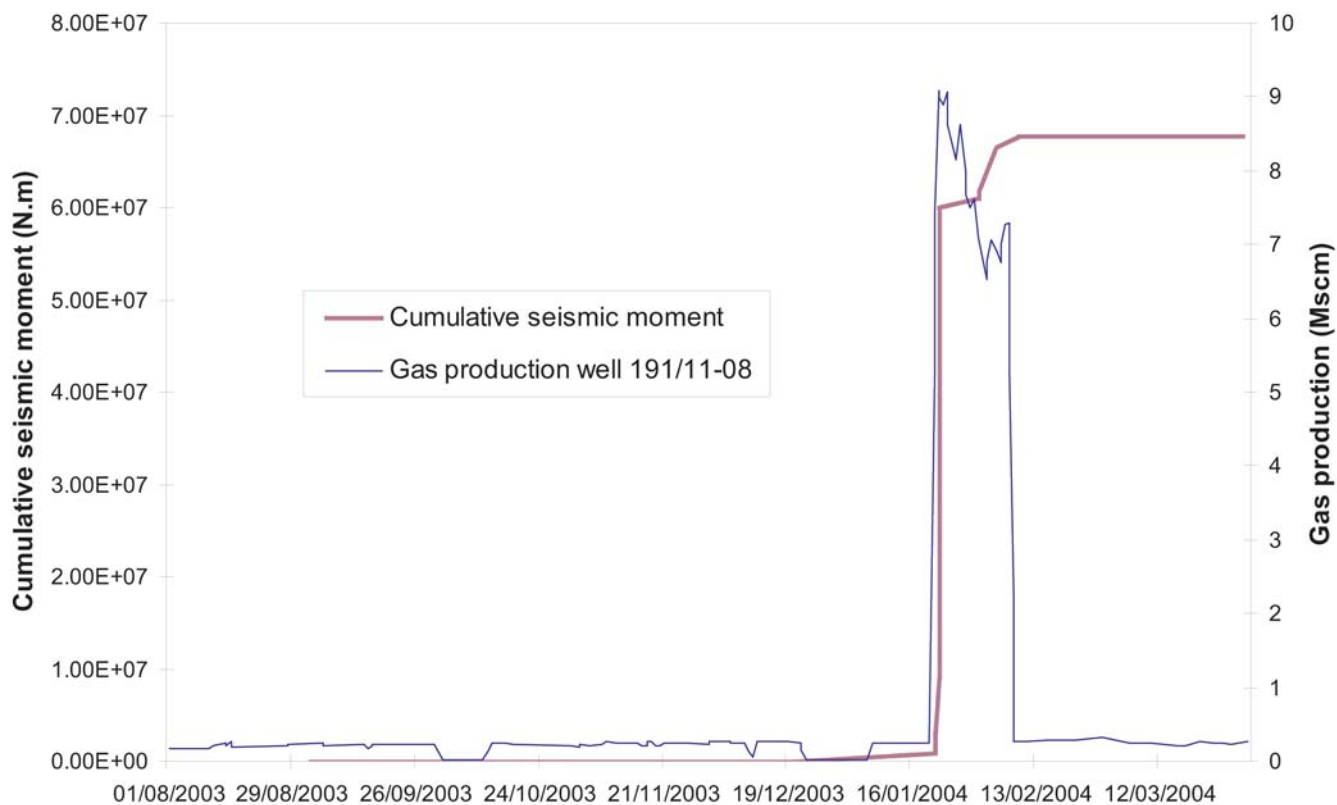


**Figure 29** Comparison of gas production in well 191/11–08 and the cumulative seismic moment of the microseismic events recorded during January and February 2004.

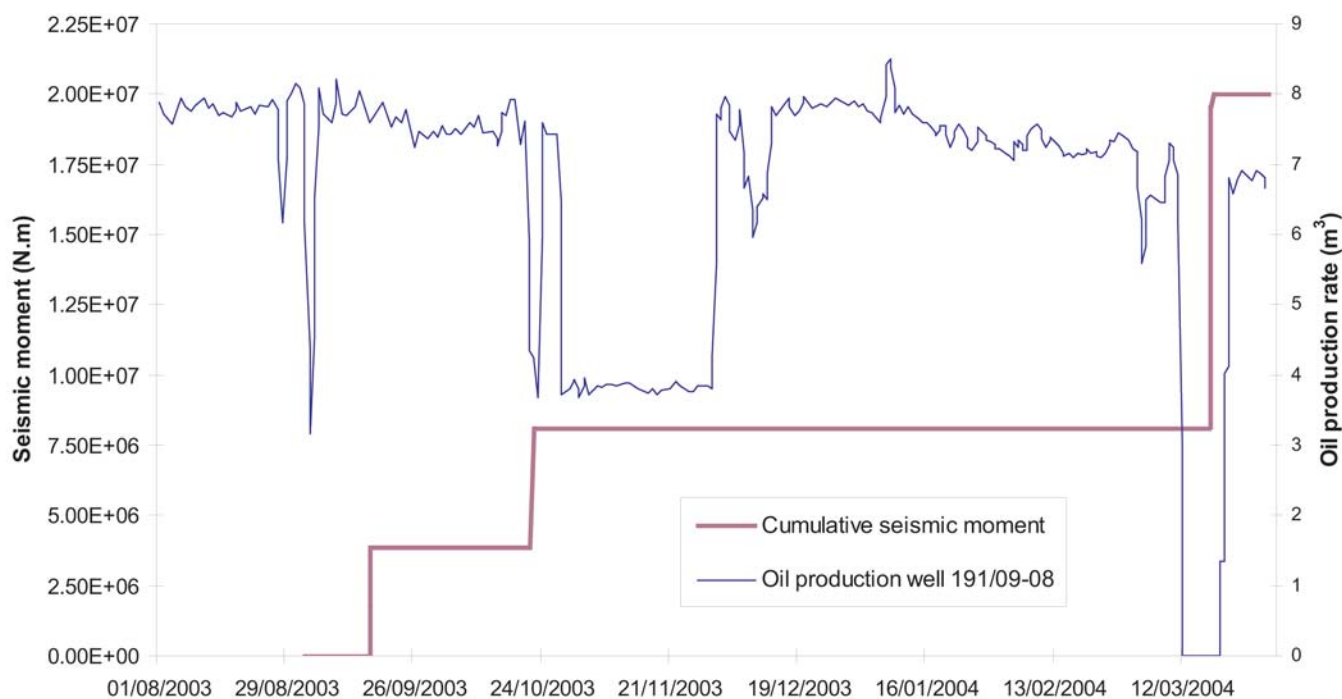


**Figure 30** Comparison of the oil production rate in well 191/09–08 and the cumulative seismic moment of events located south of the observation well.

# 3 Caprock, overlying formations and engineered seals

## 3.1 INTRODUCTION

(Yves-Michel Le Nindre)

The word ‘seal’ is the most appropriate to describe the compact lithological units which tightly close a reservoir rock. Originally, the term ‘caprock’ was used to describe a breccia complex at the top (‘cap’) of a salt diapir, which originated during the breaking through of the overlying harder rocks by the ascending salt dome. However, in most usage, ‘caprock’ is used to describe the lithological unit that overlies a reservoir unit and forms an effective ‘seal’. Two types of seal must be considered pertaining to the Midale Beds reservoir unit:

- the units immediately bounding the reservoir and normally confining the oil reserves
- the semipervious or impervious units in the overburden, which act as additional potential barriers to the migration of hydrocarbons and/or CO<sub>2</sub> upwards from the reservoir.

The units acting as barriers to the Midale reservoir unit are both Mississippian anhydrites. At the base of the Midale Vuggy Unit, the Frobisher Evaporite acts as a barrier to flow. However, this anhydrite unit is not continuous, especially south of the field. At the top of the Midale Marly Unit, the Midale Evaporite is the first effective seal. At the boundary between the Mississippian subcrop and the sub-Mesozoic unconformity, a thin anhydritised zone is present. This was formed by diagenetic migration of anhydrite along the unconformity surface. From cores that include the Mississippian–Triassic boundary, this zone appears not to be continuous. These two seals have been described by Rott (2003), Nickel (2004) and Nickel and Qing (2004).

The Triassic Lower Watrous Formation and the Middle Jurassic Upper Watrous Formation seal the sub-Mesozoic unconformity (Figure 31). Although the underlying and overlying Frobisher and Midale evaporites bound the Midale Beds

reservoir unit, they may not be sufficient to act as an effective seal against the upward migration of CO<sub>2</sub>. The Watrous aquitard, *sensu lato*, which includes the clastic Lower Watrous Formation and the evaporitic Upper Watrous Formation, is the first main barrier to prevent CO<sub>2</sub> escape from the reservoir. Therefore, diffusion and associated reaction processes through this horizon must be considered (Figure 32).

The remainder of the Mesozoic succession which overlies the Watrous Formation contains several thick and extensive shale units that are assumed to act as efficient barriers to vertical CO<sub>2</sub> migration. These are:

- the Vanguard Group aquitard (Upper Jurassic) underlying the Mannville Group aquifer (Lower Cretaceous)
- the Joli Fou aquitard (Lower Cretaceous) of the Colorado Group (Cretaceous) overlying the Mannville Group aquifer (Lower Cretaceous)
- the shales of the Colorado Group (Cretaceous) above the Viking Sandstone/Newcastle aquifer (Lower Cretaceous)
- the Bearpaw Formation shales (Upper Cretaceous) overlying the Belly River/Judith River aquifer (Cretaceous).

The Colorado Group and Bearpaw Formation shales are the principal barriers, with a thickness of several hundreds of metres each.

## 3.2 CORE ANALYSIS OF THE MIDALE EVAPORITE UNIT CAPROCK

(Niels Springer and Jonathan M Pearce)

The first caprock above the Midale Beds reservoir is the Midale Evaporite Unit, however other caprocks are present within the overlying succession. These include the Late Triassic to Early

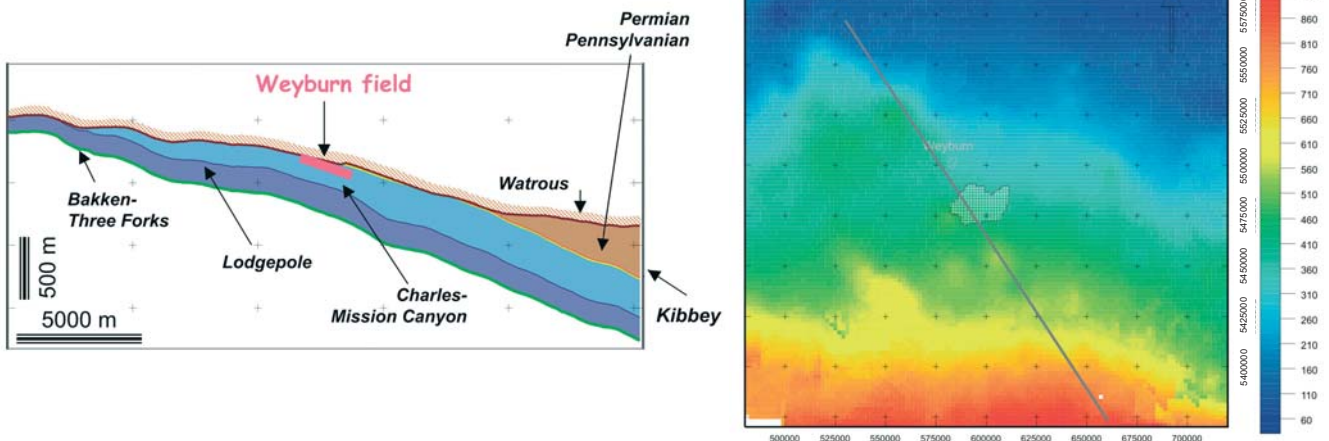


**Figure 31** Regional NNW–SSE cross-section of the Mississippian succession through the Weyburn oilfield illustrating the truncation by the Lower Watrous Formation. The isovalues depict the elevation of the unconformity surface.

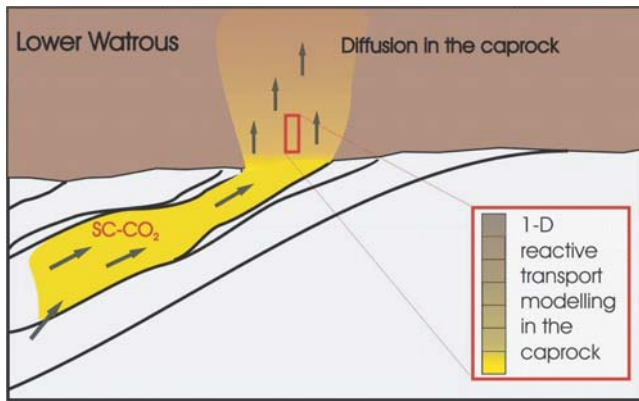


**Figure 32** Conceptual sketch of CO<sub>2</sub> diffusion in the Lower Watrous Formation. The modelled section comprises 10 elementary stacked cells; each cell is one metre thick. SC-CO<sub>2</sub> = supercritical CO<sub>2</sub>.

Jurassic Watrous Formation (Czernichowski-Lauriol et al., 2001). As part of this project, only material from the lower part of the Midale Evaporite Unit was sampled for batch and flow experiments. This core material from the Midale Marly M1 Unit/Midale Evaporite Unit transition zone was described macroscopically by Springer et al. (2002) as massive, locally anhydritised, dolomitic limestones.

The thin sections and back-scattered electron micrograph images of the Midale Marly M1 Unit/Midale Evaporite Unit transition indicate non-porous to faintly porous dolomites, comprising crystals up to 10 mm in diameter that have been locally replaced by anhydrite nodules and/or single-crystals of

anhydrite. Scattered euhedral crystals of fluorite are common (Figure 33). The samples of the Midale Marly M1 Unit/Midale Evaporite Unit transition show a scale-dependant variation in the dolomite/anhydrite ratios from plug sample to full core sample, because the dolomite appears as randomly-scattered crystal aggregates. The crystals of euhedral fluorite and alkali feldspar form up to around 20% of the anhydrite volume. There is approximately 4% clay in the Midale Evaporite Unit.

Core analysis indicates that the Midale Marly M1 Unit/Midale Evaporite Unit transition zone is of poor quality in terms of caprock seal capacity (Table 5). The average gas permeability is 0.7 mD and the expected liquid permeability is approximately 0.1 mD at reservoir conditions. This is significantly higher than levels typically recorded from good quality caprocks of less than 1 mD. Samples having better caprock properties, presumably from a higher level in the Midale Evaporite Unit, were not analysed in this project.

### 3.3 CHARACTERISATION AND HYDRO-CHEMICAL MODELLING OF THE OVERBURDEN

(Yves-Michel Le Nindre, Irina Gaus and Mohamed Azaroual)

#### 3.3.1 The Watrous Formation

The Lower Watrous Formation was deposited on a subaerial shelf and is heterolithic. It is mainly fine-grained with clasts of granitic origin with micrite lithoclasts in a clayey-dolomitic matrix. Cements are dolomicrosparite, calcisparite and anhydrite; the anhydrite may replace the carbonate and

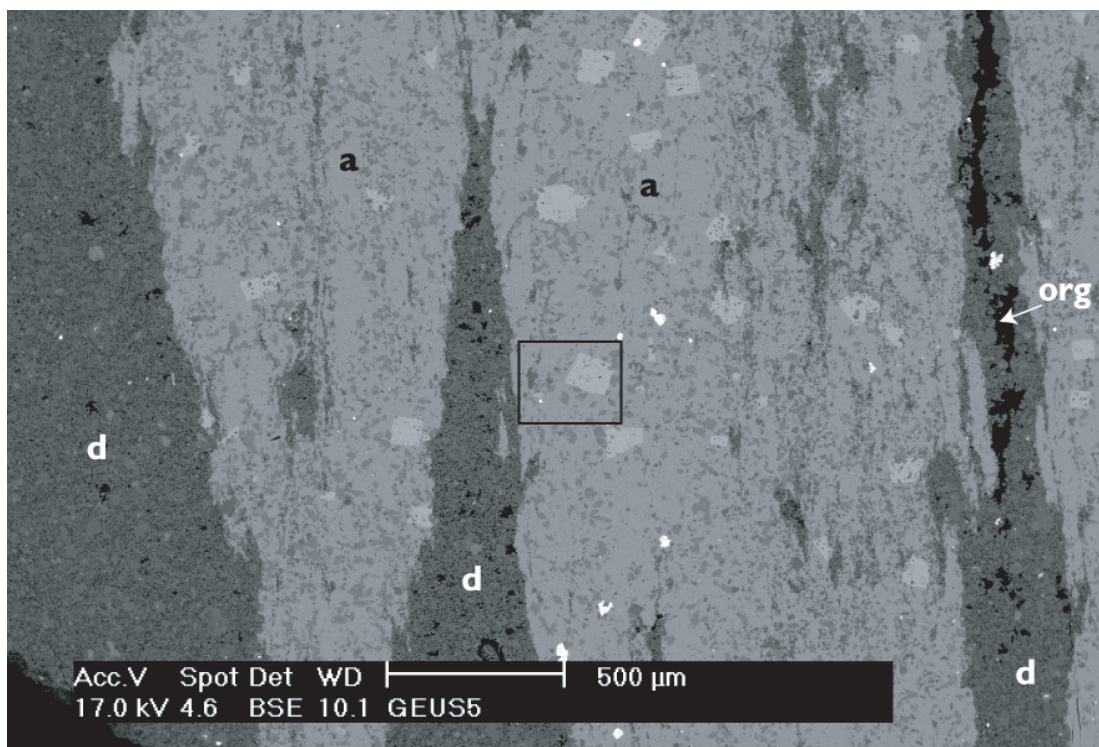


**Figure 33** A back-scattered electron micrograph of a sample of the Midale Evaporite Unit. The large areas labelled 'a' are anhydrite which has completely replaced dolomite. Dolomite ('d') is present as the prominent elongate dark grey vertical patches. The relatively small black patches in the centre of the dolomite vein on the right are believed to be sedimentary organic matter (i.e. undifferentiated kerogen). The frame in the centre of the image highlights a large, euhedral fluorite crystal.

**Table 5** Conventional core analysis data measured for the Midale Marly M1 Unit/Midale Evaporite Unit transition zone. The relatively high grain density is due to the high proportions of dolomite and anhydrite.

Lithology	BGS plugs		BGS plugs		BGS plugs
	Gas permeability (mD)		Porosity (%)		Grain density range (g/cm <sup>3</sup> )
	Range	Mean	Range (%)	Mean (%)	
Midale Marly M1 Unit/Midale Evaporite transition	0.03–1.8	0.7	5–15	10	2.84–2.46

plugs the remaining porosity. The mineralogical paragenesis was relatively constant, but mineral proportions vary rapidly laterally and vertically within a narrow range. In the potentially most porous horizons, porosity measurements indicate a maximum total porosity of about 11%, with modal pore-throat sizes of 1–10 µm. At a larger scale, a mean effective porosity of 4% and a mean permeability of 0.8 mD were assigned to the formation as a whole.

No significant fractures were observed in the Lower Watrous Formation, although minor small (1–2 mm) offset microfractures are present in the muddier units. All the facies have carbonate and/or anhydritic cement, suggesting the Lower Watrous Formation in south-eastern Saskatchewan has the potential to act as an effective seal against cross-formational fluid flow. In particular, a fine grained unit, informally identified as the 'Upper Muddy Unit', appears to especially impermeable.

For the 1D reactive transport modelling, the vertical upward direction into the caprock is modelled. Diffusion into the caprock can be described by Fick's law for diffusion in sediments (Domenico and Schwartz, 1990):

$$J = -D'_d \text{ grad}(C) \quad [6]$$

where  $J$  is the diffusional flux (moles/dm<sup>2</sup>/T),  $D'_d$  is the effective diffusion coefficient (dm<sup>2</sup>/T), and  $C$  is the concentration (moles/dm<sup>3</sup>) of a species.

In this equation, the flux of each species is related to the concentration gradient by a diffusion coefficient peculiar to that gas. Various approximations to account for the porous medium have been developed and here an approach described by Helfferich (1966), based on the porosity only is used:

$$D'_d = \frac{n}{2} D_d \text{ to } D_d \left[ \frac{n}{(2-n)} \right]^2 \quad [7]$$

where  $D_d$  is the effective diffusion coefficient in water and  $n$  is the porosity.

Taking into account that the diffusion coefficient of CO<sub>2</sub> is 1.8 x 10<sup>-9</sup> m<sup>2</sup>/s (at 20°C) and assuming a porosity of 8%, the highest value of the effective diffusion coefficient range for CO<sub>2</sub> (i.e. 3.6 x 10<sup>-11</sup> m<sup>2</sup>/s) is used for the modelling. This value is also applied for the calculation of the diffusion of all other species.

The Midale Evaporite Unit was modelled as if it was a complete caprock with an estimated thickness of 8 m. For the modelling, a 10 m section was considered, which consisted of 10 cells each 1 m thick. The 1D diffusional model

was run for a simulated 5000 years. During this period, CO<sub>2</sub> was present at the base of the Midale Evaporite unit at a constant fugacity corresponding to a pressure of 150 bar (Duan et al., 1992).

Based on the calculated reactivity, diffusion modelling gave an estimate for three parameters. These are the progression of the dissolved CO<sub>2</sub> front in the caprock, the thickness of the lower section of the caprock affected by geochemical reactions and the potential porosity change, based on a molar volume balance calculation. In the basal metre of the caprock, some carbonate dissolution is expected to occur, leading to a minor porosity increase. This is approximately +0.3 porosity units over several thousands of years. Several metres higher in the caprock, some feldspar alteration is likely to occur; this however induces a porosity decrease. This is approximately -0.2 porosity units over several thousands of years. The impact of geochemical interactions that occur as a consequence of dissolved CO<sub>2</sub> diffusion into the base of the Watrous Formation, is therefore deemed to be minor (Figure 34).

### 3.3.2 Other formations

#### 3.3.2.1 THE WATROUS AND VANGUARD AQUITARDS (TRIASSIC AND JURASSIC)

Significant salinity differences between the underlying and overlying aquifers indicate that the Triassic–Jurassic aquitards seem to be robust, at least locally. The salinity differences are mainly due to anhydrite in the Triassic and Jurassic strata. However, the attributes of these aquitards are not so clear throughout the Williston Basin, due to lack of data and facies complexity. Nevertheless, in peripheral areas where they are thin, and probably with enhanced permeabilities caused by local variations in lithology and fracturing, they allow discharge of the confined Mississippian aquifer.

#### 3.3.2.2 THE JOLI FOU AQUITARD (LOWER CRETACEOUS)

The similarity in hydraulic heads and salinity distributions in the Mannville and Viking aquifers is inconclusive in establishing the nature of the intervening Joli Fou aquitard. This aquitard may be weak, as suggested by the observed similarities; however it may be strong, as in the Alberta Basin to the west in which case the homogeneities may be caused by a similar origin and hydrodynamic characteristics of two discrete flow systems. However to the south, the Joli Fou aquitard is absent. The Mannville and Viking sandstones laterally form a single unit, the hydrogeologically continuous Dakota Sandstone.

### 3.3.2.3 THE CRETACEOUS AQUITARD

The Cretaceous aquitard system overlying the Viking Sandstone mainly comprises thick shale successions within the Colorado and Montana groups. These include the Bearpaw, Pierre, Belle Fourche, Carlisle, and Mowry shales. This aquitard also includes closed or minor aquifers. It has a strong confining effect due to its shaly nature and to the vertically inward transient flow that acts as a sink, thereby precluding cross-formational flow.

## 3.4 GEOCHEMICAL REACTIONS OF THE MIDALE EVAPORITE CAPROCK

(Christopher A Rochelle, Mohamed Azaroual and Pierre Durst)

During and after CO<sub>2</sub> injection operations, the presence of supercritical CO<sub>2</sub> will result in chemical disequilibria and the initiation of various reactions. It is important to understand the direction, rate and magnitude of such reactions. This is both in terms of their impact upon the ability of the Midale Evaporite unit, the Watrous Formation and the overlying lithological units to safely contain the injected CO<sub>2</sub>, and also in terms of the longevity of CO<sub>2</sub> containment. For example, precipitation of carbonate minerals may reduce porosity and permeability and, as a consequence, help the long-term containment of CO<sub>2</sub>.

A two-pronged approach has been used to study the impact of CO<sub>2</sub> upon caprock geochemistry:

- Laboratory experiments to simulate in situ conditions within the caprock. These are important in that they can provide the detailed, well-constrained quantitative information to aid modelling studies. These have only been conducted on samples of the Midale Evaporite Unit.
- Predictive modelling of evolving conditions within the lithology immediately overlying the reservoir. This uses data from the above experiments to improve, constrain, and build confidence in geochemical models of the shorter-term evolution of the Weyburn reservoir system. These can then be extended to predict impacts of CO<sub>2</sub> in the longer-term, after injection operations have ceased. Predictive modelling has been conducted on both the Midale Evaporite Unit and the Watrous Formation.

## 3.4.1 Experiments

A series of laboratory experiments has been undertaken in which samples of well-characterised Midale Evaporite Unit borehole material were reacted with both CO<sub>2</sub> and synthetic reservoir formation waters under simulated in situ conditions (Rochelle, Pearce, Birchall et al., 2004). The static batch experiments used fixed quantities of rock, brine and CO<sub>2</sub> that were allowed to react for a prolonged period (Rochelle et al., 2002). This approach facilitates the development of steady-state conditions; i.e. towards a point where fluid composition is stable, and where the rates of dissolution/precipitation reactions fall towards zero. The aims of this work were to identify and characterise fluid-mineral reactions caused by the presence of CO<sub>2</sub> and to provide well-defined benchmarks that can be used as test cases for comparison with predictions from geochemical computer models.

The Midale Evaporite Unit immediately overlies the Midale Marly Unit, and is the primary caprock for much of the Weyburn oilfield. It is likely that free phase CO<sub>2</sub>, as well as dissolved CO<sub>2</sub>, will come into direct contact with the Midale Evaporite Unit because the injected CO<sub>2</sub> will be more buoyant than the formation waters and rise to the base of the Midale Evaporite Unit. The experimental programme attempted to reflect this, by concentrating on static experiments with CO<sub>2</sub>-saturated formation waters. This will have tended to maximise the amounts of reaction in the experiments, facilitating the observation of any geochemical changes.

Twenty-two batch experiments were completed using samples of Midale Evaporite Unit material from the Weyburn oilfield (Rochelle et al., 2003). The experiments were conducted at conditions representative of the reservoir (i.e. 60°C, 150 bar) or close to injection wells (60°C, 250 bar), and covered time periods of over six months. A range of grain sizes of Midale Evaporite Unit samples were used (i.e. <250 µm, 250–500 µm, and small monoliths) and fluid:rock ratios were typically 10:1 or less. The Midale Evaporite Unit samples were reacted with synthetic formation water of realistic composition, and the experiments pressurised with either CO<sub>2</sub> ('reactive' experiments) or nitrogen (non-reacting 'baseline' experiments).

The evolution of a selection of solutes was followed. Relative to the nitrogen 'baseline' experiments, it was found that the impact of CO<sub>2</sub> was to:

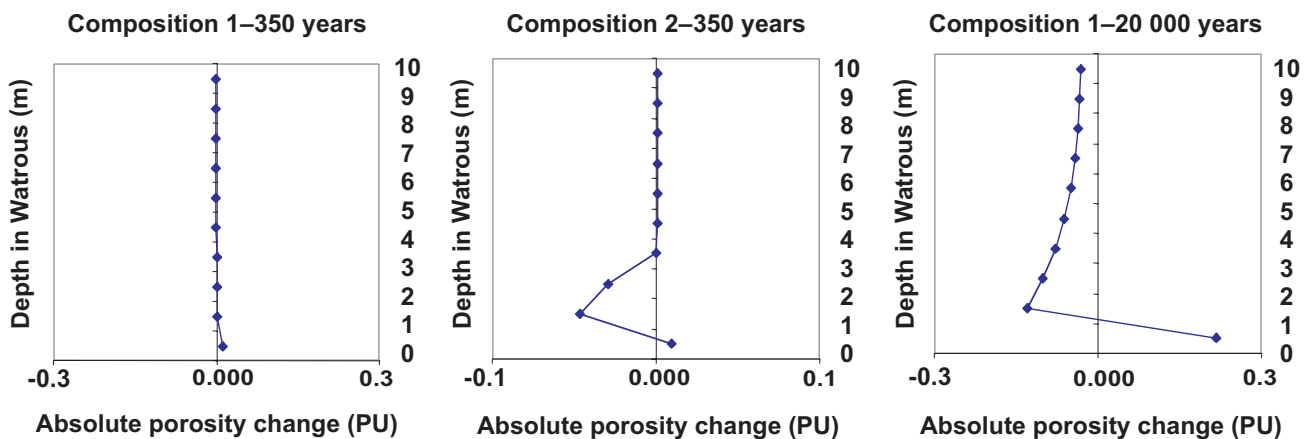
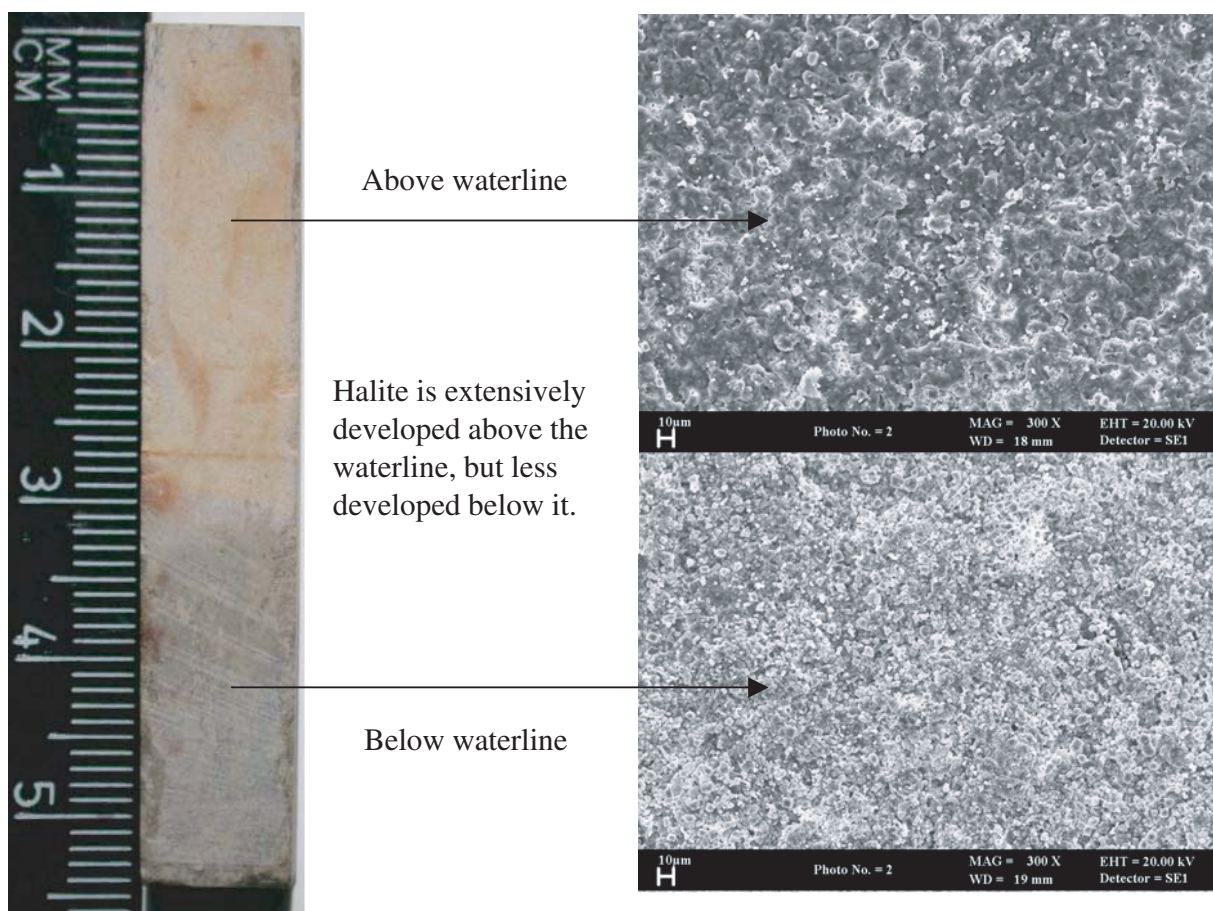


**Figure 34** Calculated porosity changes in the base of the Lower Watrous Formation for composition 1 (left) and composition 2 (middle) after 350 years and for composition 1 after 20 000 years (right).

**Figure 35** Scanning electron photomicrographs of two samples of a monolith sample of the Midale Evaporite Unit (right), demonstrating a well developed ‘tide mark’ after exposure to CO<sub>2</sub> and their relationship to the monolith sample (left).



- increase the concentrations of magnesium, manganese, silicon, HCO<sub>3</sub><sup>-</sup> and possibly aluminium (e.g. Figure 16)
- decrease the concentrations of total sulphur and pH values
- have little impact on the concentrations of calcium, strontium and barium (e.g. Figure 15)

Many of the solutes, most notably magnesium, reached steady-state conditions within about one month, indicating relatively rapid control by dolomite dissolution. It was noted that the changes in major element chemistry are different to those found in the Midale Marly Unit or Midale Vuggy Unit experiments. This suggests that one or more different reaction mechanisms were operating between the different studies. Although aluminosilicate minerals comprise a small proportion of the rock, dissolution/precipitation reactions appeared to be happening more slowly. Indeed, silicon concentrations appeared not to reach steady-state conditions, even after six months reaction.

Following reaction in CO<sub>2</sub>-rich synthetic pore waters, a clear ‘tidemark’ developed on the external surfaces of the monolith blocks, with the area above the water-CO<sub>2</sub> interface developing a lighter, creamy colour (Figure 35). Scanning electron microscopy revealed that this was due to a fine coating of halite that developed during the experiment.

Generally, there was relatively little petrographic evidence for dolomite corrosion, although anhydrite was slightly corroded in some experiments using CO<sub>2</sub>-rich pore water. Euhedral, elongate prismatic gypsum crystals developed in both the CO<sub>2</sub>-rich and nitrogen baseline

experiments, but were particularly well developed on the external surfaces of the monolith blocks in the CO<sub>2</sub>-rich experiments. These crystals grew up to 2 mm long after four weeks reaction in the CO<sub>2</sub> monolith experiments, but also grew up to 5 µm long in the experiments containing crushed grains. After 26 weeks of reaction there was little difference in the <250 µm crushed samples between the nitrogen experiment and the CO<sub>2</sub> experiment, except for a possible slight decrease in the proportion of very fine dolomite rhombs, which may suggest dissolution had been restricted to the finer grains.

### 3.4.2 Modelling

The Marly Evaporite Unit experiments used the highest salinity brines in this study (approximately 115 g/l). The simplified average mineralogy of the Midale Evaporite Unit used in the modelling is as follows: dolomite (60%), quartz and aluminosilicates (34%), anhydrite (5%) and calcite (1%).

Figure 36 illustrates that chalcedony, dolomite and sulphates (anhydrite and gypsum) achieved thermodynamic equilibrium relatively rapidly. Pyrrhotite, siderite and strontianite remained undersaturated. Calcite shows a stationary state, as in the case of the Midale Marly Unit experiments, giving a constant value of calcite saturation index (SI approximately -0.5) for the whole of the experiment. Although this mineral is a minor component of the Midale Evaporite Unit, it still appears to show similar behaviour to that in the Midale Marly and Vuggy units (Section 2.4). Chalcedony remained at thermodynamic equilibrium for the entire experiment.

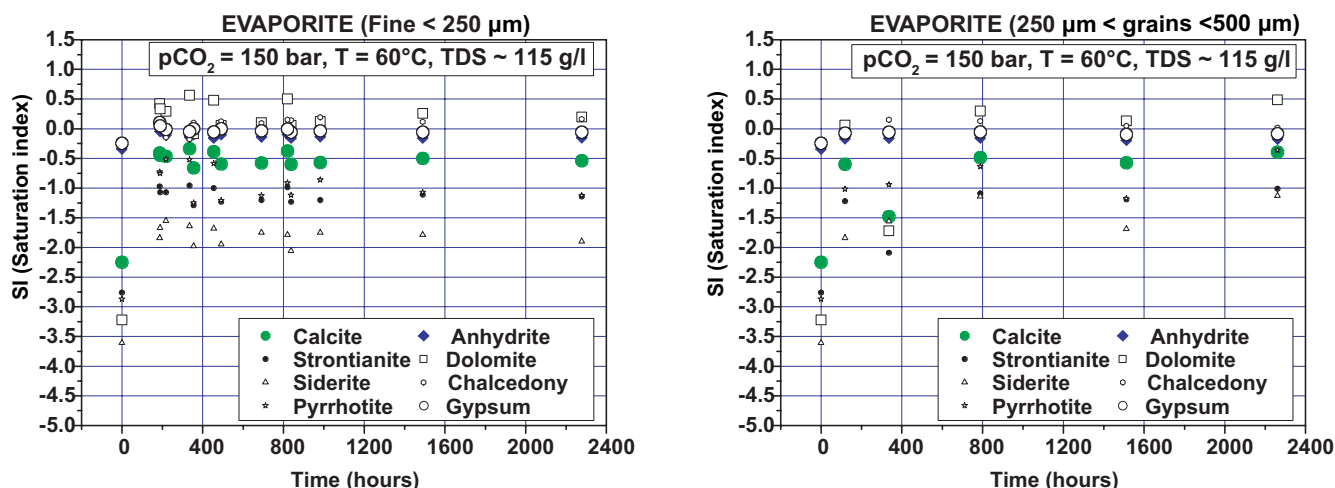


**Figure 36** The saturation index (SI) of potentially dissolving and/or precipitating minerals in the experiments.

The above modelling of a small-scale system was extended to the field scale through modelling of the diffusion of CO<sub>2</sub> into the caprock. This assumes that the caprock does not show any fracturing, as fractures might act as preferential pathways for either dissolved or supercritical CO<sub>2</sub>.

The modelled reactivity due to the diffusion (equations 4 and 5) of dissolved CO<sub>2</sub> into the base of the Midale Evaporite Unit resulted in some carbonate dissolution in the lowermost metre of that unit. Higher in the section, alteration of feldspars dominates the reactivity. Porosity changes due to this reactivity were minor, with a predicted increase in porosity in the lower metre of approximately 0.4% after 5000 years. Overall reactivity is of the same order as for the Watrus Formation.

### 3.5 GEOCHEMICAL REACTIONS OF BORE-HOLE CEMENT

(Christopher A Rochelle)

A limited number of relatively simple laboratory experiments were undertaken to assess the potential for geochemical changes resulting from the reaction of CO<sub>2</sub> with borehole cements typical of those used at the Weyburn oilfield. The pressures and temperatures used within the experiments were representative of actual in situ conditions at Weyburn (i.e. 60°C, 150 bar). These conditions will exist even after oil production and CO<sub>2</sub> injection have ceased. The experiments were of relatively short

**Table 6** Changes in weight of cement monolith samples after two weeks reaction with ‘free CO<sub>2</sub>’ and dissolved CO<sub>2</sub>. The nitrogen-pressurised experiments represent relatively non-reacting ‘baseline’ systems. SMFW = Synthetic Marly Formation Water.

Fill cement experiments				
Run no.	Monolith id.	Aqueous fluid	Gas	Weight change (%)
1133	A	None	CO <sub>2</sub>	+ 11.4
	B	None	CO <sub>2</sub>	+ 11.2
1134	C	SMFW	CO <sub>2</sub>	+ 9.9
	D	SMFW	CO <sub>2</sub>	+ 9.6
1139	A	SMFW	N <sub>2</sub>	+ 1.7
	B	SMFW	N <sub>2</sub>	+ 1.3

Tail cement experiments				
Run no.	Monolith id.	Aqueous fluid	Gas	Weight change (%)
1135	A	None	CO <sub>2</sub>	+ 3.8
	B	None	CO <sub>2</sub>	+ 4.2
1136	C	SMFW	CO <sub>2</sub>	+ 0.6
	D	SMFW	CO <sub>2</sub>	+ 0.8
1138	A	SMFW	N <sub>2</sub>	- 0.3
	B	SMFW	N <sub>2</sub>	- 0.4

duration (14 days), so only limited reaction was observed. However, enough reaction took place to provide some insights into the reactions of borehole cements with CO<sub>2</sub>.

Two samples of cement (termed 'fill cement' and 'tail cement') were prepared, and then cured under in situ conditions for 28 days. After the curing stage, they were cut into 1x1x5 cm monoliths for reaction in the experiments. These involved reaction with either; supercritical CO<sub>2</sub>, maximum amounts of dissolved CO<sub>2</sub> (i.e. in equilibrium with 150 bar of supercritical CO<sub>2</sub> at 60°C), or nitrogen-pressurised synthetic formation water ('non-reacting' base case for comparison) (Rochelle, Pearce, Bateman et al., 2004).

No significant changes in the size of the cement monoliths were found after this (albeit relatively short term) exposure to CO<sub>2</sub>. Although this does not preclude the possibility that carbonation shrinkage will occur, it does provide some evidence that this process might not be an important issue over shorter timescales

The cement monoliths gained significant amounts of weight upon exposure to CO<sub>2</sub>, with the fill cement having a greater weight increase compared to the tail cement (Table 6). However, for both fill and tail cement, greater weight gain occurred with just supercritical CO<sub>2</sub> compared to dissolved CO<sub>2</sub>. Given that the monoliths did not change in size, they must have increased in density. This appears to have been associated with a decrease in porosity in the outer parts of the monoliths, where a carbonated layer formed. It is possible that such layers may be beneficial in that they might act to protect borehole cement against complete carbonation over the longer term.

A few relatively simple flexure tests were carried out to assess the cement strength changes upon carbonation. Although data were few, it was noted that the fill cement was about twice as strong as the tail cement, both before and after exposure to CO<sub>2</sub>. Overall however, no significant changes in the tensile strength of the cement monoliths were found after albeit the relatively short term exposure to CO<sub>2</sub>.

## 4 Monitoring and characterisation of near-surface processes

### 4.1 SOIL GAS MONITORING

(David G Jones, Jean-Claude Baubron, Stan E Beaubien, Roberto Bencini, Carlo Cardellini, Domenico Granieri, Salvatore Lombardi, Lynden Penner, Fedora Quattrocchi, Michael H Strutt and Nunzia Voltattorni)

#### 4.1.1 Introduction

Soil gas concentrations and flux monitoring (i.e. surface monitoring) was carried out from 2001 to 2003 in and around the Phase 1A injection area of the Weyburn Oilfield. The objectives of this work were to:

- establish baseline soil gas values using grid sampling and profiles, and to compare these results with future datasets
- evaluate natural variations in soil gas including seasonal effects
- understand geochemical reactions and gas flow pathways in geological successions
- identify sites of higher gas flux that may be indicative of deep gas escape
- enable long term monitoring to evaluate possible escape of injected CO<sub>2</sub>
- address possible public concerns over geological storage of CO<sub>2</sub>.

More detailed accounts of this work may be found in Jones et al. (2003), Strutt, Baubron et al. (2003), Strutt, Beaubien et al. (2003) and Beaubien et al. (2004).

#### 4.1.2 Methodology

Three principal techniques were used to address these objectives:

- analysis of the concentrations of various gas species in the pore spaces of the shallow unsaturated soil horizon (soil gas)
- measurement of the mass transfer rate of CO<sub>2</sub> across the soil-atmosphere interface (gas flux)
- long-term monitoring of radon flow rates, as a proxy for CO<sub>2</sub>, using probes buried for up to a year at 2 m depth in the soil.

The gas of principal interest in this project is CO<sub>2</sub>, because it is being injected in large quantities into the underlying deep oil reservoir and due to concern that it might eventually migrate to surface. However CO<sub>2</sub> is highly soluble and can be consumed via acid-base reactions. Thus its movement, if any occurred, might be attenuated during the short period of the present monitoring. Furthermore, the interpretation of CO<sub>2</sub> data is complicated by the fact that this gas is involved in metabolic reactions, both via soil microbes and plant roots. Because of these possible sources and sinks of CO<sub>2</sub>, a large suite of other soil gas species were analysed which might help define possible flow paths that CO<sub>2</sub> may follow in the future or help resolve the origin of the present CO<sub>2</sub> anomalies. These included less reactive gases associated with the reservoir, which could be used as tracers of deep flow, such

as helium (He), methane (CH<sub>4</sub>), and radon (Rn), as well as gases that might be involved in shallow biological reactions such as ethylene (C<sub>2</sub>H<sub>4</sub>) and oxygen (O<sub>2</sub>).

Preliminary baseline soil gas data were collected in the summer and autumn of 2001 above the Phase 1A injection area of the Weyburn oilfield. At each site a hollow stainless steel probe was pounded into the soil to a depth greater than that which would be influenced by significant atmospheric gas contamination. (Figure 37). This was estimated as being in excess of 0.6 m at Weyburn. In situ monitoring of CH<sub>4</sub>, CO<sub>2</sub>, CO<sub>2</sub> flux, O<sub>2</sub>, <sup>222</sup>Rn and thoron (<sup>220</sup>Rn) was carried out on a 360 point grid (Figure 38) at 200 m spacing, with points extending to the south-west of the initial injection area. Soil gas samples were also collected in evacuated stainless steel canisters for laboratory analysis of He, light hydrocarbons, nitrogen (N<sub>2</sub>), O<sub>2</sub> and sulphur (S) species. After a rapid appraisal of the initial grid results, data were collected in the autumn of 2001 on traverses of more closely spaced sampling points (25 m apart) that crossed anomalies seen on the grid (Profiles A to F on Figure 38). Selected CO<sub>2</sub> and radon anomalies on these profiles were investigated in more detail for signs of natural pathways for deep gas escape. Continuous radon monitoring probes were installed at sites where He and radon data, in particular, indicated the potential for deep gas migration.



D G Jones, BGS © NERC

**Figure 37** Soil gas measurement in the Phase 1 CO<sub>2</sub> injection area of the Weyburn oilfield. Note the in situ soil gas probe to the right of the portable gas analyzer (red).

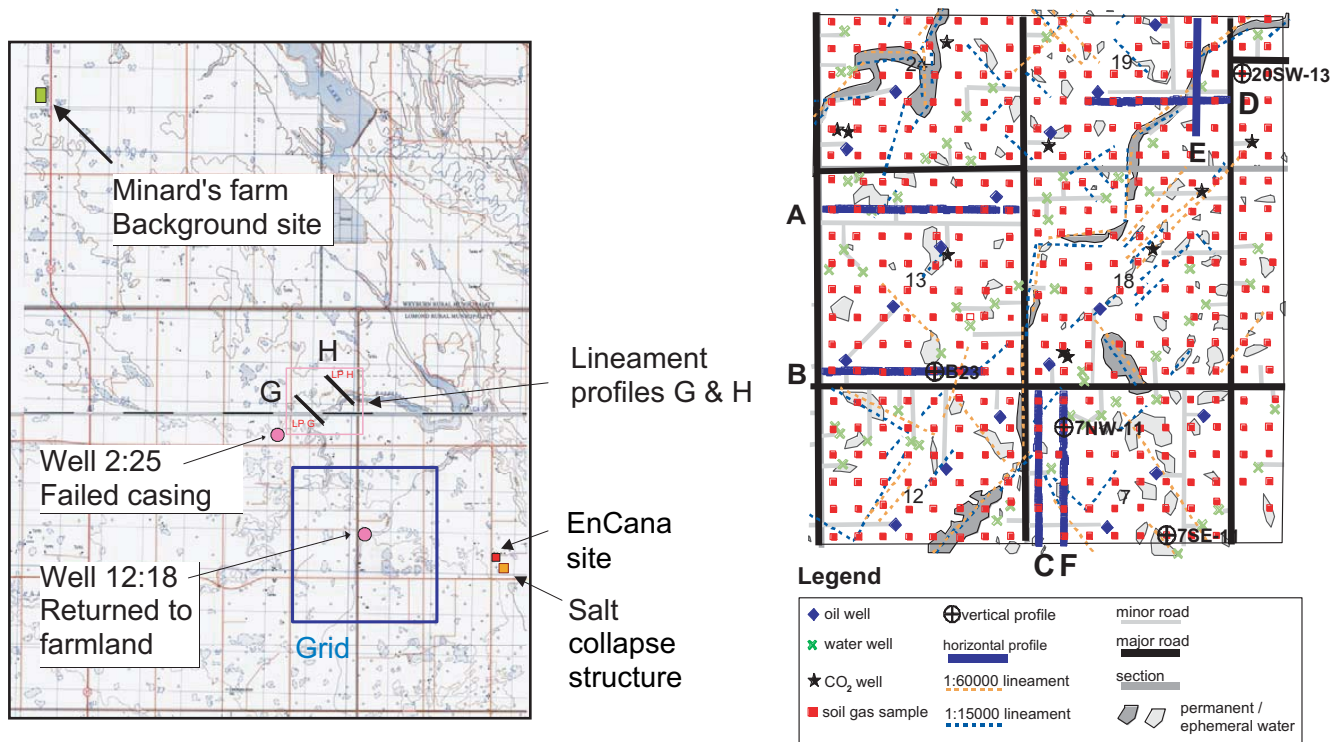


**Figure 38** Maps illustrating the locations of the various studied sites, and detail of the grid area showing sampling points, surface water, wells and air photo lineaments. The airphoto lineaments were kindly provided by J D Mollard and Associates of Regina, Canada.

The 360 point sampling grid, and most of the more detailed profiles, were repeated in the autumns of 2002 and 2003. The radon monitoring probes have been in operation virtually continuously since the autumn of 2001.

#### 4.1.3 Results

Marked changes were seen in CO<sub>2</sub> concentration and surface flux levels between each of the three datasets (Figure 39). Higher values were seen during the growing season in July 2001. Lower levels were apparent in autumn 2002 and values were further reduced in autumn 2003, when conditions were cooler and the growing season almost over. These results suggest the importance of shallow biological reactions that produce CO<sub>2</sub> as a metabolic by-product. In contrast, the radon and thoron data were found to be similar for the three years. These gases were studied primarily because they have a short half life (e.g. 3.5 days for radon) and thus the occurrence of a significant anomaly may indicate transport of deep radon carried by a stream of CO<sub>2</sub> along a highly permeable pathway, such as a fault. Instead, the relatively constant distribution of these phases during periods when the CO<sub>2</sub> concentration and flux was successively reduced, implies that these gases have a shallow in situ origin.

The temporal variation of CH<sub>4</sub> was significantly different. Although there was a decrease in outlier values with each successive campaign, there appeared to be a very slight increase over the same period. This trend may be due to the seasonal drying of the soil and subsequent increase in soil air permeability, resulting in the greater downward diffusion of atmospheric air with its constant methane concentration of approximately 2.5 ppm. The distribution of ethane (C<sub>2</sub>H<sub>6</sub>) was similar to that of CH<sub>4</sub>, although the difference from year to year with respect to outliers is far more pronounced while the distribution of the

bulk of the samples is more constant. The variations in C<sub>2</sub>H<sub>4</sub> and propane (C<sub>3</sub>H<sub>8</sub>) were markedly similar to those of CO<sub>2</sub> and CO<sub>2</sub> flux, with both the outliers and bulk of the samples decreasing significantly from year to year during each successively later season. This also implies a shallow biological origin for these gases. As the correlation between soil gas CO<sub>2</sub> and these two hydrocarbons is low, it is likely that they are produced via different metabolic pathways.

The spatial distributions of CO<sub>2</sub> and CO<sub>2</sub> flux showed a similar pattern and a good correlation from year to year (Figure 39). The majority of the anomalies are in areas that have extensive ephemeral surface-water bodies. Some of these water bodies are elongate and were mapped as surface lineaments in a separate air-photo interpretation study by Mollard and Associates of Regina. Although one interpretation of these features was that they may represent the surface expression of deep faults, present data appears to indicate that the elevated values in these areas are more likely due to shallow biological reactions in the moist, organic-rich soil. There was no clear correspondence between the soil gas CO<sub>2</sub> anomalies and the location of the CO<sub>2</sub> injection wells.

The distribution of radon and thoron anomalies lacked any clear elongated trends that might indicate the presence of a gas permeable fault or fracture system. Although radon had far fewer anomalies than CO<sub>2</sub>, some of the high radon values correspond with CO<sub>2</sub> highs, however there are also many CO<sub>2</sub> anomalies which do not have a matching radon anomaly. The distribution of thoron, by contrast, is different from both of these gases. Continuous profiling by gamma spectrometry has not, so far, shown any marked anomalies in uranium (U) or thoron series radionuclides that might be linked to radon escape through a fault or fracture system. The advantage of this method is that it could reveal a gas migration route missed by even closely spaced point gas sampling.

Carbon dioxide highs on the detailed profiles are matched by O<sub>2</sub> lows, whereas N<sub>2</sub> remains essentially constant. The same relationship is also clear in data for the grid (Figure 40). This provides strong evidence for a biogenic origin for the CO<sub>2</sub> via reactions in which O<sub>2</sub> is consumed. If significant migration of CO<sub>2</sub> from depth were occurring, both O<sub>2</sub> and N<sub>2</sub> would be diluted as CO<sub>2</sub> levels increased, similar to areas of natural deep CO<sub>2</sub> escape such as Cava dei Selci in Italy (Figure 40).

Three soil gas samples were collected in the summer of 2001 in locations with elevated CO<sub>2</sub> concentrations, for the analysis of δ<sup>13</sup>C in CO<sub>2</sub>, in order to better understand the origin of the gas. The isotopic values obtained were all well within the range of those to be expected from soil gas CO<sub>2</sub> produced by microbial or root metabolism of organic matter from local plants. However, it is difficult to draw firm conclusions from this small number of samples.

In 2003, a control or background area was sampled for the same suite of gases 10 km to the north-west of the oil-field (Figure 35). It has similar topography, land use and soil composition to the main sampling grid. Field gamma spectrometry indicated that soil composition was comparable, at least with respect to potassium, uranium and thorium. This site was in an area largely undisturbed by oil exploitation, allowing a general background comparison to the main grid dataset. There were 35 sample locations on a 7 x 5 point grid at the control site with 100 m spacing, plus two additional sites. The soil gas results from the control area were generally quite similar to those from the main grid on the oilfield suggesting that there is no general elevation of CO<sub>2</sub> levels in the soil covering the injection area and thus further supporting the lack of any escape of deep CO<sub>2</sub>.

Together with the control site, five zones of possible CO<sub>2</sub> leakage were also surveyed and sampled (Figure 38): two profiles across a river lineament that may be associated with deep faulting, two decommissioned oil wells and one site which overlies a deep salt dissolution feature.

The north-east–south-west trending river lineament, identified from air photos and satellite imagery immediately north of the main grid, generally follows an incised river valley. Although such lineaments may reflect near surface features, there is some correspondence of their location and direction with faulting in the Midale Beds. This suggests they may be a surface reflection of deep fracturing and thus have the potential to act as pathways for deep gas escape. Anomalous CO<sub>2</sub> was associated with the valley floor and minor depressions, where there was lush vegetation and a coincident depletion of O<sub>2</sub>. The relationship between CO<sub>2</sub> and other gases was variable. One CO<sub>2</sub> anomaly had a coincident He anomaly, but others had no related He feature. In general, CH<sub>4</sub> and radon were low when CO<sub>2</sub> was higher. Therefore the evidence is consistent with biogenic CO<sub>2</sub>, but there are features, such as the coincident He/CO<sub>2</sub> anomaly, and rising He levels on one traverse, that merit more detailed study.

Two perpendicular profiles of 10 sites at 25 m spacing were sampled for soil gas over the mapped centre of the salt dissolution feature which had been identified in the Prairie Evaporite Formation (Devonian) from seismic data. Background values of all gases were seen over the salt dissolution feature except for some small He anomalies that are difficult to interpret because there are no related features for other gases.

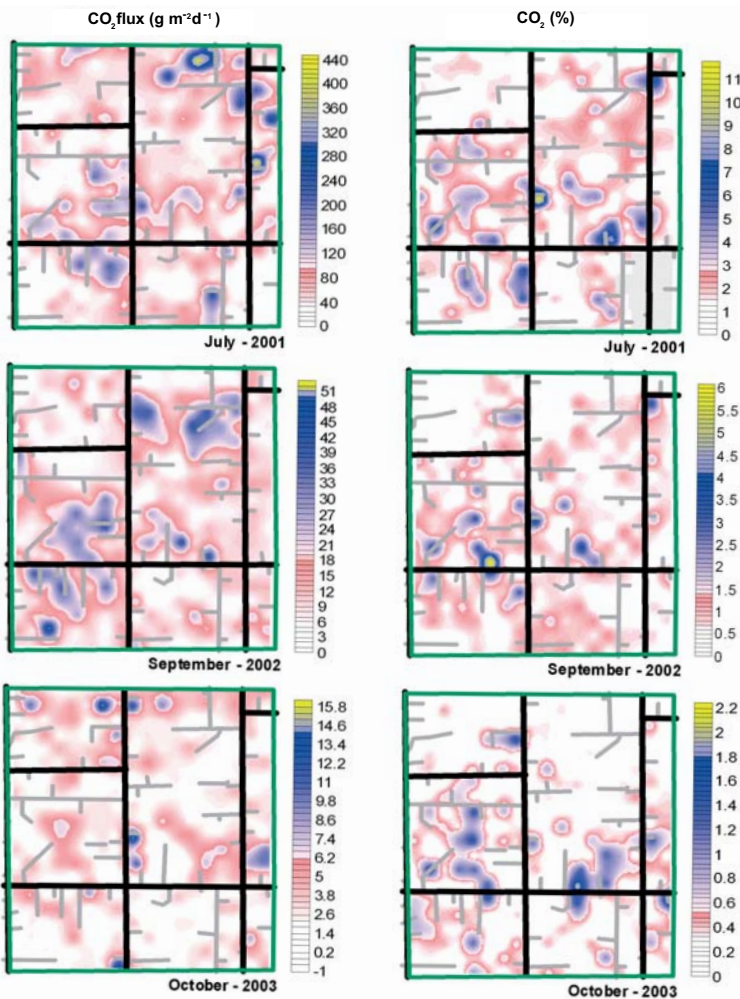


**Figure 39** Contoured distribution of CO<sub>2</sub> flux and soil gas CO<sub>2</sub> for the three sampling campaigns.

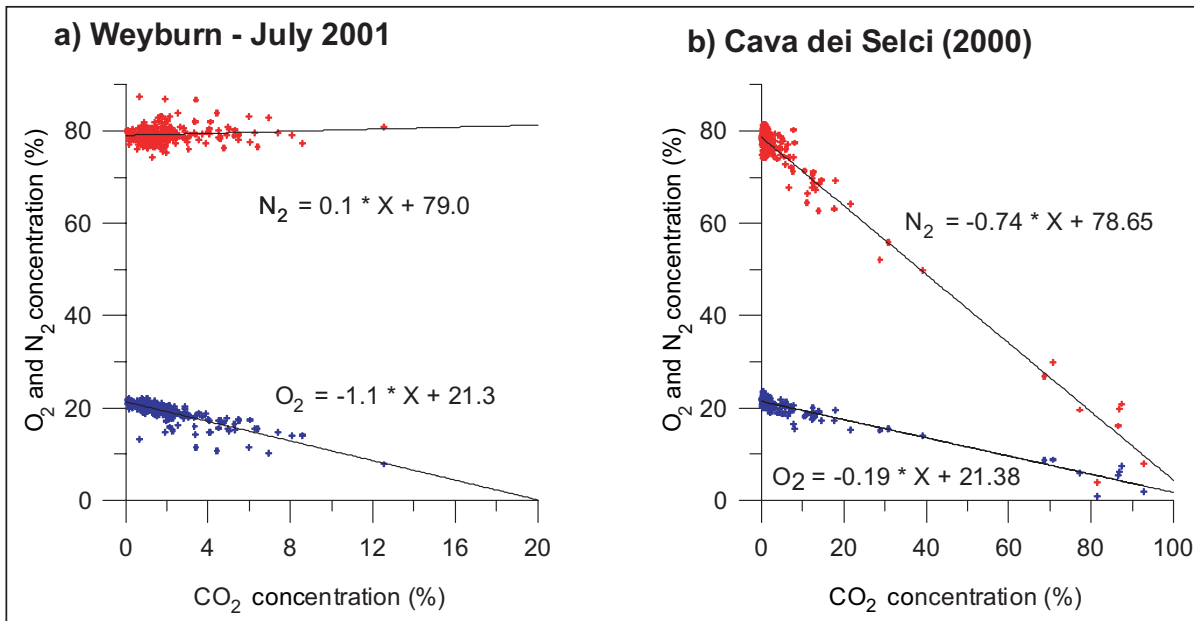


**Figure 40** Plot illustrating the relationship between CO<sub>2</sub>, O<sub>2</sub> and N<sub>2</sub> for the grid dataset from Weyburn in July, 2001 as compared to data collected from Cava dei Selci in Italy, a dormant volcanic site which has known gas vents due to deep thermometamorphic reactions. The trend of the Weyburn data is towards a maximum value of 20% CO<sub>2</sub>, implying that there is a stoichiometric consumption of O<sub>2</sub> and production of CO<sub>2</sub>. By contrast, the Cava dei Selci data trends towards a maximum of 100% CO<sub>2</sub>, indicating that the CO<sub>2</sub> is coming from outside the shallow system and diluting the O<sub>2</sub>, not consuming it.

Measuring soil gas around the two decommissioned oil wells allowed borehole integrity to be investigated. A 16-site grid was surveyed around each well. One well had been completely abandoned and the other was suspended due to failed casing. The well with failed casing had weakly anomalous CO<sub>2</sub> at two sites but this was unmatched for other gases. The fully abandoned well had background CO<sub>2</sub> values. Statistical populations of CO<sub>2</sub> and radon were generally higher for the suspended well while those for CH<sub>4</sub> and C<sub>2</sub>H<sub>6</sub> were higher for the abandoned well, as compared to the main grid, although all individual values lay well within the range observed for the grid. There was one He anomaly at the abandoned well site. The lack of correspondence between anomalies of different gases does not support significant leakage from depth along the well, but the results suggest more detailed follow up would be desirable.

Electronic radon sensors with internal memory (Barasol probes) were installed at six sites in September 2001 and data have been recorded for extended periods since then. The sites were selected from the detailed soil gas profiles located across radon and CO<sub>2</sub> anomalies seen in the initial main grid data. Detailed CO<sub>2</sub>, He, radon and thoron measurements were made around specific anomalies and radon probe sites chosen that reflected potential deep gas escape (He anomalies, higher radon) as well as 'background' sites for comparison. The clearest anomalies on two traverses with similar soil and crop types (mainly wheat) were chosen. The probes were installed in holes up to 1.9 m deep, lined with plastic pipe, the top of which was located about 40 cm below the ground surface. Once in place the pipe was covered by Goretex™ waterproof (but gas permeable) membrane and covered with soil. This allows the soil gas to flow freely to atmosphere. The instrument can record data for up to a year, which is downloaded after retrieval of the probe. After data downloading and recharging of the batteries, the probe is reinstalled and recording continues.

Measurements of radon concentration, temperature and atmospheric pressure were made every hour. The data were

modelled to provide information on gas transport mechanisms (diffusion, advection) and rates. They show seasonal variations in radon concentrations, which were modelled against atmospheric parameters, indicating the importance of pressure, rainfall and temperature on gas migration. Moreover, CO<sub>2</sub> fluxes deeper in the soil were calculated and compared to surface rates. Ultimately, the probes may reveal possible modifications of the gas transfer pressure conditions constraining the gas velocity, eventually with a contribution from the reservoir. They could then detect the first precursors of any possible CO<sub>2</sub> escape to the surface. Data from the probes showed seasonal variations in the gas flow regime and in soil permeabilities. Maximum gas velocities were in the range 5–15 cm/h, values typical of faults, whilst at the other end of the spectrum, background values were obtained that reflect diffusive gas transport. Since mid-2003, radon concentration excursions lasting for less than three hours have been observed. These suggest transient pressure phenomena, with low fluxes and high velocities. Carbon dioxide fluxes at 2 m depth were calculated to be 10–20 times lower than those at surface. This is consistent with declining biogenic CO<sub>2</sub> production with depth and suggests it may be better to monitor flux at this depth where biogenic influences are muted.

#### 4.1.4 Conclusions

A large background dataset has been obtained from soil gas monitoring at the Weyburn site. This has revealed seasonal variations in gas concentrations and fluxes. It provides an important baseline resource against which to compare future data and evaluate any escape of injected gas at the surface. All the evidence suggests that CO<sub>2</sub> in the soil gas is produced biogenically. There are no indications of any significant leakage of gas from depth. It is, however, important to maintain the monitoring effort and to focus on development of new rapid measuring techniques, enhancement of continuous monitoring and further assessment of potential pathways for deep gas migration.

## 4.2 TILL CHARACTERISATION IN THE WEYBURN OILFIELD

(Jonathan M Pearce, David G Jones, Simon J Kemp, James B Riding, Michael H Strutt and Doris Wagner)

### 4.2.1 Introduction

During 2001, soil gas monitoring (see section 4.1) indicated separate small areas with elevated levels of radon and thoron. Radon is a radioactive gas, produced naturally within some successions. It forms from the radioactive decay of thorium (Th) and uranium (U), which occur at variable concentrations in the geosphere. A possible source of variations in radon concentration may be natural variations in the concentrations of minerals that host thorium and uranium such as monazite and zircon. Permeability is also an important factor. The principle aim of this study therefore, was to determine if variations in the proportions of thorium and uranium-bearing minerals and the texture of till samples could explain variations in soil gas radon concentration. This study was a collaborative venture between the British Geological Survey and Dr Harm Maathuis of the Saskatchewan Research Council (SRC), Saskatoon, SK, Canada. Pearce et al. (2003) provides more detailed results and discussion of the material from four boreholes drilled at Weyburn. The boreholes studied were numbered A8, A13, B23 and B46 (Pearce et al., 2003). They were located adjacent to some of the long-term radon monitoring probe sites. These included sites where monitoring indicated significant advective gas flow as well as sites where only background diffusive flow was indicated.

### 4.2.2 Background

The till belongs to the Battleford Formation of the Saskatoon Group and is of late Pleistocene age. It forms part of a

proglacial, glacial and nonglacial succession which has been subdivided largely on carbonate content (Christiansen, 1992; Maathuis, 2003). The tills sampled were found to vary slightly in grain size and the degree of sorting, and they contain laterally discontinuous sandier interlayers. However, geochemical, mineralogical, palynological and sedimentological evidence strongly indicates that the material from all four boreholes is from a single till sheet.

### 4.2.3 Geochemistry, sedimentology and mineralogy of the tills, and their relationship to soil gas

The grain sizes of the till samples analysed are typical of those previously studied from other parts of southern Saskatchewan (Figure 41; Christiansen, 1967). The thorium and uranium concentrations in the sand fraction are too low to account for the whole rock concentrations. It is therefore likely that other phases also host thorium and uranium, the most likely being iron oxides developed from the breakdown of other iron-bearing minerals and clay minerals (Figure 42).

Although variable, the proportion of monazite is low (i.e. less than 1%) and cannot account for the whole rock thorium and uranium levels. It is likely that a significant proportion of the thorium and uranium is sorbed onto iron and manganese oxides, and possibly clay minerals. It is suggested therefore, that in order to determine the proportion of thorium and uranium present in this iron/manganese oxide and clay fraction, sequential extractions combined with geochemical analysis of thorium and uranium concentrations should be performed.

There is no evidence for any systematic difference in radionuclide content between boreholes; in any case, the small number of samples from each borehole would make this difficult to establish. The ranges of values for thorium

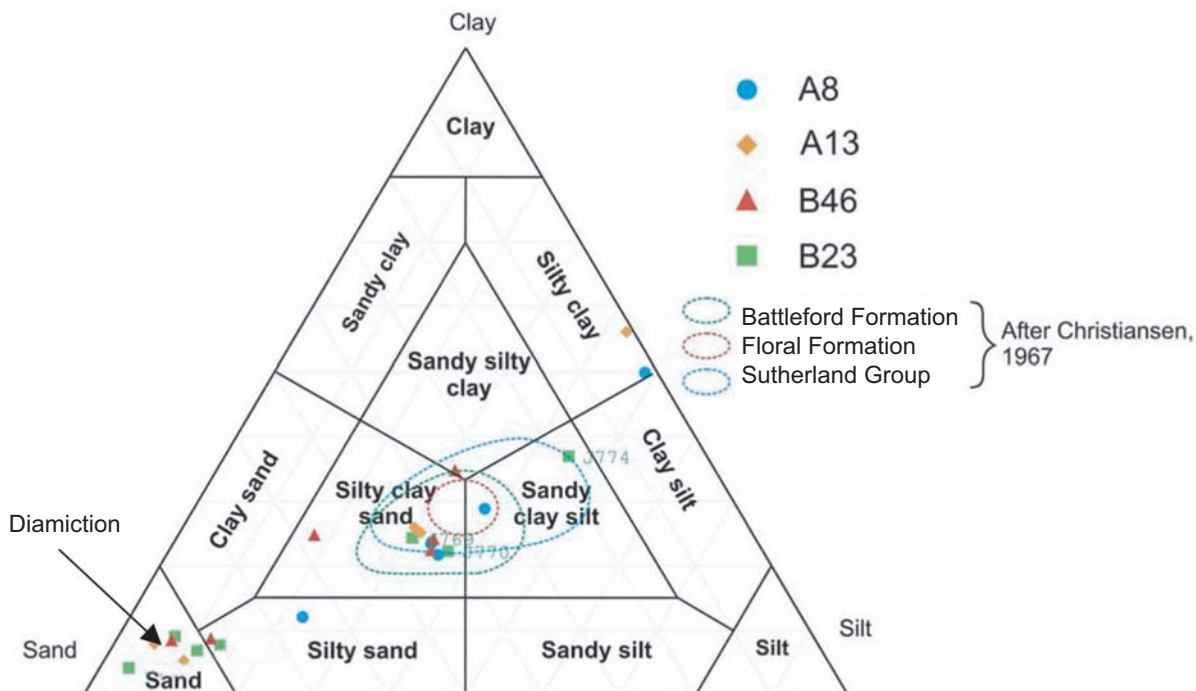


**Figure 41** Ternary diagram of grain size variations (after Shepard, 1954) for the <2 mm fraction. Note that one sample is a diamiction with >25% clasts larger than 2 mm in diameter. The grain sizes of other tills from southern Saskatchewan are from Christiansen (1967). The coloured symbols refer to borehole numbers A8, A13, B23 and B46 (Pearce et al., 2003).

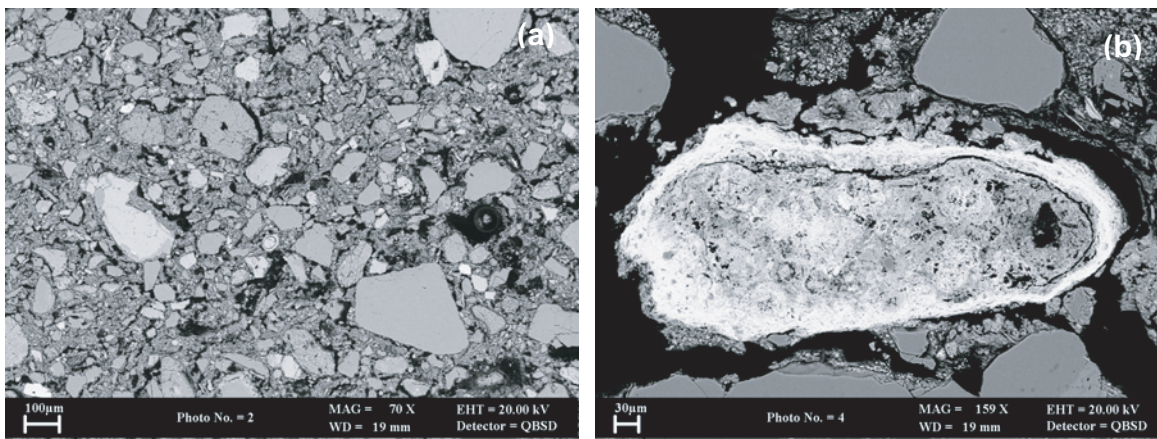


**Figure 42** (a) A typical view of till matrix with detrital angular to rounded, silt to sand sized grains in a clay matrix. Much of the coarse porosity here is an artefact of matrix shrinkage following sample drying.  
 (b) A relict, oxidised ferromagnesian grain now replaced by iron and manganese oxides, which may potentially sorb thorium and uranium released via the breakdown of monazite.

and uranium series radionuclides are similar for all four boreholes. Soil gas radon and thoron values for each site have been relatively variable from year to year, but all fall within the same broad range, with no sites being consistently higher or lower. This probably reflects small-scale variability in subsurface properties from year to year. Soil gas measurements are not made at precisely the same location (only within 1–2 m) and soil moisture/permeability will vary, reflecting the poorly sorted and heterogenetic nature of the till, in addition to differences in weather conditions prior to and during analysis from year to year. Radon measurements from the installed Barasol probes also show significant seasonal and shorter-term changes, with overlapping ranges of values at different sites. The selection of the borehole sites was made largely on the basis of different gas velocity regimes and indications, mainly from helium, of deep gas escape. This selection was based on the first two years of data. As the selection could not be extended to include sites with consistently different radon and thoron concentrations, it is unsurprising that there is no observed variation in thorium and uranium series radionuclides between sites.

Clast numbers and types were counted at the surface at all sites on the main soil gas grid during the 2003 survey and are summarised in Figure 43. There did not appear to be any systematic difference in the rock types represented across the area of the grid. However, clast numbers do vary considerably (Figure 43), consistent with the heterogeneity of the till. They are generally more abundant in the eastern half of the grid, but there are coherent patches of higher clast density throughout the area. The soil gas 'A' and 'B' profiles, where the four boreholes for this study were drilled, generally fall within areas characterised by low numbers of clasts.

There appears to be some consistency between the observed gas velocities and the grain size data, when the basal silt/clay samples are excluded. Borehole B23, with the highest velocities, has the coarsest average grain size, and hence probably the highest permeability, whereas the 'zero reference' borehole site (A8) and the lower velocity site (B46) have much finer average grain sizes and probably lower permeabilities. The data obtained so far suggest that for the four borehole sites, sediment texture, and hence permeability, is a far more important control on

radon concentrations and gas velocities. This varies seasonally according to prevailing ground conditions and, in particular, soil moisture levels.

#### 4.2.4 Palynology

A palynological investigation of 24 samples from four boreholes drilled into the till on the Weyburn oilfield was undertaken. All samples produced abundant and well-preserved palynomorphs of Devonian, Carboniferous, Late Cretaceous and Quaternary age. The relative proportions of these components proved similar throughout; Late Cretaceous dinoflagellate cysts and pollen grains are the dominant elements, indicating that the principal sedimentary input to the till is from Upper Cretaceous (Campanian-Maastrichtian) units. Devonian, Carboniferous and Quaternary grains are consistently subordinate. The Devonian palynomorphs are from Manitoba to the north-east and the Late Cretaceous palynomorphs appear to be derived locally. The abundance of palynomorphs is testament to consistently high levels of sedimentary rock input to the till successions. The relative homogeneity of the kerogen and palynofloras from the till samples has not allowed the palynological differentiation of informal till units A and B. The four samples from the supposed 'bedrock clay' yielded similar palynofloras. These samples have high organic productivities, the highest levels of Devonian input, no Carboniferous spores, the lowest Cretaceous abundances, relatively high levels of both Quaternary taxa and non-age diagnostic palynomorphs. Because the palynomorph associations are so heterogenous and similar to the overlying unequivocal till the 'bedrock clay' is probably glaciogenic in origin. Detailed palynological data were given by Riding (2003).

#### 4.2.5 Conclusions and recommendations

Despite some variations in grain size, lithology and sorting, geochemical, mineralogical, palynological and sedimentological evidence strongly indicates that the till material studied is from a single sheet of glaciogenic sediment.

Extension of this limited study comprising two sites and two control sites, to a more representative number of sites is crucial to the better understanding of variations in radon soil

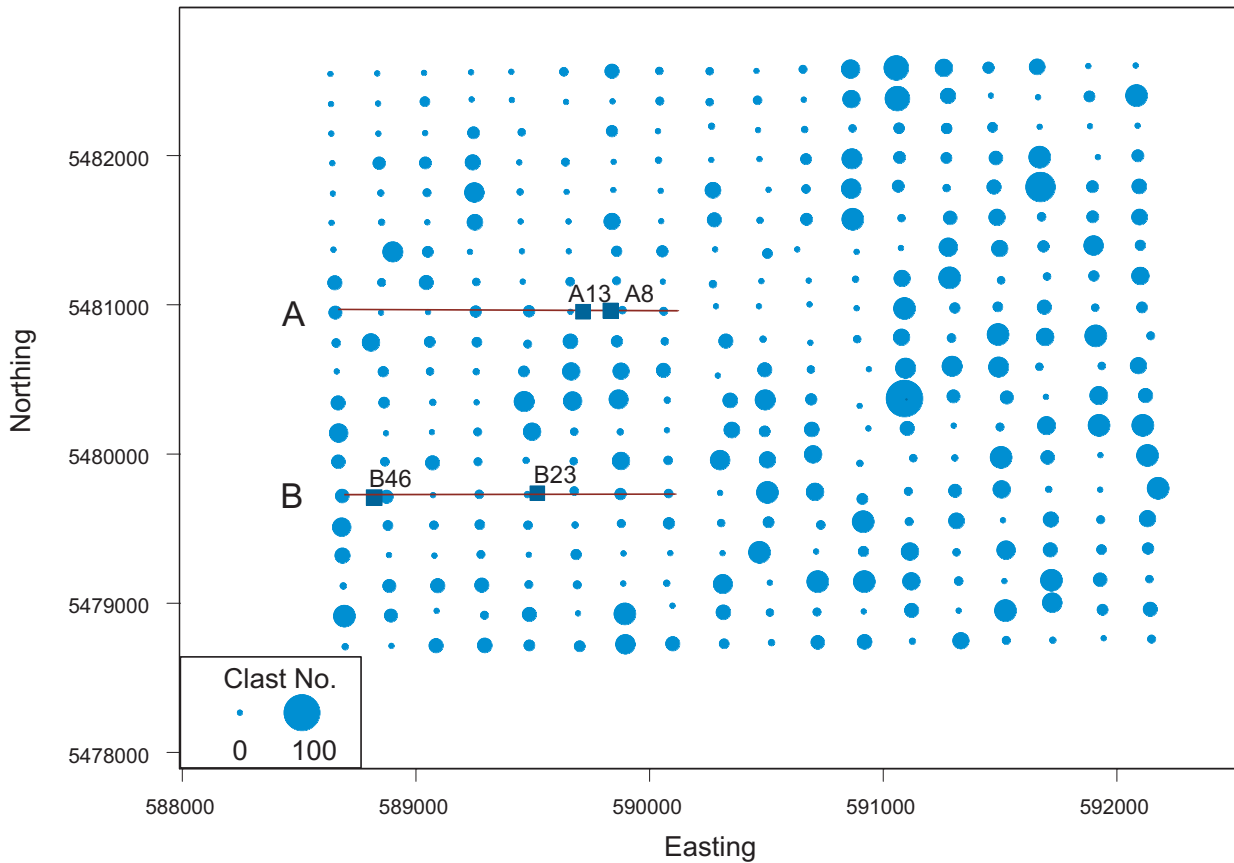


**Figure 43** Clast density. The number of clasts larger than 50 mm within 5 m of a grid point for the main soil gas grid. Profiles A and B and borehole locations are also indicated.

gas concentrations and will provide an understanding of potential CO<sub>2</sub> migration in the till. In addition to the till characterisation work undertaken in this study, it is recommended that sequential extractions combined with detailed mineralogical characterisations, are performed on selected samples which may enable the proportions of uranium sorbed to clay minerals, iron and manganese oxides, carbonates, organic

matter and occurring in more resistant minerals to be determined. In this way the proportion of uranium within the tills that is contributing to the radon concentration can be more clearly defined. Gas permeability studies on core samples would further enable changes in permeability as a result of changes in texture to be identified, which also contribute to the radon concentration measured in the soil gas.

# 5 Safety assessment studies

(Steven Benbow, Philip Maul and David Savage)

## 5.1 INTRODUCTION

To be able to quantify the likely impacts and risks associated with the geological storage of CO<sub>2</sub>, its likely long-term fate in the geological environment must be assessed and potential migration pathways and mechanisms need to be defined. The assessment of the long-term performance and safety of the geological storage of CO<sub>2</sub> is at an early stage. Many of the advances made in the last 20 years in the field of safety assessments for the geological disposal of radioactive wastes (e.g. Savage, 1995) can be applied to CO<sub>2</sub> storage. As for CO<sub>2</sub> storage, the disposal of radioactive wastes requires an understanding of complex coupled physical-chemical-mechanical processes occurring over thousands to tens of thousands of years. Systems analysis has been successfully applied in the field of radioactive waste disposal to assess the long-term fate and behaviour of radioelements in the geological environment (e.g. SKI, 1996), and is the approach taken by the North American portion of the Weyburn Project for the assessment of the performance and safety of the geological storage of CO<sub>2</sub> at Weyburn (Stenhouse, 2001). This approach dovetails with that undertaken in the EC part of the project.

Systems analysis involves the organised assembly of the features, events, and processes (FEPs) relevant to the system being studied. With regard to the geological storage of CO<sub>2</sub>, features of the storage system could include inadequately sealed boreholes, the quality (composition) of the injected carbon dioxide, or undetected geological structures. Events are usually of short duration and can be of natural or human origin, such as seismic events, faulting, or anthropogenic intrusion into the storage reservoir. There are a large number of processes that could affect the long-term evolution of the storage system and the behaviour of carbon dioxide, such as climate change, the variation of carbon dioxide's physical properties with pressure and temperature, and chemical reactions with reservoir and cap rocks. The production of databases of FEPs has proved to be valuable in the field of radioactive waste disposal. The Nuclear Energy Agency FEP database for radioactive waste (NEA/OECD, 2000) is widely used internationally. The database has been used as an audit tool to demonstrate the completeness of a number of systems-level models for the geological disposal of radioactive wastes.

Even for a well-characterised CO<sub>2</sub> storage site, there will be large and unavoidable uncertainty about the future state or evolution of the system. In the assessment of the impacts of the geological disposal of radioactive wastes, uncertainty in future states has traditionally been handled by carrying out assessment calculations for a number of stylised conceptual descriptions of future states or evolutions, termed scenarios. Scenarios were first applied to the disposal of radioactive waste in the early 1980s by Sandia National Laboratory for the US Nuclear Regulatory Commission (Cranwell et al., 1982). Processes and events that determine scenarios are referred to as 'external FEPs' or EFEPs. In the context of CO<sub>2</sub> storage, a scenario can be thought of as:

*'A hypothetical sequence of processes and events, devised to illustrate a range of possible future behaviours*

*and states of a carbon storage system, for the purposes of making or evaluating a safety case, or for considering the long-term fate of CO<sub>2</sub>'*

In developing mathematical models for the long-term fate of CO<sub>2</sub>, it can be helpful to represent the interactions between FEPs that affect the internal evolution of the system. Two general methods have been widely used:

- process influence diagrams (PIDs)
- interaction matrices.

An example of the use of PIDs is given in SKI (1996). The use of the interaction matrix was developed in the context of rock engineering systems (Hudson, 1992) and has been applied in a number of studies relevant to radioactive waste disposal (e.g. BIOMOVs, 1996). In either case, the systematic approach to the examination of how the system components relate to one another can help to identify new, previously unrecognised characteristics of the system.

## 5.2 THE FEP DATABASE

The FEP database, developed under the auspices of the Weyburn project, is generic in that it is not specific to any particular geological storage concept, but has the capability to cross-reference to project-specific databases for individual sites, thus maximising its potential usefulness. The FEPs included in the database have been chosen for their relevance to the long-term safety and performance of the geological storage system after injection of carbon dioxide has ceased, and the injection boreholes have been sealed, but some FEPs associated with the injection phase are included where these can affect long-term performance and the initial status of the storage system.

### 5.2.1 Accessing the FEP database

The database can be accessed by using the following internet link: [http://www.quintessa-online.com/CO<sub>2</sub>/](http://www.quintessa-online.com/CO2/). Once access to this site has been achieved the user needs to complete a registration process, following which a confirmatory e-mail is sent. The user can browse all the FEPs in the generic database, look at the list of references in the database, look at the list of links used in the database, and search the database.

### 5.2.2 Database structure and content

For each FEP in the database a description is provided, together with a discussion of its relevance to the long-term safety and performance of the system. Further information is provided in the form of relevant publications and websites. The database provides a central source of information on the geological storage of CO<sub>2</sub>, and can be used as part of systemic assessments of safety and performance. For each FEP entry there are fields for the FEP

Quintessa CO2 FEP Database - Microsoft Internet Explorer

Main Index Logout

Go Back | Print (You are logged in as: Russell Walke [Change your password](#))

**Database: Generic**

◀ 23/178 ▶ [Full list](#) / [External Factors](#) / [Climatic factors](#) / [Periglacial effects](#) [Edit This Record](#)  
[Suggest FEP improvement](#)

Name: 1.2.4 Periglacial effects F E P

Description: Related to the physical processes and associated landforms in cold but ice-sheet-free environments.



The diagram illustrates a cross-section of the ground in a periglacial environment. From left to right, it shows: a 'Small Deep Lake' with 'Continuous Permafrost' extending 400 m down; an 'Open Talik' (unfrozen zone) under the lake; a 'Large Deep Lake' with 'Through Talik' (unfrozen zone) extending 50 m down; a 'Bog' with 'Closed Talik' (unfrozen zone) extending 10 m down; and an 'Active Layer' (unfrozen top layer) above 'Discontinuous Permafrost'. The base of the diagram is labeled 'Unfrozen Soil and Rock'. Source: Taliks image from Physical Geography.net

Relevance to performance and safety: An important characteristic of periglacial environments is the seasonal change from winter freezing to summer thaw with large water movements and potential for erosion. Frozen sub-soils are referred to as permafrost. Meltwater from seasonal thaw is unable to percolate downwards due to permafrost and saturates the surface materials. Permafrost layers may isolate the deep hydrogeological regime from surface hydrology, or flow may be focused at "taliks" (localised unfrozen zones, e.g. under lakes, large rivers or at regions of groundwater discharge).

References: There are no references. Links: 1. [PhysicalGeography.net](#)

◀ 23/178 ▶

This record last modified: 2004-01-16.

© Quintessa Ltd. 2003...

**Figure 44** The *Periglacial Effects* FEP.

name, its description, its relevance to performance and safety issues, and references and links. To the right of the FEP name its categorisation as a feature (F), event (E) or process (P) is provided. The FEP in Figure 44 is a process, but some FEPs can be defined as more than one type of factor.

The database has a hierarchical structure with FEPs being grouped into categories and classes with an associated numbering system. If required, FEPs can be further broken down into a fourth tier of sub-FEPs. The eight categories of FEPs are summarised here.

### 5.2.3 The assessment basis

This category of FEPs determines the 'boundary conditions' for any assessment, specifying what needs to be assessed and why. The assessment basis helps to determine which FEPs need to be considered in an analysis, and which can be 'screened out' as outside the scope of the assessment. This category is atypical of the other FEP categories because it only contains classes of FEP, no actual FEPs. In effect, these FEP classes provide the context in which the FEPs described in other categories can be assessed for their relevance to the assessment being undertaken. As an example, where an assessment is concerned with potential long-term impacts to humans or the environment, the *Timescales of Interest* FEP may identify periods of up to tens of thousands of years. These very long timescales are one of the reasons why it is important to consider scenarios for the long-term evolution of the system.

### 5.2.4 External factors

This category contains the EFEPs that describe natural or human factors that are outside the system domain and which contribute to the specification of scenarios. The category has three classes: geological factors; climatic factors; and future human actions.

The climatic factors class includes natural processes and events in the atmospheric environment that are relevant to the evolution of the system. Climatic effects can result in significant changes to the accessible environment and this can affect both how CO<sub>2</sub> may be transported and the impacts that may be relevant. For example, in periglacial conditions, taliks (unfrozen regions in the periglacial environment) may affect groundwater discharge and may be potential pathways for the return of CO<sub>2</sub> to the surface. The *Periglacial Effects* FEP is shown in Figure 44. The impacts that may be of concern in this type of environment may be very different from those of concern in a temperate climate.

Many people consider that human activities could be the most important factors in CO<sub>2</sub> returning to the accessible environment. A wide range of such activities can be envisaged, and the current list of FEPs in the future human actions class is by no means comprehensive. The *Motivation and Knowledge Issues* FEP concerns the assumptions that should be made about societal memory. In the field of radioactive waste disposal it is often assumed that institutional controls can prevent inadvertent intrusion into a radioactive waste disposal facility for periods up to about three hundred years. There is, however,

plenty of experience with the location of abandoned wells of various types being 'forgotten' over much shorter periods. If knowledge of the CO<sub>2</sub> storage is lost, it is clearly possible that boreholes will be drilled into the CO<sub>2</sub> reservoir/aquifer. The probability that this will happen is difficult to determine, but will depend upon the potential economic resources present in the local geological environment and the timescales of interest.

### 5.2.5 Carbon dioxide storage

This FEP category specifies details of the pre- and post-closure storage concept under consideration. In some concepts, a closure for the CO<sub>2</sub> is present, (for example in oil and gas fields), but in others (such as saline aquifers), this may not be the case. The processes that are relevant to CO<sub>2</sub> transport will depend upon the details of the storage concept. One of the complicating factors for assessing the performance and safety of CO<sub>2</sub> storage is that impurities can have significant impacts on the subsequent evolution of the system and the potential impacts.

### 5.2.6 Carbon dioxide properties, interactions and transport

The properties of carbon dioxide can vary greatly between conditions at depth and near the surface, and a wide range of physical and chemical reactions can be important. Carbon dioxide is generally stored in its super-

critical state, but if transport processes result in it moving towards the surface, its phase will change and this will in turn affect which transport processes are important.

There are a large number of possible interactions of CO<sub>2</sub> with solid, liquid and gaseous materials in the geosphere, and it is not claimed that the list of FEPs currently in the database in this class is comprehensive. The injection of CO<sub>2</sub> can lead to physical interactions in the geosphere, such as potential fracturing or stressing of the caprock and creation of pressure gradients within the formation fluids in the reservoir. Injection of CO<sub>2</sub> will also displace fluids within the reservoir, possibly inducing microseismic events. In extreme cases, injection of CO<sub>2</sub> could lead to uplift or subsidence of the local land surface.

Some free CO<sub>2</sub> will dissolve in the aqueous phase, reducing the pH of the formation fluids and thus causing mineral dissolution-precipitation reactions with reactive minerals such as carbonates or feldspars. Some interaction processes can lead to the release of other substances that may be of concern in their own right. These include heavy metals, gas stripping of radon, and the displacement of saline formation fluids into potable water supplies. Dissolved CO<sub>2</sub> will be transported with flowing groundwater. Free gaseous CO<sub>2</sub> may be transported with other gases, particularly hydrogen sulphide.

The number of FEPs that are relevant to the transport of CO<sub>2</sub> in the geosphere is also large. Advection will occur through fractures as well as the bulk rock. Flow through fractures will depend on capillary pressures; high capillary pressures in caprocks may completely prevent the vertical movement of CO<sub>2</sub>. Flow can also be initiated by buoyancy-driven forces. CO<sub>2</sub> transport is a multiphase problem that depends upon the properties of other fluids in the system (groundwater and possibly other fluids such as hydrocarbons).

Once CO<sub>2</sub> enters the near-surface environment, a number of release processes may be relevant. Crystal Geyser in Utah (Figure 45) is a manifestation of some of these processes. Underground, the pressure is sufficient to keep the CO<sub>2</sub> in solution, but any reduction in pressure allows out-gassing to occur. The displacement of water as the CO<sub>2</sub> outgases causes a periodic, geyser-type eruption (Waltham, 2001).

### 5.2.7 The geosphere

The geosphere category of FEPs is concerned with the geology, hydrogeology and geochemistry of the storage system. Taken together, the FEPs in this category describe what is known about the natural system prior to operations commencing. The category is divided into four classes: geology; fluids; geochemistry; and resources.

In the geology FEP class, unconformities, heterogeneities, faults and fractures may be important for CO<sub>2</sub> transport back to the accessible environment. Although a caprock will generally be considered to be the primary seal for retaining CO<sub>2</sub> in a reservoir, additional seals may be part of the storage concept, and these can be important for keeping CO<sub>2</sub> away from the accessible environment over long timescales. For example, at Weyburn there is an impermeable barrier resulting from the widespread development of diagenetic anhydritised carbonate associated with the unconformity between the Mississippian beds and overlying Triassic Watrous Formation in the vicinity of the Weyburn reservoir (Figure 46). In any characterisation of a CO<sub>2</sub> storage site, it is inevitable that there may be some



J Riding, BGS©NERC

Figure 45 Crystal Geyser, Utah.

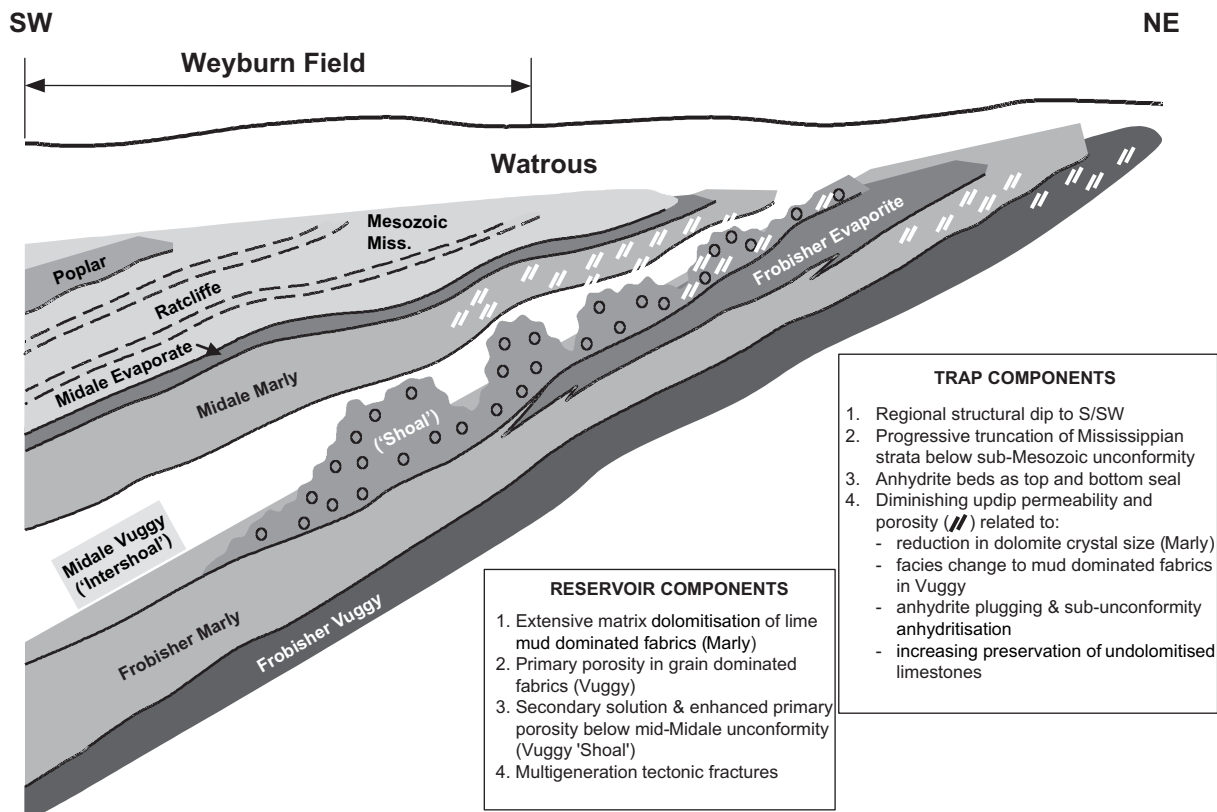


**Figure 46** Stratigraphical section at the Weyburn oilfield (from Whittaker and Rostron, 2001).

undetected features that may be relevant to CO<sub>2</sub> transport. This possibility needs to be considered in any assessment of performance and safety.

### 5.2.8 Boreholes

The boreholes category of FEPs is concerned with the way that activity by humans alters the natural system. Both boreholes used in the storage operations and those drilled for other purposes are relevant to the long-term performance of the system. The drilling of wells may directly modify the geology through formation damage. Records of wells provide an important input to society's knowledge of the system, but in general, records will be incomplete or totally absent, particularly for old wells. Monitoring wells can provide useful information before, during, and after storage operations.

Once operations have been completed, boreholes will be sealed and completed. Such boreholes provide the potential for 'short circuits' for CO<sub>2</sub> back to the accessible environment. The way that the borehole is closed to prevent human access affects the period for which the borehole can be considered to be effectively sealed. Eventually, however, seal failure may occur.

### 5.2.9 The near-surface environment

The near-surface environment category of FEPs is concerned with factors that can be important if sequestered CO<sub>2</sub> returns to the environment that is accessible by humans. Near-surface aquifers and surface water bodies and the near-surface hydrological regime and water balance will affect both the transport of CO<sub>2</sub> in the near-surface environment and the potentially important impacts. If

CO<sub>2</sub> is released to the atmosphere, the atmospheric concentrations (and hence potential impacts) will depend upon the atmospheric conditions and the surface topography. Gaseous CO<sub>2</sub> is denser than air and can therefore 'pond' in surface depressions and move down topographic gradients.

Where the relevant near-surface environment is marine, the important FEPs may be very different from a terrestrial environment. It is likely that the number of marine FEPs in the database will need to be increased as more studies into sub-seabed storage are undertaken.

### 5.2.10 Human behaviour

The characteristics of human groups in the region where impacts may be incurred will affect the magnitude of some potential impacts. Factors that need to be considered include land and water use, buildings, diet and food processing and lifestyles. The way that buildings are constructed can be very important; for example radon may be transported with CO<sub>2</sub> gas, and both may accumulate in basements.

### 5.2.11 Impacts

The impacts category of FEPs is concerned with any endpoint that could be of interest in an assessment of performance and safety. Impacts could be to humans, flora and fauna or the physical environment. Humans can die of asphyxiation if the concentration of CO<sub>2</sub> in air is as little as 5%. Less direct impacts can occur as a result of contaminant mobilisation (for example leading to contamination of drinking water supplies), physical disruption (for example from seismic events) and changes in ecology.

## 5.3 SYSTEM-LEVEL MODELLING

### 5.3.1 Model development

Because of extensive experience in reservoir modelling in the oil and gas industry, many groups involved with assessment of the long-term fate of CO<sub>2</sub> have used detailed reservoir simulation models to investigate the transport of CO<sub>2</sub> both in the short-term injection phase and the longer-term 'post closure' phase. An example of such work is given in Ennis-King and Paterson (2003). Such studies attempt to represent in detail the multiphase transport nature of the problem, but do not generally address the consequences of potential releases from the system in any detail. In the field of radioactive waste disposal these studies are analogous to the detailed flow and transport models that support performance assessment codes.

There have been a number of studies that attempt to address the consequences of release of CO<sub>2</sub> from the disposal system. An example of such a study is that of Saripalli et al. (2003). Studies such as these consider the various end points of interest, but generally make simplifying assumptions about the 'source term'. Such studies can be compared with some biosphere models developed in the field of radioactive waste disposal.

Modelling the transport of CO<sub>2</sub> and the resulting impacts for a given scenario requires consideration of all the important FEPs, but it is not generally possible (or necessary) to include a detailed representation of all of them. For example, fluid flow may be treated in a fairly simple manner (possibly in just one dimension), but this will use information from more detailed (three-dimensional) models. The representation of CO<sub>2</sub> transport in the deep geosphere part of the system can use information from reservoir simulation models.

There are some important technical challenges for CO<sub>2</sub> system-level modelling. These include:

- The properties of CO<sub>2</sub> are very different in different parts of the system, and its density and viscosity are complex functions of temperature and pressure.
- Unlike radionuclides in assessment models for radioactive waste disposal, CO<sub>2</sub> is not a 'trace' contaminant, so that the storage of large volumes of CO<sub>2</sub> at elevated pressure can directly affect the evolution of the system into which it is injected. Examples of possible CO<sub>2</sub>-induced processes are microseismicity and subsidence due to dissolution, for example in carbonate aquifers.
- The potential impacts resulting from CO<sub>2</sub> transport to the accessible environment may depend critically on the location of the release and the area of which that release occurs; impacts for a given flux to the surface may vary from insignificant to immediate loss of life depending upon the characteristics of the release.

### 5.3.2 The treatment of uncertainty

A key issue for any system-level model is the treatment of uncertainty. One of the main reasons for developing such a model is to provide a better understanding of the main features of the system that determine overall safety and of the level of uncertainty in the calculated impacts due to uncertainties in model parameters. The use of probabilistic methods is widespread in environmental assessment. Here, uncertainties in model input parameters are represented by probability density functions (PDFs), and these enable a PDF for the calculated

impacts to be produced. Probabilistic techniques can be very powerful in identifying the key sensitivities in the model, but can lead to misleading conclusions about overall risks if not used carefully.

One of the most difficult and controversial issues is the treatment of future human actions. How likely is it that at some time in the future, humans will drill into the CO<sub>2</sub> storage reservoir? If future human groups drill into the region where CO<sub>2</sub> has been stored, will they know about the presence of the CO<sub>2</sub> before they do this? If not, what could the consequences be? System-level models can help to assess the possible consequences of future human actions, but cannot resolve some of the fundamental problems associated with making assumptions about human behaviour far into the future.

### 5.3.3 The use of the FEP database

The FEP database can be used in two ways that can be described as 'top down' and 'bottom up'. In the 'bottom up' approach, the database is used directly in the development of assessment models, and the use of process influence diagrams and/or interaction matrices has already been referred to. In the 'top down' approach, the database is used as an audit tool to ensure that all relevant FEPs are included in the model, and to document why other FEPs are not considered. Some FEPs may, for example, be outside the assessment context; marine FEPs are unlikely to be relevant to a terrestrial environment for example.

The second, 'top down', use of the FEP database is likely to be the more practical and effective. The FEP audit discipline is extremely beneficial to any safety or performance assessment, and can help give confidence to stakeholders that 'nothing important' has been overlooked. For example, Stenhouse (2001) reports an audit of an earlier version of the generic FEP database described here for the purposes of the safety assessment of the Weyburn site.

## 5.4 OTHER USES OF THE DATABASE

The database has potential application as a 'knowledge base' for the geological storage of CO<sub>2</sub>. Information can be readily retrieved using the search facilities of the database. To be used in this way, the database needs to be kept up to date as new information becomes available and links to other websites need to be maintained. Users of the database can provide suggestions for new FEPs, or for additional information on existing FEPs, by using the 'Suggest FEP improvement' link.

The database can also link to project-specific databases, providing the capability to demonstrate how generically-important FEPs are represented in a specific assessment; this is termed 'FEP mapping'.

## 5.5 DISCUSSION

The generic FEP database developed as part of the IEA Weyburn CO<sub>2</sub> Monitoring and Storage Project is potentially a powerful tool in the assessment of the performance and safety of CO<sub>2</sub> storage systems. In order for this potential to be realised, it is important that the database is maintained and developed. In particular, advantage needs to be taken of the capability to link to project-specific databases.

The development of system-level models is at an early stage. Advantage can be taken of experience gained in performance assessment studies for radioactive waste disposal and reservoir simulation models used in the petroleum industry, but there are significant technical challenges to be overcome. It is suggested that such models could be developed and applied to natural systems where significant quantities of carbon dioxide are released to the accessible environment. If such models can help to produce an understanding of the key processes and potential

impacts in such systems, this will provide confidence in their suitability for application to 'engineered' systems.

Some limited economic analyses were done as part of this project. Their aim was to demonstrate that CO<sub>2</sub>-EOR operations can be commercially viable and to highlight the principal economic criteria to be considered. This section is subdivided into an assessment of the CO<sub>2</sub> source, and the profitability of the CO<sub>2</sub>-EOR operation at Weyburn. Because CO<sub>2</sub> injection at Weyburn is in its early stages, these analyses should be regarded as preliminary.

## 6 Economics

### 6.1 THE ECONOMICS OF THE CO<sub>2</sub> SOURCE: THE GREAT PLAINS SYNFUEL PLANT, NORTH DAKOTA, USA

(Nicholas J Riley)

#### 6.1.1 Introduction

The source of the injected CO<sub>2</sub> for the Weyburn EOR operation is the Great Plains Synfuels Plant, Beulah, North Dakota, USA (Figures 1 and 47), which is owned and operated by the Dakota Gasification Company, a subsidiary of the Basin Electric Power Cooperative. The oil crisis of the early 1970s exposed a profound dependency on imported fuel in the USA. The federal government therefore developed strategies to overcome any future oil crises. Out of this came the vision of the Great Plains Synfuels Plant. The vast lignite deposits of North Dakota could be transformed into versatile fuels, with a reliable supply and stable costs, providing energy security for the Prairie States. The core business of the plant is the manufacture of synthetic natural gas, or syngas, from lignite supplied by the adjacent Freedom Mine. This major coal gasification operation attempts to maximize profits by the sale of a diverse range of by-products. The nature and economics of this operation is described in this section. All data used here are in the public domain. A comprehensive history of the Dakota Gasification Company and the Great Plains Synfuels Plant was given by Stelter (2001).

#### 6.1.2 Background

The use of CO<sub>2</sub> in enhanced oil recovery (EOR) has been practiced in North America for several decades. A significant stimulus for CO<sub>2</sub> EOR development was the Oil Windfall Tax introduced in the USA in 1981, which favoured EOR use in domestic oil fields. This EOR technique has largely used CO<sub>2</sub> from natural accumulations. However, if the CO<sub>2</sub> can be obtained from an industrial source, an opportunity is provided to sell the

CO<sub>2</sub> and also to sequester a proportion of it and thus reduce emissions. In a fiscal/legislative environment where there are no financial penalties for emitting CO<sub>2</sub>, EOR provides a commercially viable route for the storage of industrially-produced CO<sub>2</sub>. The manufacture of synthetic low carbon fuels and chemical by-products from coal is a strategy to utilise this resource in a cleaner way. Synthetic fuels provide a mechanism for supplying low emission fuels and also allowing carbon to be removed relatively easily as a part of the syngas cleaning process. This avoids the problem of removing CO<sub>2</sub> from the large volume of low CO<sub>2</sub> concentration flue gases emitted from a coal burning power plant. The Great Plains Synfuels Plant is the only commercial example of synfuel manufacture linked to CO<sub>2</sub> storage. It heralds a new generation of synfuels plants which will combine energy generation with petro- and agro-chemical production. Such plants are likely to succeed in the future because they can operate on a diverse feedstock of raw fuels, even waste and/or biomass, and switch production to a variety of synthetic fuels and chemical products as the market demands.

#### 6.1.3 Outline of the Great Plains Synfuels Plant, the syngas process and by-products

The Great Plains Synfuels Plant takes 16 200 tonnes per day of crushed lignite from the nearby Freedom Mine which is fed into 14 Lurgi dry-bottom gasifiers. The plant is capable of using waste products such as used car tyres and refinery sludges. These have been tried experimentally but the normal feedstock is lignite. A strong factor in the economics of the plant is the relatively low cost of this lignite, which is in part due to extremely low transportation costs. Lignite supplied to the adjacent Basin Electric Antelope Valley Power Station in 2000 was sold for \$8.76 per short tonne. There are significant cost benefits across the Basin Electric Power Cooperative and its member co-operatives including cheap electricity and cost sharing between the synfuels plant and the power plant in regard to water supply and infrastructure. These benefits have been estimated at in excess of \$30m per year.

**Figure 47** Aerial photograph of the Great Plains Synfuels Plant, Beulah, North Dakota, USA.



Photo courtesy of the Dakota Gasification Company

Oxygen and steam are injected into the gasifier, causing high temperature partial combustion of the lignite at 1200°C. The resultant gases are cooled to remove phenol, tar oil and water. Raw synthesis gas is separated and modified, using a cobalt molybdenum catalyst, to a H<sub>2</sub>:CO ratio > 3:1. It is then fed into the Rectisol Unit, where it is purified in a low temperature methanol wash. This selectively removes CO<sub>2</sub>, naphtha and sulphur compounds. The cleaned synthesis gas contains 61.8% hydrogen, 20.0% carbon monoxide, 16.9% methane, 0.60% carbon dioxide, 0.45% argon and 0.25% nitrogen. The clean synthesis gas is passed over a reduced nickel catalyst to produce methane and water. Daily production of 3050 tonnes of synthetic natural gas is mainly supplied to domestic and industrial consumers, with a proportion used onsite for the manufacture of anhydrous ammonia. The Rectisol Unit produces 13 000 tonnes per day of CO<sub>2</sub>, of which up to 5000 tonnes per day is supplied to Weyburn.

The Great Plains Synfuels Plant has developed a number of by-products and these have become economically important, decreasing exposure to volatile gas prices.

The by-product capacities at December 2000 were as follows:

Anhydrous ammonia	350 kt
Ammonium sulphate	150 kt
Dephenolised cresylic acid and tar oil cresylic acid	15 kt
Phenol	15 kt
Liquid nitrogen	91 M litres
Naphtha	26.5 M litres
Krypton and xenon	3.1 M litres
Carbon dioxide	1.1 billion m <sup>3</sup>

The anhydrous ammonia and ammonium sulphate are used as fertilisers. The remainder are used by the petrochemical and chemical industries. Other by-products have been explored, but so far not developed; these include aviation fuel, ethanol, hydrogen, methanol and synthetic diesel. Revenues from by-products in 2000 reached \$78.2 million, which was approximately 30% of total sales revenue of the Great Plains Synfuels Plant

#### 6.1.4 The CO<sub>2</sub> stream

The level of impurity in the CO<sub>2</sub> supplied from the Great Plains Synfuels Plant is ideal for use in enhanced oil recovery. This is because 100% pure CO<sub>2</sub> is less effective as a gas in EOR than slightly impure CO<sub>2</sub>. Carbon dioxide dissolves more readily into oil when small impurities are present. The presence of hydrogen sulphide as an impurity is also an advantage because this gas further enhances the ability of the injected CO<sub>2</sub> to mix with the oil. Since the Weyburn oilfield reservoir already contains hydrogen sulphide, the introduction of this gas into the reservoir presents no additional problems. One disadvantage of the syngas source of CO<sub>2</sub> is the trace presence of methyl mercaptan. Mercaptans have an extremely strong odour; the human nose can detect minute concentrations. For this reason, methyl mercaptan is deliberately added to natural gas supplies so that leaks can be detected. The problem with its presence in the CO<sub>2</sub> stream is that otherwise inconsequential leaks during normal operation of surface infrastructure (e.g. changing valves or seals) can cause annoyance to local people living near the Weyburn plant. The CO<sub>2</sub> supply comprises 96% CO<sub>2</sub>, 2.3% C<sub>2+</sub> hydrocarbons, 0.9% hydrogen sulphide, 0.7% methane, 0.1% carbon monoxide, <300 ppm nitrogen, <50 ppm oxygen and <20 ppm of water.

#### 6.1.5 The price of CO<sub>2</sub>

The net income from CO<sub>2</sub> supply over a 15-year contract for supply to EnCana Resources was stated by the Dakota Gasification Company to be approximately \$15–18m per year. It is difficult to estimate from these figures what the price of CO<sub>2</sub> delivered to EnCana Resources is because cost recovery of the pipeline construction (\$110m), plus operating, maintenance and compression costs will all be included in the final price. Assuming that the CO<sub>2</sub> is sold at c. \$1 Mscf (thousand standard cubic feet), the price per tonne will be about \$20. This is likely to be the upper price limit due to potential competition from natural CO<sub>2</sub> sources within Canada. The pipeline has extra capacity and sections were designed in anticipation of joining new supply spurs to the main pipeline. If future CO<sub>2</sub> contracts are won from other oilfield operators, the net revenue for the remaining 8000 tonnes per day CO<sub>2</sub> capacity would be far greater than that derived from the contract with EnCana Resources to supply Weyburn. This is assuming that the contract with EnCana Resources covers the cost of the main pipeline and supplying the CO<sub>2</sub>.

#### 6.1.6 The syngas market

In 2000, the total marketed production of gas from natural gas and oil wells in North Dakota was 52 426 MMscf (million standard cubic feet). Syngas supplied 49 190 MMscf. North Dakota has no underground or liquid natural gas storage facility. Reliable and affordable gas supply has become increasingly important because demand has risen, especially from industrial users. In 2000, the total consumption by consumers was 36 553 MMscf of which, residential consumption was 10 963 MMscf, commercial usage 10 787 MMscf and industrial demand 14 795 MMscf. No significant amounts of gas were used for electricity generation. When the Great Plains Synfuels Plant was conceived, the capacity exceeded consumption in North Dakota, but in recent years consumption has outstripped syngas supply. Four pipeline companies take the syngas, which is blended with natural gas before being supplied to consumers. Gas payment contracts with the pipeline companies are complex and an outline of their development was given by Riley (2002). According to Sinor Consultants Inc., during 2000 the Dakota Gasification Company broke even when natural gas prices reached \$2.50 per dekatherm, adding about \$450 000 revenue per month for each \$0.10 increase per dekatherm. In 2000 DGC hedged more than half of its natural gas production at a price of approximately \$2.80 per dekatherm. For this reason and because of price capping in the long term supply contracts to the pipeline companies, it became more profitable to switch interruptible syngas capacity into fertiliser manufacture, because natural gas prices rose steeply in late 2000.

### 6.2 THE ECONOMICS OF ENHANCED OIL RECOVERY USING CO<sub>2</sub>: THE WEYBURN CASE

(Panchali Guha)

#### 6.2.1 Introduction

Publicly available data on the Weyburn oilfield operation were used to delineate some of the expected costs and benefits of CO<sub>2</sub>-enhanced oil recovery (EOR) projects. Since many of the economic and financial data that would be required for a full economic analysis are confidential corporate information, the results here are not definitive. However, it is anticipated that they are indicative of the costs and benefits that may be expected in similar EOR projects.

## 6.2.2 Incremental production

Enhanced oil recovery using CO<sub>2</sub> flooding at the Weyburn oilfield commenced in September 2000, and is expected to continue up to 2025. The oilfield is expected to produce an additional 130 million barrels of medium-gravity crude oil over the 25-year time period of the project. The incremental production is expected to follow an approximately bell-shaped curve, tapering off towards the end of the life of the operation.

## 6.2.3 Revenue from CO<sub>2</sub>-EOR

Using the expected production profile and estimates of future oil prices, the stream of future revenues from CO<sub>2</sub>-EOR can be determined. This calculation is complex as oil prices are subject to a high degree of uncertainty, and it is virtually impossible to forecast future price movements. According to the EnCana 2002 Annual Report, the benchmark West Texas Intermediate (WTI) crude oil price in 2002 was \$26.15 per barrel.

## 6.2.4 Costs

The total cost of a CO<sub>2</sub>-EOR project will comprise the cost of purchasing the CO<sub>2</sub>, capital expenditure and operating expenditure. According to EnCana Resources, the capital costs and cost of CO<sub>2</sub> purchase will together account for approximately US \$900 million including inflation throughout the Weyburn CO<sub>2</sub>-EOR operation.

### 6.2.4.1 COST OF PURCHASING CO<sub>2</sub>

Obtaining the CO<sub>2</sub> normally accounts for the largest proportion of the costs of a CO<sub>2</sub>-EOR operation. When the CO<sub>2</sub> is obtained from anthropogenic sources, rather than natural accumulations, the cost is even higher. This is because the price that the EOR operator pays for CO<sub>2</sub> incorporates the costs of capture, separation and compression of the CO<sub>2</sub> at source, which are all substantial. Moreover, there is also the cost of transporting the CO<sub>2</sub> from the source to the EOR site. In the case of the Weyburn operation, the CO<sub>2</sub> pipeline and compressor was paid for by the supplier of CO<sub>2</sub>, the Dakota Gasification Company. The length of the pipeline is approximately 330 km, and the total cost of constructing the pipeline and compressor was \$110 million.

Based on literature information, the market price of CO<sub>2</sub> is estimated to be around \$20 per tonne. The total volume of CO<sub>2</sub> purchased by EnCana Resources for purposes of CO<sub>2</sub>-EOR is expected to be about 20 million tonnes.

### 6.2.4.2 CAPITAL EXPENDITURE

The following is a list of some of the main items of capital expenditure in the Weyburn CO<sub>2</sub>-EOR operation (Hancock, 1999; Way and Hancock, 1999).

- **The cost of developing injection patterns** Seventy-five injection patterns will be developed in the CO<sub>2</sub> target area over the lifetime of the operation. Nineteen patterns were developed in 2000, four in 2002, and nine in 2003. The remainder will be developed in the future as recycled CO<sub>2</sub> becomes available for injection. The patterns, which were configured as inverted nine spot water flood patterns, need to be modified for purposes of CO<sub>2</sub> injection.
- **The drilling of new wells** New horizontal injection and production wells need to be drilled, and suspended and abandoned producing wells need to be reactivated. In total, it is estimated that 54 new wells will be drilled, and more than 600 wells will be upgraded, converted or reactivated.
- **New pipeline** For the entire complex of 75 injection patterns, more than 900 km of new pipeline will be needed.

This includes:

- carbon dioxide injection trunk lines to the satellites and CO<sub>2</sub> injection flow lines to the injection wells
- emulsion production lines from the production wells to the satellites
- carbon dioxide production trunk lines from the satellites to the central compressor station
- emulsion trunk lines from the satellites to the central treating plant
- new water injection flow lines from the existing water injection stations to the new water/CO<sub>2</sub> injection wells
- up to 19 new production satellites.
- **The cost of adding new equipment** to the central oil treatment plant in order to enable it to handle high-pressure gas, including a new free water knock-out vessel, a new battery gas compressor and a new flare system.
- **Four CO<sub>2</sub> recycle compressors** are required for the recompression and recycling of CO<sub>2</sub>.

### 6.2.4.3 OPERATING EXPENDITURE

Operating costs involved in the injection process include the cost of labour, auto usage and operating supplies. Operating costs are also incurred in the recycling of produced CO<sub>2</sub>, and in the clean up and disposal of produced water. Power consumption tends to be a significant component of the operating costs. Large quantities of power are required to pump oil and water from the production wells and move the mixture to the treatment and distribution facilities. Recompression of the produced CO<sub>2</sub> for purposes of recycling is also a power-intensive process. According to EnCana Resources, the overall operating cost of CO<sub>2</sub>-EOR at Weyburn is approximately \$5 per barrel of incremental oil recovered.

## 6.2.5 The interface between CO<sub>2</sub> sequestration and enhanced oil recovery

Operations such as Weyburn demonstrate that using CO<sub>2</sub> from anthropogenic sources for the purposes of EOR can be profitable. If, in the future, there are changes in the policy environment such that oilfield operators are eligible to receive incentives for carbon storage, the economics of EOR projects utilising anthropogenic CO<sub>2</sub> may improve even further. However, there are some important caveats. While it has been estimated that more than 80% of the world's oil reservoirs may be suitable for CO<sub>2</sub> flooding based on oil recovery criteria alone, a much smaller proportion of these are likely to be suitable for underground carbon storage. Even where an oilfield is considered to be suitable for storage, the potential conflict between EOR and storage objectives must be recognised. Where EOR is the sole objective, effort is focused on reducing the volume of CO<sub>2</sub> that is required to recover a barrel of oil, since it is expensive for the EOR operator to buy and/or recycle CO<sub>2</sub>. However, where EOR and CO<sub>2</sub> storage are combined, two objectives must be simultaneously satisfied: (i) to maximise incremental oil production, and (ii) to maximise the amount of CO<sub>2</sub> that is left behind when the reservoir is abandoned. Hence, the engineering design objective is likely to be significantly different in these two cases.

Where the oilfield is judged to be suitable, and suitable incentives are provided, there may be a much larger storage response than under current conditions, in which the economics of EOR alone dictates how much CO<sub>2</sub> will be stored underground. For instance, if payments are made to oilfield operators for carbon storage, this will greatly alter the economics of the entire operation, leading to greater storage and probably also to higher oil production, over and above the current economic limit dictated by EOR.

## 7 Conclusions

*(James B Riding and Christopher A Rochelle)*

The Weyburn oilfield has proven to be an outstanding laboratory for the study of CO<sub>2</sub> storage; this is based on its comprehensive well/field data, the extensive core material and the accessibility of the site. The European part of the IEA Weyburn CO<sub>2</sub> Monitoring and Storage Project has derived significant scientific knowledge related to the storage of CO<sub>2</sub> in a commercial miscible CO<sub>2</sub>-EOR operation. The structure of the research is intended to serve as a model, which can be applied to other CO<sub>2</sub> storage operations. Furthermore, the results from this project should help guide policy development on the abatement of greenhouse emissions from energy generation using underground storage. This project has also been notable for the many successful international collaborations that have taken place within the large project team. These have been both intra-European and transatlantic collaborations.

A range of approaches was used to monitor different parts of the Weyburn oilfield system. In the main however, these were focussed towards an understanding of how injected CO<sub>2</sub> would be controlled by, or would impact, hydrogeological, hydrochemical and geochemical processes. This focus allowed the European research team to provide complementary information to other monitoring activities, for example active seismic surveys, that were being conducted in North America. Monitoring of conditions at depth within the Midale reservoir unit was via direct sampling of reservoir fluids, and passive seismic methods. Surface monitoring focussed on determining the concentration of a suite of gases within the soil.

Monitoring changes in the composition of the reservoir fluids for dissolved gases, trace elements and strontium isotopes over three successive years clearly illustrated the effects of reactions between CO<sub>2</sub>, formation water and host rock. Not only were there increases in dissolved CO<sub>2</sub>, but the changes in fluid chemistry clearly demonstrated that significant amounts of reaction with the Midale reservoir unit had occurred. In terms of strontium isotopes, this reaction was large enough to mask a significant proportion of the signature of 40 years of water flooding. When displayed as contour maps, such geochemical changes can be also used to monitor broad scale movement of CO<sub>2</sub> within the Weyburn oilfield. Continued monitoring of reservoir fluids in the Phase 1A and succeeding injection areas will be needed to follow these changes and to assess the overall geochemical evolution of the Weyburn oilfield system.

This study has also shown that it is possible to monitor microseismicity within an active oilfield CO<sub>2</sub> injection operation. However, the deployment of the equipment was delayed until near the end of the project, partly as a consequence of the practical difficulties of working on a active oilfield. A preliminary interpretation of the data obtained, shows that numerous events were recorded in and around the Midale reservoir, though most could be attributed to either well completion or production activities, i.e. effectively oilfield noise. However, the magnitude of these events did not exceed those expected with water flooding or conventional gas injection. Continued microseismic monitoring is likely to provide information on CO<sub>2</sub> movement itself, but this may require sensor

arrays to be deployed for extended periods in dedicated wells.

Monitoring of gases within the soil horizon above the Phase 1A injection area was mainly aimed at determining natural baseline concentrations and assessing how these might change seasonally. The data were then used to understand better how gases move within the shallow geosphere at Weyburn. As well as CO<sub>2</sub> concentrations and CO<sub>2</sub> flux rates, a range of other gases were monitored that might be indicative of gas migration from depth, for example helium, methane and radon. Also monitored were gases that might be involved in shallow biological processes such as ethylene and oxygen. A range of techniques and equipment were used, with some analysis being conducted on site, and others being done later in the laboratory from preserved samples. Most of the sampling was undertaken over three successive autumn sampling campaigns, however some automated radon-measuring equipment was left in place for several months at a time to record seasonal variability. An extensive suite of data on baseline gas concentrations and fluxes was obtained, which shows variations between seasonal changes, and also between dry areas and damp ground. However, all the evidence suggests that the CO<sub>2</sub> measured in the soil is produced biogenically within the soil itself. There are no indications of any significant leakage of gas from depth.

It will be important to continue the periodic monitoring of soil gases at Weyburn. Not only will this indicate any CO<sub>2</sub> migration to the surface, in the unlikely event that this should occur, but it will also allow the development of new analytical tools and strategies that could be applied to other storage sites. In particular, it would be most useful to develop equipment and techniques to facilitate rapid measurements over large areas, and for continuous monitoring at specific locations.

A variety of approaches have been used to assess and verify a range of key processes in different parts of the Weyburn reservoir system. Like the monitoring activities outlined above, these were focussed towards an understanding of how injected CO<sub>2</sub> would be controlled by, or would impact, the local hydrogeology, hydrochemistry and geochemistry. This again provided complementary information to other activities being conducted in North America.

An understanding of the processes happening at depth within the Weyburn oilfield was achieved through predictive modelling constrained and verified by both field and laboratory data. Prior to an assessment of the impact of injected CO<sub>2</sub>, it was necessary to have a good understanding of the pre-CO<sub>2</sub> baseline conditions within both the reservoir and the rocks overlying it. This involved sourcing background literature information, as well as undertaking new and detailed mineralogical analyses of rock samples from Weyburn oilfield borehole cores.

Published data on the structure, hydrogeology and water chemistry of the host Mississippian aquifer were combined into a model of a 240 x 230 km block centered on Weyburn. This highlighted the particularly large salinity gradient that exists in the region of the Weyburn field. The highest salinity is in the southeast and lowest in the northwest. This is

important because of its impact on changing water density and solubility of CO<sub>2</sub>. When compiled into a model of the Weyburn oilfield system, it is predicted that this salinity gradient will act to focus fluid flow parallel to the salinity gradient. As a consequence, it is predicted that the natural flow within the aquifer would be capable of transporting dissolved CO<sub>2</sub> in an east-north-east direction, but only about 25 km over 100 000 years. The solubility of CO<sub>2</sub> within these saline formation waters is unlikely to exceed 1 mole (44 g) per 1 kg of water. This regional scale model could be developed and refined further, by focussing down to a 10 km scale around the injection patterns. This would need to consider the complexities of a multilayer aquifer system, though many of the parameters required to do this, for example formation thickness, in situ pressure, permeability, salinity etc., have now been produced during this first phase of the Weyburn project.

An assessment of the sealing capacity of the aquicludes above the Mississippian aquifer focussed mainly on the Midale Evaporite Unit, which is a local seal, and the Watrous Formation, a regional seal. Transport of dissolved CO<sub>2</sub> into these units, was assessed by modelling diffusional processes. For the Watrous Formation, the impact of CO<sub>2</sub> was predicted to be minor, extending just a few metres even after several thousand years. In the lowermost metre of this formation, a minor porosity increase was predicted, though a slightly smaller porosity decrease was predicted just a few metres above this. A similar low reactivity was found in the modelling of the Midale Evaporite. In terms of geochemical interactions with unfractured natural seals therefore, the CO<sub>2</sub> is predicted to have little impact.

Detailed observations of processes occurring when CO<sub>2</sub> is added to samples of the Midale Beds were achieved via laboratory experiments under simulated in situ conditions, i.e. 60°C, 150–250 bar. These experiments simulated both static systems (representative of regions away from injection wells, or timescales after the cessation of CO<sub>2</sub> injection) and flowing systems (representative of regions closer to wells). The information from these experiments was used to identify reaction processes and to provide well-constrained test cases with which to validate the capabilities of predictive models.

Static experiments used a full range of units within the Midale Beds, i.e. Marly, Vuggy and Evaporite, and reacted fixed quantities of rock and synthetic formation water for up to six months. The presence of CO<sub>2</sub> initiated mineral dissolution, but steady-state compositions for elements derived from carbonate and sulphate mineral dissolution were achieved in about one month. Silicate minerals appeared to react much slower than the carbonates, and this continued throughout the six month duration of the experiments. It was noticeable that the Marly and Vuggy samples showed some similar behaviour, with increases in aqueous concentrations of elements such as calcium in the presence of CO<sub>2</sub>. Although most mineralogical changes were very minor, the Vuggy experiments also exhibited significant amounts of secondary gypsum precipitation. Experiments using samples of the Midale Evaporite showed significantly different behaviour. The presence of CO<sub>2</sub> appeared to leave calcium concentrations unchanged, but increased magnesium concentrations. The overall interpretation of these experiments is that calcite, the source of calcium, and/or dolomite, the source of calcium and magnesium, achieved saturation relatively rapidly. Silicate minerals did not reach saturation, and that the fluid/rock ratio in the experiments favoured gypsum formation over that of anhydrite.

Experiments where CO<sub>2</sub>-saturated fluid was flowed through a core or packed column of Midale Marly Unit material exhibited different behaviour to those described above. Significant corrosion was observed where the fluid first contacted the rock, i.e. where they were most out of equilibrium, but this became progressively less obvious away from the fluid inlet point. The corrosion was due to the dissolution of calcite and dolomite, and this led to increases in outlet concentrations of dissolved elements such as calcium and magnesium. However, the relatively rapid reaction of carbonate phases, followed by an equally relatively rapid approach towards equilibrium, is consistent with what is observed in the static batch experiments described above. One observed difference however, was the liberation and migration of fine particles of clay in the flow experiments. These were released when the carbonate matrix surrounding them was dissolved in the CO<sub>2</sub>-rich formation water, and they show the potential for impeding fluid flow if their migration leads to a lowering of permeability. Current predictive geochemical coupled models do not take non-chemical 'fines liberation' into account, even though they are a consequence of dissolution. This could be an important area to include into future developments of these codes.

It is significant that there is some consistency between observations from centimetre scale laboratory experiments and kilometre scale field measurements described above. Both show significant and relatively fast reaction between CO<sub>2</sub>-rich formation water and carbonate phases, even though they are five to six orders of magnitude different in scale. That similar processes appear to be occurring over such a range of scales, increases confidence in being able to extend the use of models tested on laboratory systems to field scale operations.

A limited number of relatively simple laboratory experiments were undertaken to scope the potential for reaction of CO<sub>2</sub> with borehole cements typical of those currently used at the Weyburn oilfield. Small monoliths of cured fill cement and tail cement were exposed to CO<sub>2</sub> in both supercritical dissolved form. No significant changes in the size of the cement monoliths were found after short-term exposure to CO<sub>2</sub>. Although this does not preclude the possibility that carbonation shrinkage will occur, it does provide some evidence that this process might not be an important issue over shorter timescales.

Both cement types gained weight on exposure to CO<sub>2</sub>, which was more pronounced with just supercritical CO<sub>2</sub> compared to dissolved CO<sub>2</sub>. The fill cement showed a greater weight increase, approximately 11%, compared to the tail cement, approximately 4%. This increase was associated with the formation of carbonate reaction rims, which penetrated up to several millimetres into the monoliths. Associated with these were carbonated reaction fronts with significantly reduced porosity. It is possible that such layers may be beneficial in that they might act to armour borehole cement against complete carbonation over the longer term.

A few relatively simple flexure tests were carried out to assess cement strength changes upon carbonation. Although data were few, it was noted that the fill cement was about twice as strong as the tail cement, both before and after exposure to CO<sub>2</sub>. Overall however, no significant changes in the tensile strength of the cement monoliths were found after, albeit relatively limited, exposure to CO<sub>2</sub>.

The European part of the IEA Weyburn CO<sub>2</sub> Monitoring and Storage Project has successfully completed an ambitious programme of research focussed towards an understanding of how injected CO<sub>2</sub> is controlled by, or would impact, hydrogeological, hydrochemical and geochemical

processes. Additionally, the monitoring of conditions at depth within the Midale reservoir unit was carried out using a variety of techniques. This approach has allowed the European team to provide information to other monitoring activities within the overall international project. The Weyburn CO<sub>2</sub> injection operation is unique, in that it is a

major onshore EOR operation into a carbonate reservoir that has prodigious amounts of oilfield data. It has provided an outstanding opportunity to study all aspects of CO<sub>2</sub> storage. The structure of the project can be used as a model for the study of other CO<sub>2</sub> storage operations and the results from will guide policy development in this important area.

## 8 Acknowledgments

The European Commission is gratefully acknowledged for its generous co-funding of this work, which is EC project number NNE5–2000–00096 (contract ENK5-CT-2000–00304). Denis O’Brien of the EC has been an extremely helpful, supportive and proactive project officer. Many other bodies have provided sponsorship to this project. These include five project partners, i.e. BGS, BRGM, GEUS, INGV and Quintessa Limited, and the UK Department of Trade and Industry via Future Energy Solutions. John Gale of the IEA Greenhouse Gas Research and Development Programme helped greatly in publicising the project. Malcolm Wilson (University of Regina) is thanked for his efforts to initiate this international project, and in its execution and administration. The Petroleum Technology Research Centre (PTRC), Regina, Canada has provided links to the North American researchers on Weyburn through regular communication and regular project meetings. In particular, Waleed Jazrawi, Roland Moberg and Kyle Worth of PTRC have helped trans-Atlantic communications. Waleed Jazrawi, the former Programme Director of the North American Weyburn project, was tireless in his efforts to facilitate integration of the two teams of researchers. He was ably assisted throughout by the project integrator, Roberto Bencini of INGV.

The Petroleum Technology Research Centre, Regina also generously funded specific activities which fell outside the EC contract, such as the soil gas sampling at certain sites and the till characterisation work.

This project could not have proceeded without the support and goodwill of the operator of the Weyburn oilfield, EnCana Resources. EnCana Resources have given much logistical support to the European researchers who visited Weyburn to undertake fieldwork and/or sampling activities. David Stachniak of EnCana Resources, Calgary is thanked for his support throughout the project. He acted as project liaison between the European research team and the company. His efforts ensured that all reasonable requests made by the research providers were efficiently met. Ken Ferguson, and colleagues at the Weyburn unit, gave much invaluable assistance at the oilfield to all visiting researchers. Soil gas sites were surveyed by Condon Surveying Group; thanks are due to Lowell Peterson and his colleagues.

Staff at the University of Calgary, and in particular Maurice Shevalier, are thanked for their help during sampling trips for well fluids, for their provision of samples, and for allowing access to their data.

Bill Gunter and Ernie Perkins of the Alberta Research Council are thanked for all their helpful discussions about geochemistry.

# References

- ANDERSON, G M. 1983. Some geochemical aspects of sulfide precipitation in carbonate rocks. 61–67 in Proceedings of the International Conference on Mississippi Valley Type Lead-Zinc Deposits. KISVARSAN, G, GRANT, S K, PRATT, W P, and KOENIG, J W (editors). University of Missouri-Rolla, Missouri, USA.
- AUDIGANE, P, and LE NINDRE, Y-M. 2004. Hydrodynamic modelling of the Mississippian aquifer at Weyburn, Saskatchewan, Canada. *Bureau de Recherches Géologiques et Minières Report*, BRGM/RP-52786, (restricted).
- AZAROUAL, M, KERVÉVAN, C, DURANCE, M-V, DURST, P. 2004. SCALE2000 (V3.1) *User's Manual; software for thermodynamic and kinetic calculations*. BRGM (Bureau de Recherches Géologiques et Minières) Editions.
- AZAROUAL, M, DURST P, GAUS I, and CZERNICHOWSKI, I. 2004. EU Weyburn Monitoring Project - Long term redictive reactive transport modelling of CO<sub>2</sub> in the Weyburn CO<sub>2</sub> storage reservoir. *Bureau de Recherches Géologiques et Minières Report*, BRGM/RP-53273-FR.
- BACHU, S. 1995. Flow of variable-density formation water in deep sloping aquifers: review of methods of representation with case studies. *Journal of Hydrology*, Vol. 164, 19–38.
- BACHU, S, GUNTER, W D, and PERKINS, E H. 1994. Aquifer disposal of CO<sub>2</sub>: hydrodynamic and mineral trapping. *Energy Conversion and Management*, Vol. 35, 269–279.
- BACHU, S and HICHON, B. 1996. Regional-scale flow of formation waters in the Williston Basin. *American Association of Petroleum Geologists Bulletin*, Vol. 80, 248–264.
- BATEMAN, K, BIRCHALL, D J, ROCHELLE, C A, PEARCE, J M, CHARLTON, B D, REEDER, S, SHAW, R A, TAYLOR, H, TURNER, G, and WRAGG, J. 2004. Geochemical interactions between super-critical CO<sub>2</sub> and the Midale Formation. VI: Flow experiments with Midale Marly. *British Geological Survey Commissioned Report*, CR/04/010N.
- BEAUBIEN, S, STRUTT, M H, JONES, D G, BAUBRON, J-C, CARDELLINI, C, LOMBARDI, S, QUATTROCHI, F, and PENNER, L A. 2004. D20 Report: Soil Gas surveys in the Weyburn oil field (2001–2003). *British Geological Survey Commissioned Report*, CR/04/030N.
- BIOMOVS. 1996. An overview of the BIOMOVS II study and its findings. *BIOMOVS II Technical Report 17*, Swedish Radiation Protection Institute.
- BRUCKSCHEN, P, BRUHN, F, VEIZER, J, and BUHL, D. 1995. <sup>87</sup>Sr/<sup>86</sup>Sr isotopic evolution of Lower Carboniferous seawater: Dinantian of western Europe. *Sedimentary Geology*, Vol. 100, 63–81.
- CAPASSO, G, and INGUAGGIATO, S. 1998. A simple method for the determination of dissolved gases in natural water. *Applied Geochemistry*, Vol. 13, 631–642.
- CHRISTIANSEN, E A. 1967. Tills in Southern Saskatchewan, Canada. 167–183 in *Tills: A Symposium* GOLDTHWAIT, R P, (ed.). Ohio University Press.
- CHRISTIANSEN, E A. 1992. Pleistocene stratigraphy of the Saskatoon area, Saskatchewan, Canada: an update. *Canadian Journal of Earth Sciences*, Vol. 29, 1767–1778.
- CRANWELL, R M, GUZOWSKI, R W, CAMPBELL, J E, and ORTIZ, N R. 1982. Risk methodology for geologic disposal of radioactive waste: scenario selection procedure. *Sandia Report SAND80-1429*, Sandia National Laboratory, Albuquerque, New Mexico, USA.
- CZERNICHOWSKI-LAURIOL, I, LE NINDRE, Y-M, AZAROUAL, M, QUATTROCCHI, F, PEARCE, J M, and SPRINGER, N. 2001. The Weyburn CO<sub>2</sub> Monitoring Project - Baseline hydrogeology, hydrochemistry and mineralogy. *Bureau de Recherches Géologiques et Minières Report*, BRGM/RP-51414-FR, (restricted).
- DOMENICO, P A, and SCHWARTZ, F W. (1990). *Physical and chemical hydrogeology*. (New York: John Wiley and Sons).
- DUAN, Z, MOLLER, N, and WEARE, J H. (1992). An equation of state for the CH<sub>4</sub>-CO<sub>2</sub>-H<sub>2</sub>O system: 1. Pure systems from 0° to 1000°C and 0 to 8000 bar. *Geochimica et Cosmochimica Acta*, Vol. 56, 2605–2617.
- ENNIS-KING, J, and PATERSON, L. 2003. Rate of dissolution due to convective mixing in the underground storage of carbon dioxide. 507–510 in *Greenhouse Gas Control Technologies, Volume I*, GALE, J, and KAYA, Y, (editors). (Oxford: Elsevier Science Limited.)
- HANCOCK, S K. 1999. Project brings commercial-scale CO<sub>2</sub> miscible flooding to Canada. *Oil and Gas Journal*, October 1999.
- HECK, T J, LEFEVER, R D, FISCHER, D W, and LEFEVER, J. 2002. Overview of the petroleum geology of the North Dakota Williston Basin. [http://www.state.nd.us/ndgs/resources/wbpetroleum\\_h.htm](http://www.state.nd.us/ndgs/resources/wbpetroleum_h.htm)
- HELFFERICH, F. (1966). 65–100 in *Ion exchange, A Series of Advances*. MARINSKY, J A (editor). (New York, Marcel Dekker.)
- HUDSON, J. 1992. *Rock engineering systems: theory and practice* (Chichester: Ellis Horwood.)
- JONES, C E, JENKYN, H C, COE, A L, and HESSELBO, S P. 1994. Strontium isotope variations in Jurassic and Cretaceous seawater. *Geochimica et Cosmochimica Acta*, Vol. 58, 3061–3074.
- JONES, D G, BEAUBIEN, S, STRUTT, M H, BAUBRON, J-C, CARDELLINI, C, QUATTROCHI, F, and PENNER, L A. 2003. Additional Soil Gas Monitoring at the Weyburn unit (2003). Task 2.8 Report for PTRC. *British Geological Survey Commissioned Report*, CR/03/326N.
- KENDALL, A C, and WALTERS, K L. 1978. The age of metasomatic anhydrite in Mississippian reservoir carbonates, southeastern Saskatchewan. *Canadian Journal of Earth Sciences*, Vol. 15, 424–430.
- KENT, D M. 1984. Depositional setting of Mississippian strata in southeastern Saskatchewan: A conceptual model for hydrocarbon accumulations. 19–30 in *Oil and gas in Saskatchewan*. LORSONG, J A, and WILSON, M A, (eds). Saskatchewan Geological Society Special Publication, No. 7.
- KHARAKA, Y K, MAEST, A S, CAROTHERS, W W, LAW, L M, LAMOTHE, P J, and FRIES, T L. 1987. Geochemistry of metal-rich brines from central Mississippi Salt Dome Basin, USA. *Applied Geochemistry*, Vol. 2, 543–561.
- LE NINDRE, Y-M, CZERNICHOWSKI-LAURIOL, I, BACHU, S, and HECK, T. 2002. Preliminary characterisation of regional hydrogeology at the CO<sub>2</sub> sequestration site of Weyburn (SK-Canada). 1633–1636 in *Greenhouse Gas Control Technologies, Volume II*. GALE, J, and KAYA, Y, (editors). (Oxford: Elsevier Science Limited.)
- MAATHUIS, H. 2003. Till characterisation in the Weyburn soil gas investigation area. IEA Weyburn CO<sub>2</sub> Monitoring Project Task 2.2.6. *Saskatchewan Research Council Publication*, No. 11635–1E03.
- MALIK, Q M, and ISLAM, M R. 2000. CO<sub>2</sub> injection in the Weyburn field of Canada: Optimization of enhanced oil recovery and greenhouse gas storage with horizontal wells. *Society of Petroleum Engineers/Department of Energy Improved Oil Recovery Symposium, Tulsa Oklahoma, 3rd-5th April 2000; Society of Petroleum Engineers (SPE) Paper Number 59327*, 16 p.
- MATHISEN, A, and SHEHATA, M. 1987. The Midale Beds log-core correlations in Tatagwa Oil Field, southern Saskatchewan, Canada. *Bulletin of Canadian Petroleum Geology*, Vol. 35, 443–453.

- MUNDY, D J C, and ROULSTON, P E. 1998. Diagenesis and porosity development of a subcropped Mississippian carbonate oil reservoir, an example from the Alida Beds of the Pheasant Rump Pool, southeast Saskatchewan. 86–102 in *Eighth International Williston Basin Symposium*. CHRISTOPHER, J E, GILBOY, C F, PATERSON, D F, and BEND, S F, (editors). Saskatchewan Geological Society Special Publication, No. 13.
- NEA/OECD 2000. Features, events and processes (FEPs) for geologic disposal of radioactive waste. Nuclear Energy Agency/Organisation for Economic Development, Paris, France.
- NICKEL, E H. 2004. Subtask 2.4.2. Report on the sealing units of the Weyburn reservoir: mapping, petrography, and geochemistry. *Bureau de Recherches Géologiques et Minières Internal Report*, (restricted).
- NICKEL, E H, and QING, H. 2004. Geochemical and petrographic characterization of the unconformity-related seal in the Weyburn Midale Pool, southeastern Saskatchewan. *Summary of Investigations 2004, Volume 1, Saskatchewan Geological Survey, Saskatchewan Industry and Resources, Miscellaneous Report, 2004–4.1, CD-ROM, Paper A-10*.
- OLSEN, D, and STENTOFT, N. 2004. The Weyburn Monitoring Project. Core analysis tests to ascertain changes in fluid flow properties as a consequence of reaction with CO<sub>2</sub>. *Danmarks og Grønlands Geologiske Undersøgelse Rapport*, nr. 2004/1, (restricted).
- PARKHURST, D, and APPELO, C A T. 1999. User's Guide to PHREEQC (Version 2). *Water-Resources Investigations Report*, No. 99–4259.
- PEARCE, J, and SPRINGER, N. 2001. A mineralogical review of the Midale Beds (Mississippian) from the Weyburn Oilfield, south-eastern Saskatchewan. *British Geological Survey Commissioned Report*, CR/01/146N.
- PEARCE, J M, WAGNER, D, JONES, D G, KEMP, S J, RIDING, J B, and STRUTT, M H. 2003. Till characterisation above the Weyburn oilfield. *British Geological Survey Commissioned Report*, CR/03/318N.
- QUATTROCCHI, F. 1999. In search of evidence of deep fluid discharges and pore pressure evolution in the crust to explain the seismicity style of the Umbria-Marche 1997–1998 seismic sequence (Central Italy). *Annali di Geofisica*, Vol. 42, 609–636.
- QUATTROCCHI, F, GUERRA, M, PIZZINO, L, and LOMBARDI, S. 1999. Radon and helium as pathfinders of fault systems and groundwater evolution in different Italian areas. *Il Nuovo Cimento*, Vol. 22, 309–316.
- QUATTROCCHI, F, PIK, R, ANGELONE, M, BARBIERI, M, CONTI, M, GUERRA, M, LOMBARDI, S, MARTY, B, PIZZINO, L, SACCHI, E, SCARLATO, P, and ZUPPI, G M. 2000. Geochemical changes at the Bagni di Triponzo thermal spring, during the Umbria-Marche 1997–98 seismic sequence. *Journal of Seismology*, Vol. 4, 56–587.
- RIDING, J B. 2003. A palynological investigation of the till succession from the Weyburn oilfield, Weyburn, Saskatchewan, Canada. *British Geological Survey Commissioned Report*, CR/03/292N.
- RIDING, J B, CZERNICHOWSKI-LAURIOL, I, LOMBARDI, S, QUATTROCCHI, F, ROCHELLE, C A, SAVAGE, D, and SPRINGER, N. 2003. The IEA Weyburn CO<sub>2</sub> Monitoring and Storage Project - the European dimension. 1629–1632 in *Greenhouse Gas Control Technologies, Volume II*. GALE, J, and KAYA, Y, (editors). (Oxford: Elsevier Science Limited.)
- RILEY, N J. 2002. The Weyburn CO<sub>2</sub> Monitoring Project — Economic modelling of CO<sub>2</sub> sequestration: Provisional report on the Great Plains Synfuels Plant (the CO<sub>2</sub> source). *British Geological Survey Commissioned Report*, CR/02/019N.
- ROCHELLE, C A, BIRCHALL, D J, and BATEMAN, K. 2002. Geochemical interactions between supercritical CO<sub>2</sub> and the Midale Formation. Introduction to fluid-rock interaction experiments. *British Geological Survey Commissioned Report*, CR/02/289N.
- ROCHELLE, C A, BIRCHALL, D J, CHARLTON, B D, REEDER, S, SHAW, R A, TAYLOR, H, and WRAGG, J. 2002. Geochemical interactions between supercritical CO<sub>2</sub> and the Midale Formation. II: Initial results of preliminary test experiments. *British Geological Survey Commissioned Report*, CR/02/290N.
- ROCHELLE, C A, BIRCHALL, D J, PEARCE, J M, CHARLTON, B D, REEDER, S, SHAW, R A, TAYLOR, H, TURNER, G, WRAGG, J, BATEMAN, K, and MCKERVEY, J A. 2003a. Geochemical interactions between supercritical CO<sub>2</sub> and the Midale Formation. III: Experiments investigating reactions of the Midale Marly. *British Geological Survey Commissioned Report*, CR/03/332N.
- ROCHELLE, C A, BIRCHALL, D J, PEARCE, J M, CHARLTON, B D, REEDER, S, SHAW, R A, TAYLOR, H, TURNER, G, BATEMAN, K, and MCKERVEY, J A. 2003b. Geochemical interactions between supercritical CO<sub>2</sub> and the Midale Formation. IV: Experiments investigating reactions of the Midale Evaporite. *British Geological Survey Commissioned Report*, CR/03/333N.
- ROCHELLE, C A, BIRCHALL, D J, PEARCE, J M, CHARLTON, B D, REEDER, S, SHAW, R A, TAYLOR, H, TURNER, G, BATEMAN, K, and MCKERVEY, J A. 2003c. Geochemical interactions between supercritical CO<sub>2</sub> and the Midale Formation. V: Experiments investigating reactions of the Midale Vuggy. *British Geological Survey Commissioned Report*, CR/03/334N.
- ROCHELLE, C A, PEARCE, J M, BATEMAN, K, BIRCHALL, D J, CHARLTON, B D, REEDER, S, SHAW, R A, TAYLOR, H, TURNER, G, and MCKERVEY, J A. 2004. Geochemical interactions between supercritical CO<sub>2</sub> and borehole cements used at the Weyburn oilfield. *British Geological Survey Commissioned Report*, CR/04/009N.
- ROCHELLE, C A, PEARCE, J M, BIRCHALL, D J, and BATEMAN, K. 2004. The Weyburn project: Summary report for Task 3.1. Experimental geochemical studies of CO<sub>2</sub>-porewater-rock interaction. *British Geological Survey Commissioned Report*, CR/04/020N.
- ROTT, C. 2003. Sealing potential of the Mississippian Alida Beds. IEA Weyburn CO<sub>2</sub> Monitoring and Storage Project, Internal Report (unpublished).
- SALVI, S, QUATTROCCHI, F, ANGELONE, M, BRUNORI, C A, BILLI, A, BUONGIORNO, F, DOUMAZ, F, FUNICIELLO, R, GUERRA, M, LOMBARDI, S, MELE, G, PIZZINO, L, and SALVINI, F. 2000. A multidisciplinary approach to earthquake research: implementation of a geochemical geographic information system for the Gargano site, southern Italy. *Natural Hazards*, Vol. 20, 255–278.
- SARIPALLI, K P, MAHASANAN, N M, and COOK, E M. 2003. Risk and hazard assessment for projects involving the geological sequestration of CO<sub>2</sub>. 511–516 in *Greenhouse Gas Control Technologies, Volume I*. GALE, J, and KAYA, Y, (editors). (Oxford: Elsevier Science Limited.)
- SAVAGE, D, (editor). 1995. *The Scientific and Regulatory Basis for the Geological Disposal of Radioactive Waste*. (New York: John Wiley and Sons.)
- SHEPARD, F P. 1954. Nomenclature based on sand-silt-clay ratios. *Journal of Sedimentary Petrology*, Vol. 24, 151–158.
- SKI 1996. SKI Site-94: Deep repository performance assessment project. SKI Report SKI 96:36. Swedish Nuclear Power Inspectorate, Stockholm, Sweden.
- SPRINGER, N, STENTOFT, N, FRIES, K, LINDGREEN, H, and VOIGT, B. 2002. The Weyburn CO<sub>2</sub> Monitoring Project, Core Analysis. *Danmarks og Grønlands Geologiske Undersøgelse Rapport*, nr. 111.
- STELTER, S. 2001. The New Synfuels Energy Pioneers. Dakota Gasification Company, Bismarck, North Dakota.
- STENHOUSE, M J. 2001. Application of systems analysis to the long-term storage of CO<sub>2</sub> in the Weyburn reservoir. Monitor Scientific Report MSC1-2025-1, Monitor Scientific LLC, Denver, Colorado, USA.

- STRUTT, M H, BEAUBIEN, S E, BAUBRON, J-C, BRACH, M, CARDELLINI, C, GRANIERI, R, JONES, D G, LOMBARDI, S, PENNER, L, QUATTROCCHI, F, and VOLTATTORNI, N. 2003. Soil gas as a monitoring tool of deep geological sequestration of carbon dioxide: preliminary results from the EnCana EOR project in Weyburn, Saskatchewan (Canada). 391–396 in *Greenhouse Gas Control Technologies, Volume I*. GALE, J, and KAYA, Y, (editors). (Oxford: Elsevier Science Limited.)
- STRUTT, M H, BAUBRON, J-C, BEAUBIEN, S E, BRACH, M, CARDELLINI, C, GRANIERI, D, JONES, D G, LOMBARDI, S, PENNER, L A, QUATTROCCHI, F, and VOLTATTORNI, N. 2003. Soil gas as a monitoring tool of deep geological sequestration of carbon dioxide: preliminary results from the EnCana EOR project in Weyburn, Saskatchewan (Canada). *Second National Conference on Carbon Sequestration, Washington, DC, May 5–8, 2003*, abstract.
- THIÉRY, D. 1990. Software MARTHE. Modelling of aquifers with a rectangular grid in transient state for hydrodynamic calculation of heads and flows. Release 4.3. *Bureau de Recherches Géologiques et Minières Report*, BRGM/EAU R37762.
- WALTHAM, A C. 2001. Crystal Geyser - Utah's cold one. *Geology Today*, Vol. 17, 22–24.
- WAY, W P, and HANCOCK, S K. 1999. Weyburn CO<sub>2</sub> miscible flood project - Field production and pipeline operation impacts. *Eighth Petroleum Conference of the South Saskatchewan section, the Petroleum Society of the Canadian Institute of Mining, Metallurgy and Petroleum, Regina*, October 18–21, 1999.
- WEGELIN, A. 1984. Geology and reservoir properties of the Weyburn field, southeastern Saskatchewan. 71–82 in *Oil and gas in Saskatchewan*. LORSONG, J A, and WILSON, M A, (editors). Saskatchewan Geological Society Special Publication, No. 7.
- WEGELIN, A. 1987. Reservoir characteristics of the Weyburn Field, southeastern Saskatchewan. *Journal of Canadian Petroleum Technology*, Vol. 26, 60–66.
- WHITE, D J, BURROWES, G, DAVIS, T, HAJNAL, Z, HIRSCH, K, HUTCHEON, I, MAJER, E, ROSTRON, B, and WHITTAKER, S. 2004. Greenhouse gas sequestration in abandoned oil reservoirs: The International Energy Agency Weyburn pilot project. *GSA Today*, Vol. 14, 4–10.
- WHITTAKER, S G, and ROSTRON, B. 2001. Geologic storage of CO<sub>2</sub> in a carbonate reservoir within the Williston Basin, Canada: an update. 385–390 in *Fifth International Conference on Greenhouse Gas Control Technologies*. (Oxford: Pergamon.)

